INFORMATION TO USERS

This manuscript has been reproduced from the microfilm master. UMI films the text directly from the original or copy submitted. Thus, some thesis and dissertation copies are in typewriter face, while others may be from any type of computer printer.

The quality of this reproduction is dependent upon the quality of the copy submitted. Broken or indistinct print, colored or poor quality illustrations and photographs, print bleedthrough, substandard margins, and improper alignment can adversely affect reproduction.

In the unlikely event that the author did not send UMI a complete manuscript and there are missing pages, these will be noted. Also, if unauthorized copyright material had to be removed, a note will indicate the deletion.

Oversize materials (e.g., maps, drawings, charts) are reproduced by sectioning the original, beginning at the upper left-hand corner and continuing from left to right in equal sections with small overlaps.

Photographs included in the original manuscript have been reproduced xerographically in this copy. Higher quality 6" x 9" black and white photographic prints are available for any photographs or illustrations appearing in this copy for an additional charge. Contact UMI directly to order.

Bell & Howell Information and Learning
300 North Zeeb Road, Ann Arbor, MI 48106-1346 USA
800-521-0600

Application of Artificial Intelligence Techniques for Inductively Coupled Plasma Spectrometry

Christine Sartoros

A Thesis Submitted to the Faculty of Graduate Studies and Research in partial fulfillment of the requirements of the degree of Doctor of Philosophy

August 1998

Department of Chemistry
McGill University
Montreal, Quebec
Canada

The following text has been reproduced and is included as instructed from the "Guidelines Concerning Thesis Preparation", Faculty of Graduate Studies and Research, McGill University, in order to inform the external reader of Faculty Regulations:

> "Candidates have the option of including, as part of the thesis, the text of one or more papers submitted or to be submitted for publication, or the clearly-duplicated text of one or more published papers. These texts must be bound as an integral part of the thesis.
>
> If this option is chosen, **connecting texts that provide logical bridges between the different papers are mandatory**. The thesis must be written in such a way that it is more than a mere collection of manuscripts; in other words, results of a series of papers must be integrated.
>
> The thesis must still conform to all other requirements of the "Guidelines for Thesis Preparation". **The thesis must include**: A Table of Contents, an abstract in English and French, an introduction which clearly states the rationale and objectives of the study, a review of the literature, a final conclusion and summary, and a thorough bibliography or reference list.
>
> Additional material must be provided (e.g., in appendices) and in sufficient detail to allow a clear and precise judgment to be made of the importance and originality of the research reported in the thesis.
>
> In the case of manuscripts co-authored by the candidate and others, **the candidate is required to make an explicit statement in the thesis as to who contributes to such work and to what extent.** Supervisors must attest to the accuracy of such statements at the doctoral oral defense. Since the task of the examiners is made more difficult in these cases, it is in the candidate's interest to make perfectly clear the responsibilities of all the authors of the co-authored papers."

Abstract

The development of intelligent components for the automated analysis of samples by inductively coupled plasma (ICP) spectrometry is presented. An expert system for diagnosing an ICP atomic emission spectrometry (AES) system using a blank solution was developed as a warning system. This expert system was able to warn the system of major malfunctions and was able to identify most problems. Three pattern recognition techniques were compared in their ability to recognize similar geological samples in small databases. Two of these techniques, k-Nearest Neighbours and Bayesian Classification, worked extremely well with over 96% success. The development of an objective function for multi-element optimizations in ICP-AES is presented. Various aspects of the application of a Simplex optimization were explored for the optimization of the ion optics of an ICP-mass spectrometry (MS) system. An algorithm for the automatic selection of internal standards for analytes in difficult samples in ICP-MS is presented.

Résumé

Cette thèse présente le développement d'éléments 'intelligents' pour l'analyse d'échantillons par spectroscopie à plasma inductif. Un système sophistiqué a été développé pour diagostiquer un plasma à couplage inductif en utilisant un blanc. Il s'est avéré que ce système a été capable de diagnostiquer des malfonctions majeures et d'identifier les problèmes les plus courants. Par la suite, trois techniques de reconnaisance ont été comparées, le but de l'opération étant d'analyser l'habileté respective de chacune des techniques à reconnaître des échantillons géologiques similaires dans une base de données. Deux de ces techniques, K-Nearest Neighbors et Bayesian Classification, ont obtenu un taux de succès remarquablement élevé. Le project présente donc le développement d'une fonction générale pour l'optimisation de multiples éléments. A cette fin, plusieurs aspects de l'application de la méthode d'optimisation du Simplex ont été explorés pour l'optimisation de l'optique ionique d'un spectomètre de masse. Finalement, le projet présente un algorithme dont le but primordial est de sélectionner automatiquement des étalons internes afin d'aider à l'évaluation d' échantillons difficiles.

Contributions to Original Knowledge

1. A diagnostic procedure using a blank solution was developed for an inductively coupled plasma atomic emission spectrometer to warn the instrument operator of possible malfunctions.

2. Three pattern recognition techniques were evaluated for the problem of sample classification using elemental composition with variable size databases.

3. An objective function for multi-element optimization in inductively coupled plasma atomic emission was developed.

4. A Simplex optimization of the ion optics on an inductively coupled plasma mass spectrometer was evaluated in terms of (i) the most appropriate objective function for multi-element optimizations, (ii) the best initial points of Simplex, (iii) the performance of single-element versus multi-element optimizations, and (iv) the selection of the element to be used for single element optimizations.

5. A procedure for the automatic selection of internal standards for elements in difficult samples was developed using a cluster analysis algorithm.

Acknowledgments

First, I would like to thank my research advisor, Eric Salin, for his advice and guidance, and especially for his encouragement and patience.

There have been several people who have worked directly on the Autonomous Instrument project: Douglas Webb, the original designer of the Autonomous Instrument, and Wayne Branagh, designer and developer of the framework of the current Autonomous Instrument. I would like to express my gratitude to the latter, his assistance and insights were invaluable.

I would like to express my appreciation to Doug Goltz who helped me understand the workings of an ICP-MS and worked with me on a project that became one of the components of the Autonomous Instrument.

I would also like to thank everyone in Eric's lab and Prof. Burns lab, past and present, for offering their expertise and friendship.

I would also like to acknowledge the financial support from Fonds pour la Formation de Chercheurs et l'Aide à la Recherche (FCAR) of the Province of Quebec.

Finally, I thank my family and friends for their support, encouragement and patience.

Table of Contents

List of Tables

List of Figures

Chapter 1

1 Introduction

Man has always believed that humans are the only creatures on the Earth that are capable of rational thought. In attempts to express power and intelligence, man has sought to control his environment. Man's aspiration to become godlike has lead to his desire to create artificial beings. Man is continuously trying to improve the quality of life by creating machines to perform labor intensive and repetitive tasks. From the invention of the wheel to the development of the land rover sent to Mars, man continually evolves and so does his technology. The advent of computers has provided a wealth of opportunity for improvement in all aspects of life. In business and finance, computers are found in banking machines, the stock market, and most stores enabling consumers to buy purchases using their bankcards. In education, schools are introducing computers to students to help them learn subjects such as mathematics, geography and history. Many examinations, such as those for a driver's license, are now being taken on computers instead of on paper. In aviation, many pilots train in computer simulators long before they fly a plane. The same types of simulators, using virtual reality, are helping people conquer their fears of flying. In biology, the Human Genome Project, an effort to map the human genetic code, would not be possible without computers to sort and store the data. In astronomy, computers have made space exploration possible, from shuttle launches to the Hubble Space Telescope, and recently missions to Mars. In chemistry, computers control most instruments. The latest spectrometers have no knobs to adjust or buttons to press, almost every aspect of the spectrometer is accessed by computer.

Since their development, analytical instruments and their associated techniques have been well described in journals, conference proceedings, and books. Learning the individual steps in an analytical process may take a person a long time. In addition, good analytical results are often only achieved with a great deal of experience. To an operator, with very little experience and faced with a particular problem, selecting the appropriate analysis procedure and analytical instrument can be a very difficult task.

There are several reasons why expert systems (defined below) are receiving attention[1,2] for use in the analytical laboratory. First, experts are confident in demonstrating their decision-making process but have difficulty explaining their decision processes. Second, experts may not like to disclose the rules they use for decision making. Third, transferring knowledge from one human to another can be a laborious, lengthy, and expensive process. Transferring knowledge from one expert system to another can be as simple as copying or cloning a program or data file. Fourth, an expert system produces consistent results whereas a human expert can be unpredictable due to emotional factors such as stress or being under pressure.

1.1 Expert Systems

There have been many definitions of expert systems since the beginning of their existence and the most general and complete, although lengthy, is given by Michaelson *et al.*[3]

> Expert systems are a class of computer programs that can advise, analyze, categorize, communicate, consult, design, diagnose, explain, explore, forecast, form concepts, identify, interpret, justify, learn, manage, monitor, plan, present, retrieve, schedule, test, and tutor. They address problems normally thought to require human specialist for their solution.

This definition emphasizes the range of capabilities of an expert system although no expert system to date has included all these features.

1.1.1 Importance of Expert Systems

The importance of expert systems can be illustrated by two early expert systems, MYCIN[4] and PROSPECTOR[5]. MYCIN, one of the first expert systems, was developed as a decision aid for doctors. The doctor would feed a medical patient's symptoms into the computer program. Based on this information, MYCIN would diagnose infectious blood disease. It would also provide a recommendation as to which therapies would be appropriate to treat the disease diagnosed. In a medical facility that handles many infectious diseases cases a year, an expert system such as MYCIN can be valuable. Its ability to aid doctors in making quick and accurate diagnosis of the cases enables a facility to handle more patients, more effectively. The PROSPECTOR expert system was

developed to aid geologists in assessing whether a given region would be a favorable site for the exploration of minerals. PROSPECTOR would ask the operator for information such as what rocks and minerals were observed in a particular region. The expert system would then provide its conclusions as to whether the available information supports the presence of a particular ore in a given site. An expert system such as PROSPECTOR is a useful tool to a geologist with a vast territory to explore.

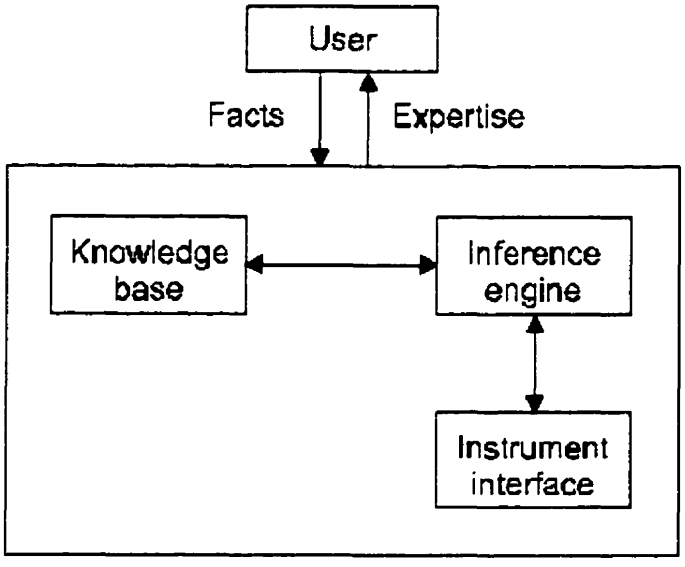

Figure 1.1 Flowchart of an expert system.

1.1.2 Description of Expert Systems

The user interface is a link between the system and the outside world (Figure 1.1). The user can input data or can ask questions and then receive comments, advice, explanations or conclusions. Some expert systems control instruments through an instrument interface. The purpose of this interface is to transfer information from the instrument to the system and provide a method for performing actions the system deems necessary. The knowledge base contains information entered by an expert or knowledge engineer (person who implements the expert system) in that domain in the form of rules and facts useful for solving problems in a domain. The information in the knowledge base usually takes on the form of IF/THEN rules called production rules. IF/THEN rules specify that IF certain conditions are met THEN certain facts apply, or IF certain situations exist

THEN certain actions may be taken. IF/THEN rules have other features[6]: (i) Each rule is an independent piece of information, (ii) new rules may be added to the knowledge base independent of other rules, and (iii) old rules can be modified without affecting other rules in the knowledge base. Due to the simplistic nature of IF/THEN rules, it is easier to follow the reasoning behind a decision and answer questions such as "How?" and "Why?". The inference engine uses the rules and facts in the knowledge base and finds possible solutions to the problem.

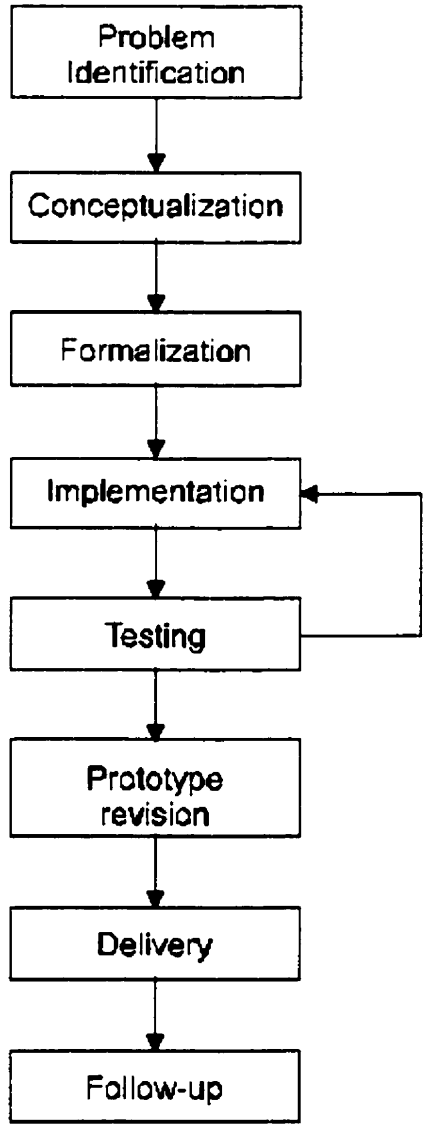

Figure 1.2 Development of an expert system.

1.1.3 Expert System Development

There are several phases that characterize the development of an expert system[7,8] (Figure 1.2).

Identification phase:

This phase consists of identifying the essential components of the expert system, namely, the characteristics of the problem, the available resources, and the goal of the system.

Conceptualization phase:

Using the information from the identification phase, the knowledge engineer will create the structure of the prototype system using diagrams and flowcharts.

Formalization phase:

This phase involves the selection of the language or tool for the implementation of the expert system. High-level languages, such as C and Pascal, offer computing speed and flexibility; however, they lack capabilities such as dealing with symbolic computation that expert systems require. Declarative languages such as PROLOG and LISP provide mechanisms that are superior to other languages for dealing with symbolic data and expressing logical inference[9]. A disadvantage of these languages is that they suffer from a need for greater computational resources and reduced portability of the final code, particularly PROLOG. The alternative to programming languages is to acquire a commercially available expert system shell. These shells contain the control structure of the expert system. The knowledge engineer simply needs to add the knowledge base. Since the shell contains a standard structure format, the knowledge engineer saves time although there is a loss of flexibility.

Implementation phase:

Once the programming language or expert system shell has been selected, the knowledge expert programs all the information into the expert system.

Testing phase:

Upon completion of the implementation of the prototype system, the system must undergo a series of rigorous tests to ascertain its performance. It is difficult to specify exactly the knowledge in an expert system. If major modifications are required, the results obtained from the testing phase can be used back in the implementation phase to help the knowledge acquisition.

Prototype revision:

Based on the results of the testing phase, minor modifications are made and the system undergoes fine-tuning.

Delivery and Follow-up:

The delivery phase includes the installation of the application, manuals and system documentation. Even after an application has been delivered, software maintenance, patches or upgrades may be required.

1.2 Limitations of Expert Systems

Expert systems attempt to model the human reasoning approach using a rule-based approach. Developers of expert systems are required to determine the rules a human expert would use and to implement them in IF/THEN format. Novices in the various fields are expected to obtain the rules from the experts. They often do not ask the right questions and hence do not obtain the necessary knowledge. The human experts, on the other hand, may have more difficulty explaining their decision-making process than using it. This results in many interviews between the two and a lengthy development process. The second problem is that improving an expert system requires that it is able to learn through experience and most expert systems are incapable of this[10]. Several expert system development techniques have been explored in order to overcome these limitations.

1.2.1 Pattern Recognition

It is a characteristic of human beings presented with an object to recognize it and classify it as belonging to a certain group. Having never seen a particular object before, its properties are examined and it is placed in a group of objects with similar properties or a new group is created. This can be seen in young children with their toys and older people with their hobbies of collection. This is a valuable trait human possess not only in their daily routines, but it also has great value in different fields of careers. In science, the ability to classify and group objects, data, and ideas, is essential. Although humans are very good at recognizing and classifying various patterns, when presented with large amounts of data, particularly numerical, they have considerable difficulty with the task. Analytical instruments, today, generate large quantities of numerical data, which make it almost impossible for the human operator to keep up.

1.2.1.1 Supervised vs. Unsupervised

Samples are analyzed and described by a set of measured values. The task is to derive and apply a formal method (e.g., mathematical scheme) of grouping the samples such that the samples in a group (class) are similar and are also different from samples in other groups (classes). In unsupervised analysis the number of classes and the characteristics of the classes are not known prior to the analysis but are determined from the analysis[11]. In supervised pattern recognition, the number of classes and their characteristics are known. The samples in the training set are associated with a particular class and this information is used to develop the method for the classification of unknown samples.

1.2.2 Inductive Learning

One of the most promising techniques for generating rule-based expert systems and recognizing patterns has been inductive learning[12]. Inductive learning is a process by which classification rules are generated from a set of examples. This set consists of examples that have been previously solved by human experts. The set of rules that is generated is used as the knowledge base in the expert system. This process eliminates the

need for extensive interviews between the developer and human expert. There are several inductive learning algorithms but the most widely used has been ID3 developed by Quinlan[13], which has its origins in Hunt's Concept Learning Systems (CLS)[14]. Quinlan later developed C4.5, an extension of ID3.

1.2.2.1 C4.5

The C4.5 induction algorithm applies information theory to determine which attribute best divides the examples in a data set into distinct classes. For example, consider that the data in Table 1.1 describe the conditions for determining whether an analysis will be problematic. Each example consists of four attributes: Matrix, Feed Rate, Element, and Suppression. Each example belongs to one of two classes: Problematic or Easy.

Table 1.1 Data for determining whether analysis would be problematic

Matrix	Feed Rate	Element	Suppression	Class
High	90	K	High	Easy
High	60	K	High	Problematic
High	30	Mg	Low	Problematic
High	90	Na	Low	Easy
Medium	90	K	High	Problematic
Medium	30	Na	High	Problematic
Medium	60	K	Low	Easy
Medium	90	Na	Low	Easy
Medium	30	K	High	Problematic
Low	60	K	High	Easy
Low	90	Mg	Low	Easy
Low	30	Na	High	Easy
Low	60	Mg	Low	Easy

Consider an example selected at random from the data set, S, and said to be of class, C_j, it has a probability of

$$\frac{freq(C_j, S)}{|S|}$$

and the information it contains is given by

$$-\log_2\left(\frac{freq(C_j,S)}{|S|}\right)\text{bits.}$$

A bit is a scalar value used as a unit of measure of the amount of information that can be extracted. The information in the entire data set S is calculated using

$$\text{info(S)} = -\sum_{j=1}^{k}\left[\left(\frac{freq(C_j,S)}{|S|}\right)*\log_2\left(\frac{freq(C_j,S)}{|S|}\right)\right]$$

For the data in Table 1.1, the information in the data set would be

$$\text{info(S)} = -\frac{8}{13}\log_2\left(\frac{8}{13}\right)-\frac{5}{13}\log_2\left(\frac{5}{13}\right) = 0.961\text{ bits.}$$

There are eight examples in the data set that belong to the class Easy and five examples belonging to the class Problematic. Once the C4.5 algorithm has calculated the information of a data set, it then looks at each attribute and determines which one would best divide the data set. The information expected from a division by an attribute is calculated using

$$\text{info(S)} = -\sum_{j=1}^{k}\left[\left(\frac{|S_i|}{|S|}\right)*\text{info}(S_i)\right]$$

where S_i is the information in a subset and calculated as described previously. For example, the information expected when the attribute Matrix is used to divide the data set into three subsets (High, Medium, Low) is calculated

$\text{info}_{\text{Matrix}}(S) = \text{info}_{\text{Matrix}}(\text{High}) + \text{info}_{\text{Matrix}}(\text{Medium}) + \text{info}_{\text{Matrix}}(\text{Low})$

$$=\frac{4}{13}\left(-\frac{2}{4}\log_2\frac{2}{4}-\frac{2}{4}\log_2\frac{2}{4}\right)+\frac{5}{13}\left(-\frac{2}{5}\log_2\frac{2}{5}-\frac{3}{5}\log_2\frac{3}{5}\right)+\frac{4}{13}\left(-\frac{4}{4}\log_2\frac{4}{4}-\frac{0}{4}\log_2\frac{0}{4}\right)$$

$= 0.681$ bits.

The information gained by such a division is determined by

$\text{gain}_{\text{Matrix}}(S) = \text{info(S)} - \text{info}_{\text{Matrix}}(S) = 0.961 - 0.681 = 0.280$ bits.

The gain criterion was used by the ID3 algorithm for the selection of the attribute that would best divide the data set. The criterion gives good results but it has a serious shortcoming. It would give a strong bias in favor of attributes with a large number of

values. To compensate for this, Quinlan suggested the following ratio instead of gain when he developed the C4.5 algorithm

$$\text{GainRatio}_{\text{Matrix}}(S) = \frac{\text{gain}_{\text{Matrix}}(S)}{\text{split info}_{\text{Matrix}}(S)}$$

where the split information is calculated using

$$\text{split info}_{\text{Matrix}}(S) = -\sum_{i=1}^{n}\left[\frac{|S_i|}{|S|} * \log_2\left(\frac{|S_i|}{|S|}\right)\right]$$

$$= -\frac{4}{13}\log_2\frac{4}{13} - \frac{5}{13}\log_2\frac{5}{13} - \frac{4}{13}\log_2\frac{4}{13} = 0.845 \text{ bits}$$

and the gain ratio becomes

$$\text{GainRatio}_{\text{Matrix}}(S) = \frac{0.280}{0.845} = 0.331$$

This process is repeated with the other attributes and the GainRatios for Feed Rate, Element, and Suppression are 0.218, 0.0598, and 0.131, respectively. Since the attribute Matrix yields the largest value for the GainRatio, it is used to subdivide the data set. This procedure of examining GainRatios and subdividing the data set is repeated until subdivision of the data set gives no further improvements.

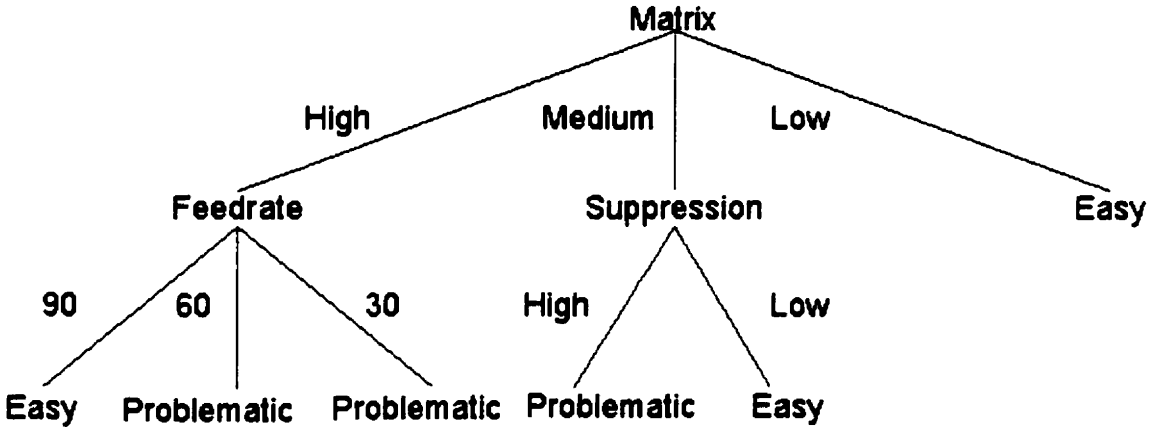

Figure 1.3 Decision tree produced for the example of determining when an analysis would be problematic.

The output of the C4.5 inductive learning engine is a decision tree. For example, consider the output of the previous problem (Figure 1.3). The way to read the tree is to first start at the top (Matrix). In the decision tree, each node represents a non-categorical

attribute (e.g., Matrix) and each branch corresponds to a possible value of that attribute (e.g., High). A leaf of the tree (e.g., Problematic) specifies the result of the classification. Once at the top of the tree, the first decision to be made is what kind of matrix is present. There are three branches with the associated values of High, Medium, and Low. If the Medium branch is followed, the next decision to be made is the kind of suppression observed. A High suppression results in a Problematic conclusion whereas a Low suppression produces an Easy conclusion.

1.3 Expert Systems for Analytical Chemistry

Artificial intelligence techniques, such as expert systems, are playing an increasingly important role in providing intelligent components in current analytical instrumentation. These instruments can select the most suitable method available, optimize operating conditions, and detect and, in some cases, repair malfunctions. Despite advances in commercial instruments, no instrument to date incorporates all the intelligent components necessary to form a completely autonomous instrument.

1.3.1 Fault Diagnosis

A major concern with instrument operation is whether the data obtained is valid. Many things can go wrong in an analysis from the time of sample insertion to the output of results. Any component of the instrument can malfunction after extensive use. The ability to diagnose possible malfunctions in a system is an asset to any laboratory. It takes a trained operator to recognize when the system is not functioning properly. There are few operators who possess this ability and many rely on an instrument manufacturer's technical support services to assist them. An expert system, which has incorporated knowledge obtained from experienced operators, to diagnose faults in a system is an invaluable and sought after tool.

1.3.2 Optimization

Most instruments in chemical analysis have many parameters that can be varied to obtain satisfactory analysis results. The instrumental parameters can sometimes have many

settings and finding the right combination for all the parameters is not a trivial task. To go through all possible combinations can be a very time-consuming approach and quite costly if this procedure has to be repeated on a regular basis. Alternatives to this approach are to use optimization algorithm such as genetic algorithms[15], simulated annealing[16], and Simplex[17].

1.3.2.1 Optimization Algorithms

In analytical chemistry, a widely used optimization algorithm has been the Simplex algorithm. The Simplex algorithm is a multi-parameter direct-search optimization that varies all of the parameters simultaneously. This makes it useful when the optimum setting for one parameter is dependent on the other parameter settings. The algorithm uses the response at various points to direct itself toward the optimum. The Simplex algorithm, in N dimensions, begins by selecting N+1 points and ordering them from best to worst. It then makes use of reflections, expansions, and contractions, to move around the surface towards a maximum. For example, in two dimensions (Figure 1.4), three points would be selected and labeled as Best (B), Next Best (N), and Worst (W). The Worst point would then be reflected (R) through the median of the Best and Next Best points. Based on this new value, a contraction (C) or an expansion (E) is performed. This is repeated until a maximum is obtained.

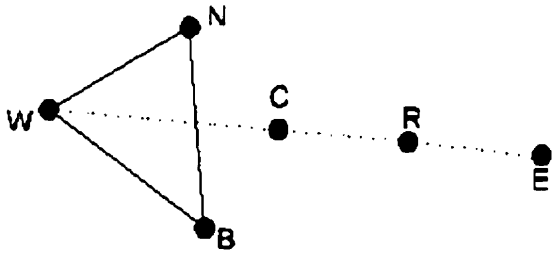

Figure 1.4 Illustration of possible directions of Simplex algorithm.

1.4 Applications of Expert Systems in Chemistry

1.4.1 Molecular Spectroscopy

1.4.1.1 IR, NMR, and MS

One of the first and most notable expert systems in chemistry was the Dendral project. It began in 1964 with Lederberg's development of an algorithm for generating canonical names and structural description of molecules[18]. Later, Dendral broadened to include interpretation of analytical chemical data. Dendral programs are designed to aid organic chemists interpret data from unknown compounds and have become the templates for many expert systems developed in chemistry.

The interpretation of molecular spectra, whether it be in infrared (IR) spectrometry, nuclear magnetic resonance (NMR) spectrometry or mass spectrometry (MS), can be a very complex process. A spectroscopist requires experience in this domain in addition to extensive knowledge of spectrum-structure correlations. Many expert systems have been developed in the fields of IR spectrometry, NMR spectrometry and MS for the interpretation of spectra and structure elucidation[19-26]. These expert systems were constructed to provide spectroscopists with tools to facilitate recognition of substructures and to provide assistance in the construction of molecular structures based on substructures. Andreev *et al.*[19] formulated the principle heuristics used by an expert to interpret IR spectra and implemented some of them in an expert system written in Pascal, EXPIRS (EXPert in InfraRed Spectroscopy). The expert system's main function is the structure elucidation of organic compounds. Luinge[20] developed a similar expert system for the interpretation of IR spectra, EXSPEC, which he wrote in LPA MACPROLOG. Three main modules made up the EXSPEC system. The first was an interpretation module. This module inferred structural fragments from an IR spectrum. Knowledge in this module was represented by IF/THEN rules; for example, IF there is a strong band near 1700 THEN the compound probably contains a >C=O group[20]. The second module was a rule generator. This module automatically generated interpretation rules from example data. The third module was a structure generator. This module constructed all possible isomeric structures from a molecular formula and a given set of fragments. ISIA

(InfraRed Interpretation Aid)[21] was an expert system which recognized major functional groups and sub-structures of functional groups based on user's description of spectral data. This expert system was developed using a commercially available expert system shell, Leonardo Expert System. PAIRS (Program for the Analysis of IR Spectra)[22], written in Fortran and the CONCICE interpreter, provided an explanation of the rationale behind its interpretation process. HIPS (Heuristic Interpretation of Protein Spectra)[24] was a hybrid expert system. It did not solely employ If-Then rules but used a combination of an expert system with pattern recognition. A genetic algorithm was used to find the best pattern match provided by the expert system. This system was written using a number of tools including a commercially available expert system shell, KEE shell, a programming language, LISP, and Gates Toolbox on a Sun Sparc-1 workstation. Expert system's have also found other uses in molecular spectroscopy. Moore *et al.*[27] developed an expert system to assist in the sampling and interpretation of Fourrier Transform Infrared (FT-IR) spectra of organic and inorganic compounds. In the beginning, the expert system would provide a recommendation as to the best technique for sample preparation. It would then perform sample identification by providing assistance with band identification. This was accomplished by searching a database of band positions with position windows that the band was expected to fall within. This expert system was written in the 1st Class expert system shell. Scott *et al.*[28-30] used a combination of an expert system and pattern recognition in the estimation of molecular weight from low-resolution mass spectra. The algorithm employed a sequential design; it began by using an unsupervised pattern recognition technique, SIMCA, and it then applied a filtering step and a molecular weight estimator. Catasti *et al.*[31] developed an expert system, PEPTO, written in Turbo Prolog for automatic peak assignment of 2-D NMR spectra of proteins.

1.4.2 Chromatography

There have been several expert systems developed for gas chromatography (GC) covering several aspects of automation. Du *et al.*[32] designed and developed an expert system, GCdiagnosis, to aid in the diagnosis of faulty analysis by GC. The expert system was written in Visual Basic 2.0 for Windows 3.x and relied on manual input from the

user. GCdiagnosis provided the identity of faulty components and improper operation based on the appearance of the chromatograms that result from a required experiment. Hasenoehrl *et al.*[33] designed an expert system based on principle component analysis (PCA) for the characterization of functional groups from GC-IR. DIM (Data Interpretation Module)[34] was created to automate the interpretation of gas chromatograms for organochlorine compounds. In a fully automated laboratory, its tasks would include data assessment, data interpretation, and result reporting. DIM was developed in the real-time expert system shell G2 (Gensym) and employed principle component regression (PCR) pattern recognition. Expert systems have found slightly more use in high performance liquid chromatography (HPLC) than with GC. An expert system has been designed for the selection of factors for a ruggedness test, which is valuable for finding the analytical conditions that give the best performance in HPLC[35]. DASH (Drug Analysis System in HPLC)[36] was created to give advice on HPLC conditions for analysis of basic compounds. CRISE (CRIteria SElection)[37,38] was developed to assist chromatographers in the selection of suitable optimization criteria and CHIRULE[39] suggests a chiral stationary phase which would be suitable for use in developing a separation method for a new target molecule. Other method development expert systems in HPLC include ECAT (Expert Chromatographic Assistance Team)[40] and ESCA (Expert System for Chemical Analysis)[41].

1.4.3 Electrochemistry

Electrochemical techniques are well suited for the application of expert systems. Esteban *et al.*[42-45] developed an expert system to give advice on the different steps involved in the selection of the appropriate methodology for the determination of several elements by polagraphic and voltammetric techniques. The elements studied were Cu, Zn, Cd, Pb, In, Co, Ni and Tl. The advice given by this expert system was separated into four categories: sample pretreatment, electroanalytical measurement, qualitative analysis, and quantitative analysis. The knowledge in each category was implemented with IF/THEN rules. Another type of expert system developed by Palys *et al.*[46] was for the automatic elucidation of electrode reaction mechanisms.

1.4.4 Atomic Spectroscopy

1.4.4.1 Atomic Absorption Spectroscopy

Stillman *et al.*[47-50] developed a complete expert system for automated metal analysis by flame atomic absorption (FAA) spectrometry. The expert system was composed of many modules that performed various tasks.

AAmethods, AAselect	Using rules and a method-selection database, these modules select the appropriate method of analysis.
AAcontrol	This module performs all the tasks related to the atomic absorption spectrometer. It is responsible for real-time sample introduction and scheduling of the autosampler and capturing real-time data.
AAanalysis, AAQC	These modules collect and evaluate the data obtained from AAcontrol. They extract information and provide an assessment of the quality of the data.
AAdiagnosis	It is a fault diagnosis module that diagnoses probable causes of instrument malfunctions or incorrect data values.
AAtrend, AAreport, AAassurance	These modules provide a report of the evaluated analysis data and information. They also apply guidelines to assure process and production quality.
AAteach	This module provides a training capability targeted toward laboratory personnel or students. It teaches using simulations and question and answer sessions.

The system works as follows. The manager obtains a sample from a customer and consults with both the customer and regulatory agency to determine the criteria to be used in the analysis. The module AAassurance is used by the manager and the analyst to implement the laboratory quality assurance program. The operator identifies the blank, standard, and sample solutions to be used for the analysis. The module AAcontrol then establishes the sequence of tubes and beakers to be used for the analysis. The method of analysis is chosen by the modules AAmethods and AAselect and the analysis is initiated. The absorbance profile of the solution being analyzed is sent to the module AAQC. The AAQC and AAdiagnosis modules determine whether the measurement meets preset criteria. This is accomplished by the extraction of the parameters from the training set with the application of production rules. Once the acceptability of the measurement has been determined, an appropriate message is sent back to the AAcontrol module which proceeds with the analysis. The modules AAtrend and AAreport provide a report of the analysis of the experimental data which can be presented to the customer. Penninckx *et al.*[51] developed an expert system, written in Visual Basic, for the detection of matrix interferences and method validation in atomic absorption spectrometry (AAS). Another expert system in AAS was written in Toolbook 1.0 Software, for the selection of dissolution methods prior to atomic absorption analysis of pharmaca.

1.4.4.2 X-ray Fluorescence, X-ray Diffraction, FIA

Arnold *et al.*[52] developed an expert system written in Pascal for energy-dispersive X-ray fluorescence spectrometry. The aim in designing this expert system was to automatically interpret the data and return the elemental composition of the sample associated with a spectrum. The expert system consisted of three components: (1) A knowledge base which contains information on energy-dispersive X-ray fluorescence spectrometry in IF/THEN rules; (2) a database containing reduced spectral data and an array of certainty factors associated with each element; and, (3) an inference engine which performs manipulation of the knowledge. Janssens and Van Espen[53] developed an expert system for the qualitative interpretation of wavelength dispersive X-ray fluorescence

spectrometry. This expert system included two modules. The first was the pre-processor module, PREXRF, written in BASIC. This module encompassed the following functions for the manipulation of spectral data: (1) Filtering of the digital original spectrum and derivation of line spectra; (2) selection of the database section that is applicable to the actual experimental conditions; (3) correction for gross deviations in the wavelength axis; (4) spectral pattern matching of the unknown sample spectrum and candidate element spectrum; (5) calculation of probabilities of line coincidences by Bayesian reasoning; and, (6) calculation and identification of Compton lines. The second module, INFERXRF, implemented in PROLOG, contained the knowledge base and inference engine. The rules in the inference engine were used for the selection of the most appropriate lines, the identification of elements present and the spectral stripping of the determined element in the raw spectrum. An expert system developed by Adler *et al.*[54] employed a knowledge base containing fuzzy set rules for the qualitative and semi-quantitative interpretation of X-ray diffraction spectra. Brandt and Hitzmann[55] developed an expert system for fault detection and diagnosis in flow injection analysis (FIA). This expert system could detect faults in the sampling, flow, reaction, detector, and automation systems. The knowledge base comprised IF/THEN rules such as the following:

> IF the measurement data in the initial phase of the flow injection cycle differ from a straight line THEN Injection disturbed.

1.4.4.3 Atomic Emission Spectroscopy

In inductively coupled plasma atomic emission spectrometry (ICP-AES), an automated sample preparation and plasma spectrometric system for the analysis of geological materials[56] has been operational since 1981. This expert system involves complete automation from prospecting to processing the analytical data. The entire process begins with the selection and grinding of the samples. One gram of sample is weighed on an electronic balance and both its origin and weight are stored in computer memory. This information is used later for computing element concentrations. Sodium peroxide is added automatically and the reaction takes 45 min. at 460°C. At the end of the decomposition process, a clear solution is produced for multi-element analysis by ICP-AES. In an 8-hour time period 250 samples can be prepared. A quality control

procedure is implemented by monitoring the Cd II / Cu I ratio and adjusting gas flow rates accordingly. When satisfactory operating conditions are obtained the analysis begins. Upon analysis of the sample, if the relative standard deviations (RSDs) obtained are not within tolerance the analysis is repeated. If after 3 repetitions the RSDs are unacceptable, the system is halted and a warning is activated. Otherwise, the intensity data is processed. The method of external calibration is the only calibration methodology implemented in this system. Interferences are measured for element channels. Corrections are applied based on results from experiments on synthetic samples. Major, minor, and trace elements were all analyzed successfully in geochemical prospecting samples.

Pomeroy *et al.*[57,58] had in their possession a direct current plasma echelle CID spectroscopic system for AES. This instrument has the advantage that it can record simultaneously all wavelengths between 220 nm and 520 nm and produce large amounts of data. They designed and built two expert systems. The first, auto-qualitative analysis, was used to determine what elements were present in a sample. The process began with the acquisition of two spectra: a blank and a sample. The blank subtracted spectrum was calculated and stored. The signal-to-noise ratio (SNR) of each line was then calculated and used to predict the presence of an element in the sample. There are several rules in the decision process:

1. If 50% of the lines of an element have a SNR > 5 then the element is present in the sample.
2. If the most intense line of an element has a SNR > 5 then the element may be present in the sample at a very low concentration.
3. Otherwise, the element is not present in the sample.

An advantage of this approach is that no prior knowledge of the sample is required in the decision process. The authors decided that this expert system was good for determining what elements were present in a sample but what they wanted to know was the quantity of the element in the sample. For this purpose, they designed their second expert system for semi-quantitative analysis. The approach they used was to employ the method of internal standardization. They obtained initial calibration curves and did not need to

recalibrate. Over a fifteen-day period their results never varied more than ±20%. This system is used when speed is of utmost concern and accuracy is not as important.

Webb and Salin[59] developed an expert system for line selection using an atomic emission rapid scanning spectrometer. LINEX (LIne EXpert), written in Prolog, used elemental compositions of a given sample to generate a line search strategy that minimized the number of lines to be measured. The presence of an analyte was determined by checking line ratios and verifying the possibility of line interferences. If an analyte was present in the sample it was spectrally stripped from the net signal and the expert system would go on to the next element.

Yang *et al.*[60,61] developed an expert system for the prediction of spectral interferences in ICP-AES. PESLS (Primary Expert System for Line Selection) was written in C++ and consisted of three modules. The first module performed a simulation of an ICP discharge. The second module performed a simulation of the process of excitation and ionization. Both these modules were written in Fortran 77. The third module required the first two modules and performed a simulation of spectral line shapes and the selection of the best spectral line under non-local thermal equilibrium (LTE) conditions. They found that the expert system's predictions under non-LTE conditions were much closer to reality than those under LTE conditions.

Webb *et al.*[62] designed a fully automated ICP-AES, the Autonomous Instrument. They employed a Thermo Jarrell Ash Model 25 scanning ICP-AES spectrometer that could scan wavelengths in the range 160 nm to 900 nm. The sequence the expert system used began with acquiring prior knowledge such as where the sample came from, its volume, and the accuracy required. The next step was to search the database for a similar sample and to use the same operating conditions. If the sample was not a quality control (QC) sample then a semi-quantitative analysis was performed to estimate the concentration of elements in the sample. A calibration methodology was selected based on the semi-quantitative scan data and on the user constraints. If the sample were a QC sample then a full analysis would be performed.

QUID Expert[63] was developed using the knowledge obtained from Mermet's[64] research on ICP-AES instrument diagnosis. This expert system required that a test standard solution be run. This solution contained the elements magnesium, barium, and

zinc. QUID Expert would identify problems related to the nebulizer, drift, energy transfer, sample transfer, and the optical components.

1.5 Application of Optimization Algorithms in ICP Spectrometry

The optimization of the operating conditions of an ICP spectrometer may improve accuracy and precision of results. In ICP-AES, there have been several studies of a single element Simplex optimization of the operating conditions[65-67]. Terblanche *et al.*[66] found that optimizing the instrument using the signal-to-background ratios of elements generated higher reproducibility in results compared to using their detection limits. Ebdon *et al.*[67] found the best operating conditions for use with different organic solvents. There have been several studies of multi-element optimizations in ICP-AES[68-70]. Many studies on optimization of ICP atomic emission spectrometers have been for the minimization of interference effects in difficult to analyze samples[68,70,71]. Recent studies[72-75] in optimization of ICP-MS have made use of the Simplex technique. Evans and Caruso[73] and Schmit and Chauvette[76] used the Simplex technique and demonstrated its applicability to the optimization of the ion lens voltages. Evans and Ebdon[77] and van der Velde-Koerts and de Boer[72] demonstrated the use of the Simplex technique in the optimization of the plasma operating parameters. All of these studies optimized the system for maximum analyte signal and minimum interferences. Ford *et al.*[78] used the Simplex technique for the optimization of the plasma parameters and the ion optics using signal-to-background ratios.

1.6 Toward Autonomous ICP Spectrometers

With advances in technology, analytical instruments can now produce enormous quantities of data in relatively short periods of time. Of all the data produced only a small select fraction is necessary. There is also concern that there is a shortage of skilled personnel to operate these instruments. Laboratories emphasize the importance of accuracy and precision thus putting pressure on the operators who are trying to select the best calibration methodology for the analyses. This results in a very difficult situation;

there are more samples hence higher throughput is required, which means more data for unskilled operators. The solution is to develop software that would handle the data intelligently.

The goal of the Autonomous Instrument Project is to relieve human operators of the burden of dealing with the flood of data and to assist in the decision-making process for more accurate and precise results. Originally, the concept behind the Autonomous Instrument was to build a complete system but this was not acceptable to manufacturers. It was then decided to break up the Autonomous Instrument into modules that could be, if desired, run independently. These modules could be combined to form a complete system that could operate without a human operator.

The Autonomous Instrument has evolved over the years to its present modular design (Figure 1.5). Although it looks like an integrated system, each component is a module that can stand alone; some of these modules contain smaller modules that can also be used on their own (Table 1.2). The first module consists of all the startup procedures particular to the instrument such as wavelength calibration, turning the plasma on and any other events that should occur in the initialization of the instrument. The second module is the Real Time Blank Diagnosis (RTBD) module. This module would be loaded immediately after startup and would be setup to run as a background process. It would analyze each blank solution run and would warn the user if there were a problem with the system. If the RTBD module has warned the user of a possible problem or at the user's request, QUID Expert may be used. QUID Expert[63] is a diagnostic module based on the research of J-M. Mermet *et al.*[64] This module runs a test solution and monitors several atomic and ionic lines. The information extracted from these lines allows the diagnosis of the major components of an inductively coupled plasma (ICP) system.

The three remaining modules deal with different types of analysis. The Quality Control (QC) module analyzes samples and verifies that they are all within specification using a pattern recognition component. The analysis of an unknown sample module is a large module, which contains smaller modules such as a pattern recognition module, a calibration methodology selection module, and a module predicting whether a sample would produce inaccurate results. The third type of analysis is Learning to Run New

Samples (LNS) which would also be a large module. It will contain optimization and methodology selection modules and is presently in the planning stage.

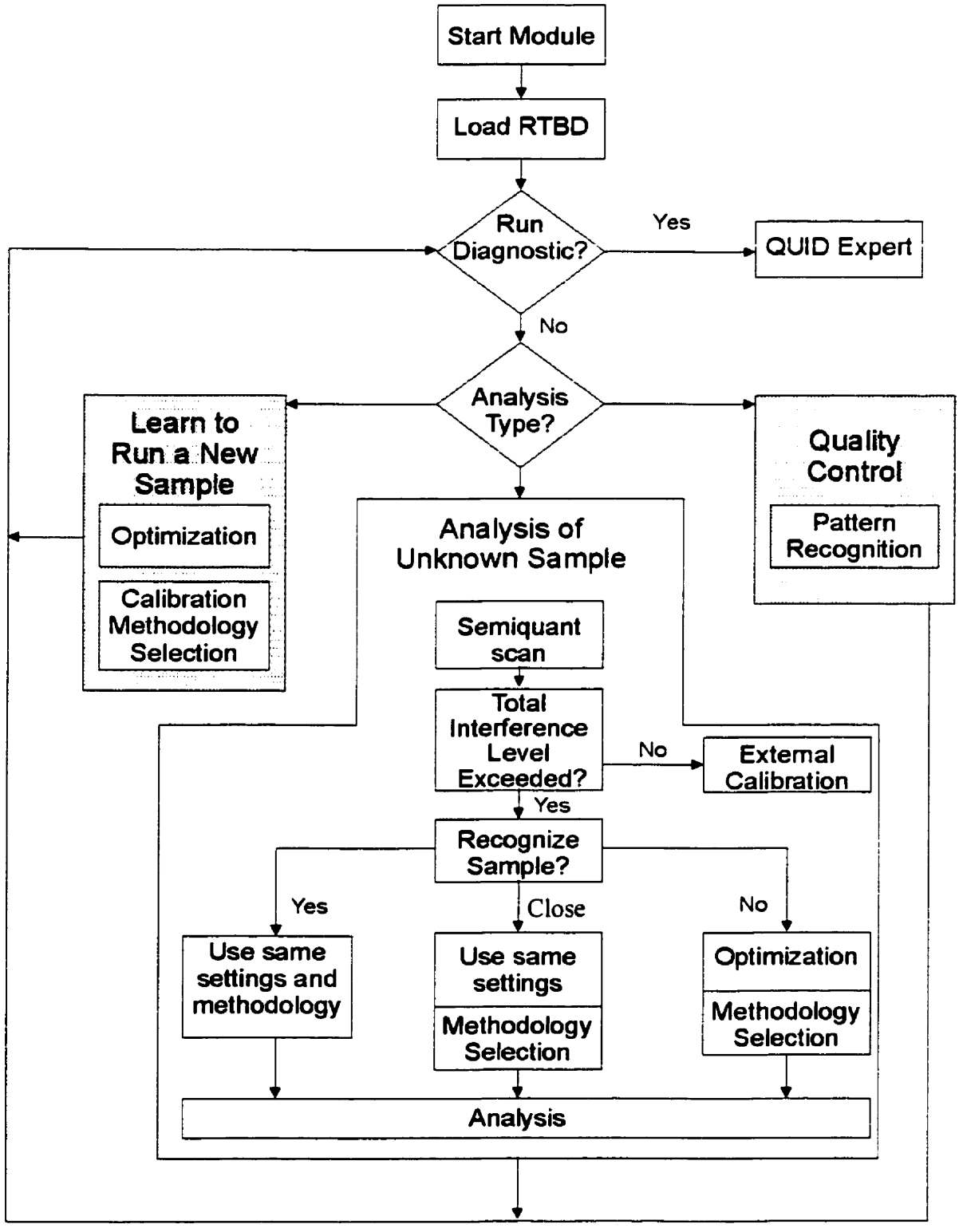

Figure 1.5 Diagram of the Autonomous Instrument system.

Table 1.2 Components of the Autonomous Instrument.

Major modules	Components
Real Time Blank Diagnosis module	Expert system
QUID Expert	Expert system
Analysis of unknown sample	Pattern recognition Optimization Methodology selection
Learn to run a new sample	Optimization Methodology selection
Quality control	Pattern recognition

1.7 Thesis Outline

Chapter 2 describes the development of a warning system which can diagnose an ICP-AES in real-time and decide whether a complete diagnosis should be performed.

Chapter 3 is an evaluation of three pattern recognition techniques for use in the Autonomous Instrument system.

Chapter 4 describes the development of an objective function for multi-element optimizations in ICP-AES.

Chapter 5 details studies on optimization of the ion optics in an ICP-MS which includes a comparison of objective functions and a comparison of single element and multi-element optimizations.

Chapter 6 describes the development of a system that can automatically select internal standards for analyses of analytes in difficult samples in ICP-MS.

Chapter 7 describes the work that remains to be done to complete the modules of the Autonomous Instrument.

1.8 Contributions to thesis

The author carried out the experimental work in Chapters 2, 3 and 4. The results of these chapters were submitted or published as the following manuscripts:

> "Inductively Coupled Plasma-Atomic Emission Spectrometer Warning Diagnosis Procedure Using Blank Solution Data", C. Sartoros and E.D. Salin, *Spectrochimica Acta*, 1998, 53B, 741.

> "Pattern Recognition for Sample Classification using Elemental Composition -Application for Inductively Coupled Plasma Atomic Emission Spectrometry", C. Sartoros and E.D. Salin, *J. Anal. At. Spectrom.*, 1997, 12, 827.

> "Comparison of Two Objective Functions for Optimization of Simultaneous Multi-Element Determinations in Inductively Coupled Plasma Spectrometry", C. Sartoros and E.D. Salin, *J. Anal. At. Spectrom.*, 1997, 12, 13.

Chapter 5 contains experimental work used to evaluate the application of Simplex optimization to the ion optics of an inductively coupled plasma mass spectrometer. The design of the experiments and the work carried out was done by a postdoctoral fellow, Dr. Douglas M. Goltz, and the author. This work was published as the following manuscript:

> "Program Considerations for Simplex Optimization of Ion lenses in ICP-MS", C. Sartoros, D.M. Goltz, and E.D. Salin, *Applied Spectroscopy*, 1998, 52, 643.

Chapter 6 contains experimental work to evaluate the use of a cluster analysis algorithm for the selection of internal standards in ICP-MS. This work has been accepted for publication as:

"Automatic Selection of Internal Standards in ICP-MS", C. Sartoros and E.D. Salin, *Spectrochimica Acta.*

Dr. E.D. Salin was available throughout and contributed helpful discussion and guidance regarding project direction, experimental planning and data interpretation.

1.9 References

1 Kattan, M., *AI Expert*, 9(4), 1994, 32.

2 Waterman, D.A., A Guide to Expert Systems, Addison-Wesley Publishing Company Inc., Massachusetts, 1986.

3 Michaelson, R.H., Michie, D., and Boulanger, A., "The Technology of Expert Systems", *BYTE*, 1985, 10(4), 303.

4 Buchanan, B.G. and Shortliffe, E.H., eds., Rule-Based Expert Systems: The MYCIN Experiments of the Stanford Heuristic Project, Addison-Wesley Series in Artificial Intelligence, Massachusetts, 1984.

5 Michie, D., ed., Introductory Readings in Expert Systems, Gordon and Breach Science Publishers, NY, 1982.

6 Bratko, I., PROLOG Programming for Artificial Intelligence, 2nd ed., Addison-Wesley Publishing Company, Singapore, 1990.

7 Firebaugh, M.W., Artificial Intelligence: A Knowledge-Based Approach., Boyd and Fraser, Boston, MA, 1988.

8 Kroschwitz, J.I., exec. Ed., Encyclopedia of Chemical Technology, Wiley Interscience, New York, 4th ed., 1991, 9, 1082.

9 Wade, A.P., Crouch, S.R., and Betteridge, D., *Trends Anal. Chem.*, 1988, 7, 358.

10 Yoon, Y. and Guimaraes, T., *Information and Management*, 1990, 24, 209.

11 Adams, M.J., Chemometrics in Analytical Spectroscopy, Royal Society of Chemistry, UK, 1995.

12 Salin, E.D. and Winston, P. H., *Anal. Chem.*, 1992, 64, 49A.

[13] Quinlan, J.R., C4.5 Algorithms for Machine Learning, Morgan Kaufmann Publishers, San Mateo, 1993.

[14] Hunt, E.B., Marin, J., and Stone, P.S., Experiments in Induction, Academic Press, NY, 1966.

[15] Michalewicz, Z., Genetic Algorithms + Data Structures = Evolution, 2nd ed., Springer-Verlag Berlin Heidelberg, 1994.

[16] Shaffer, R.E. and Small G.W., *Anal. Chem.*, 1997, 69, 236A.

[17] Nelder, J.A. and Mead, R., *Computer Journal*,1964, 7, 308.

[18] Lindsay, R.K., Buchanan, B.G., Feigenbaum, E.A., and Lederberg, J., Applications of Artificial Intelligence for Organic Chemistry: The DENDRAL Project, McGraw-Hill Advanced Computer Science Series, NY, 1980.

[19] Andreev, G., Argirov, O., and Penchev, P., *Anal. Chim. Acta*, 1993, 284(1), 131.

[20] Luinge, H.J., *Anal Proc.*, 1990, 2(10), 266.

[21] Jin, J.Y., Adams, M.J., and Sumiga, J.H, *Anal. Proc.*, 1993, 30(3), 169.

[22] Wythoff, B.J., Buck, C.F., and Tomellini, S.A., *Anal. Chim. Acta*, 1989, 217, 203.

[23] Harrington, P., Street, T., Voorhees, K., Radicati, F., and Odom, R., *Anal. Chem.*, 1989, 61, 715.

[24] Wehrens, L., Lucasius, C., Buydens, L., and Kateman, G., *Anal. Chim. Acta.*, 1993, 27(2), 313.

[25] Hong, H. and Xin, X., *Anal. Chim. Acta*, 1992, 262(1), 179.

[26] Moldveanu, S. and Rapson, C.A., *Anal. Chem.*, 1987, 59, 1207.

[27] Moore, D.S., White, J.S., and Harbin, B.A., *Anal. Chim. Acta.*, 1994, 294(1), 85.

[28] Scott, D.R., *Anal. Chim. Acta*, 1994, 285(1), 209.

[29] Scott, D.R., Levitsky, A., and Stein, S.E., *Anal. Chim. Acta*, 1993, 278(1), 137.

[30] Scott, D.R., *Anal. Chim. Acta*, 1992, 265(1), 43.

[31] Catasti, P., Carrara, E., and Nicoline, C., *J. Comput. Chem.*, 1990, 11, 805.

[32] Du, H., Lahiri, S., Huanh, G.S., and Stillman, M.J., *Anal. Chim. Acta*, 1994, 296(1), 21.

[33] Hasenoehrl, E.J., Perkins, J.H., and Griffiths, P.R., *Anal. Chem.*, 1992, 64(7), 705.

[34] Elling, J.W., Mniszewski, S.M., Zahrt, J.D., and Klatt, L.N., *J. Chromatogr. Sci.*, 1994, 32(6), 213.

[35] Van Leeuwen, J.A., Vandeginste, B.G.M., Kateman, G., Mulholland, M., and Cleland, A., *Anal. Chim. Acta*, 1990, 28(1), 145.

[36] Maris, F., Hindriks, R., Vink, J., Peeters, A., Vanden-Driessche, N., and Massart, L., *J. Chromatogr.*,1990, 506, 211.

[37] Bourguignon, B., Vankeerberghen, P., and Massart, D.L. *J Chromatogr.*, 1992, 592(1-2), 51.

[38] Shoenmakers, P.J., Peeters, A., and Lynch, R.J., *J. Chromatogr.*, 1990, 506, 169.

[39] Stauffer, S.T. and Dessy, R. E., *J. Chromatogr. Sci.*, 1994, 32(6), 228.

[40] Williams, S.S., *Trends Anal Chem.*, 1990, 9(2), 63.

[41] Buydens, L. Shoenmakers, P., Maris, F., and Hindriks, H., *Anal. Chim. Acta*, 1993, 272, 41.

[42] Ruisánchez, I., Larrechi, M.S., Rius, F.X., and Esteban, M., *Trends Anal. Chem.*, 1992, 11(4), 135.

[43] Esteban, M., Ruisánchez, I., Larrechi, M.S., and Rius, F.X., *Anal. Chim. Acta*, 1992, 268(1), 95.

[44] Esteban, M., Ruisánchez, I., Larrechi, M.S., and Rius, F.X., *Anal. Chim. Acta*, 1992, 268(1), 107.

[45] Esteban, M., Ariño, C., Ruisánchez, I., Larrechi, M.S., and Rius, F.X., *Anal. Chem. Acta*, 1994, 285(1), 193.

[46] Palys, M.J., Bos, M., and Van der Linden, W.E., *Anal. Chim. Acta*, 1993, 284(1), 107.

[47] Lahiri, S. and Stillman, M.J., *Anal. Chem.*, 1992, 64(4), 283A.

[48] Browett, W.R.L and Stillman, M.J., *Prog. Analyt. Spectrosc.*, 1989, 12, 73.

[49] Lahiri, S., Yuan, B., and Stillman, M.J., *Anal. Chem.*, 1994, 66, 2954.

[50] Zhu, Q. and Stillman, M.J., *J. Chem. Inf. Comput. Sci.*, 1996, 36, 497.

[51] Penninckx, W., Vankeerberghen, P., Massart, D.L., and Smeyers-Verbeke, J., *J. Anal. At. Spectrom.*, 1995, 10(3), 207.

[52] Arnold, T., Otto, M., and Wegschieder, W., *Talanta*, 1994, 41(7), 1169.

[53] Janssens, K. and Van Espen, P., *Anal. Chim. Acta*, 1986, 184, 117.

[54] Adler, B., Schütze, P., and Will, J., *Anal. Chim. Acta*, 1993, 271(2), 287.

[55] Brandt, J. and Hitzmann, B., *Anal. Chim. Acta*, 1994, 291(1-2), 29.

[56] Borsier, M., *Spectrochim. Acta Rev.*, 1991, 14(1), 79.

[57] Pomeroy, R.S., Kolczynski, J.D., and Denton, M.B., *Appl. Spectrosc.*, 1991, 45(7), 1111.

[58] Pomeroy, R.S., Kolczynski, J.D., and Denton, M.B., *Appl. Spectrosc.*, 1991, 45, 198.

[59] Webb, D.P. and Salin E.D., *J. Anal. At. Spectrom.*, 1989, 4, 793.

[60] Yang, P., Ying, H., Wang, X., and Huang, B., *Spectrochim. Acta*, 1996, 51B, 877.

[61] Yang, P., Ying, H., Wang, X., and Huang, B., *Spectrochim. Acta*, 1996, 51B, 889.

[62] Webb, D.P., Hamier, J, and Salin E.D., *Trends Anal. Chem.*, 1994, 13, 44.

[63] Sartoros, C., Alary, J-F, Salin, E.D., and Mermet, J.-M., *Spectrochim. Acta*, 1997, 52B, 1923.

[64] Poussel, E. and Mermet, J.M., *Spectrochim. Acta*, 1993, 48B, 743, and references therein.

[65] Edbon, L., Cave, M.R., and Mowthorpe, D.J., *Anal. Chim. Acta*, 1980, 115, 179.

[66] Terblanche, S.P., Visser, K., and Zeeman, P.B., *Spectrochim. Acta*, 1981, 36B, 293.

[67] Ebdon, L., Evans, E.H., and Barnett, N.W., *J. Anal. At. Spectrom.*, 1989, 4, 505.

[68] Moore, G.L., Humphries-Cuff, P.J., and Watson, A.E., *Spectrochim. Acta.*, 1984, 39B, 915.

[69] Leary, J.J., Brookes, A.E., Dorrzaff, A.F., Jr., and Golightly, D.W., *Appl. Spectrosc.*, 1982, 36, 37.

[70] Kalivas, J.H., *Appl. Spectrosc.*, 1987, 41, 1338.

[71] Belchamber, R.M., Betteridge, D., Wade, A.P., Cruickshank, A.J., and Davison, P., *Spectrochim. Acta*, 1986, 41B, 503.

[72] van der Velde-Koerts, T., and de Boer, J.L.M., *J. Anal. At. Spectrom.*, 1994, 9, 1093.

[73] Evans, E.H., and Caruso, J.A., *Spectrochim. Acta*, 1992, 47B, 1001.

[74] Schmit, J.P., and Chauvette, A., *J. Anal. At. Spectrom.*, 1989, 4, 755.

[75] Evans, E.H., and Ebdon, L., *J. Anal. At. Spectrom.*, 1991, 6, 421.

[76] Schmit, J.P., and Chauvette, A., *J. Anal. At. Spectrom.*, 1989, 4, 755.

[77] Evans, E.H., and Ebdon, L., *J. Anal. At. Spectrom.*, 1991, 6, 421.

[78] Ford, M.J., Ebdon, L., Hutton, R.C., and Hill, S.J., *Anal. Chim. Acta*, 1994, 285, 23.

Chapter 2

Prior to performing any analysis, it is important for the Autonomous Instrument to know that the instrument is working properly. The Autonomous Instrument should have the capability to identify malfunctions that may occur, determine the possible causes of these malfunctions and suggest possible remedies. A complete diagnostic procedure is implemented in the module QUID Expert. This module can diagnose malfunctions in all the major components of an ICP-AES using a standard test solution. The standard test solution must be reproducible and run on a regular basis, which could be time consuming.

The question is "when should this solution be run?". The simplest answer is "when the instrument begins operation". Unfortunately, the instrument may run for many hours and would not know if a malfunction had occurred during its operation. The Real Time Blank Diagnosis (RTBD) module has been added to the Autonomous Instrument as a warning system. This module uses a blank solution to monitor the instrument during its operation. A feedback loop is used to warn the Autonomous Instrument of a possible malfunction. This module will alert the Autonomous Instrument of the need to run the QUID Expert module. This chapter describes the RTBD module. This work was published in Spectrochim. Acta., 1998, 53B, 741

2 Inductively Coupled Plasma-Atomic Emission Spectrometer Warning Diagnosis Procedure Using Blank Solution Data

2.1 Abstract

Lines available while running a blank solution were used to monitor the analytical performance of an inductively coupled plasma atomic emission spectrometry (ICP-AES) system in real time. Using H and Ar lines and their signal-to-background ratios (SBRs), simple rules in the form of a prediction table were developed by inspection of the data. These rules could be used for predicting changes in RF power, carrier gas flow rates, and sample introduction rate. The performance of the prediction table was good but not excellent. Another set of rules in the form of a decision tree was developed in an automated fashion using the C4.5 induction engine. Performance of the decision tree was superior to that of the prediction table. It appears that blank spectral information can be used to predict with over 90% accuracy when an ICP-AES is breaking down, however it is not as definitive at identifying the exact fault as some more exhaustive approaches involving the use of standard solutions.

2.2 Introduction

Inductively coupled plasma atomic emission spectrometer (ICP-AES) systems are now automated such that they can easily run for long periods with less experienced operators. The high data throughput and operator level suggest the quality of the data obtained can be somewhat questionable. An essential module that is absent in these automated instruments is a self-diagnosing procedure which would warn the operator when there was a malfunction in one of its components. The software provided with instruments does notify the user of major malfunctions such as loss of gas pressure, plasma off, or communication failure between computer and instrument, but it will not tell the user of more subtle failures such as nebulizer blockage, optics degradation, gas pressure reduction, *etc.* Mermet and his colleagues have been able to identify problems in ICP-AES instruments by devising several simple experiments that can evaluate the performance of an ICP sequential system[1]. These experiments use a standard test solution containing 5 ppm of barium, magnesium, and zinc, and monitor seven atomic and ionic lines including those of argon. The information extracted from the measurements of a line profile, absolute line intensities, relative standard deviation (RSD) of intensities, signal-to-background ratios (SBRs), and ionic to atomic line intensity ratios, allows diagnosis of the major components of an ICP system including the optics, the sample introduction system, the generator, and the detector. While the tests are easy to perform, the interpretation of the data could be difficult for an inexperienced operator. To overcome this problem an expert system called QUID Expert was developed[2]. The program was developed to run in the Windows™ environment so that it runs concurrently with most manufacturers' software. QUID Expert is based on Mermet's work and uses the information obtained from the ionic and atomic lines in a series of rules, some of which use statistics, to determine when the spectrometer's performance is degrading and where the probable fault lies. QUID Expert appears to be a useful tool when the instrument's performance is of utmost importance.

A drawback of QUID Expert is that a standard test solution must be run on a regular basis or whenever a problem is suspected. Excessive use of the test solution can

decrease throughput of the system while sparse use can allow degradation to be unnoticed. With this in mind, we decided to develop a procedure which would identify potential problems during normal instrument operation. The purpose of this application would not be to pinpoint the malfunction, as QUID Expert does, but to operate as an early warning system. When a malfunction is detected, one would run QUID Expert to verify the malfunction and determine its cause(s). The best way to maintain throughput is to use a solution that is run on the instrument on a regular basis: the blank. It is the single solution that will normally be run multiple times and periodically on the instrument. Using the blank solution does not increase the analytical cost since it must be run anyway. The information that would be available in an aqueous acid blank would be accrued from the hydrogen lines, the argon lines, and the background signal (Table 2.1). The Ar I 404 nm line and two background positions were selected for this study since they were used in QUID Expert for several of the tests. The four most prominent hydrogen lines were selected since they are related to the water input through the sample introduction system[3]. The major components of the instrument emphasized in this study were the generator and torch (energy transfer) and the sample introduction system (nebulizer gas rate, nebulizer efficiency, nebulizer precision) since these components are more subject to rapid degradation than the optics.

Rules were generated to predict the instrument's behavior based on information obtained from line intensities, RSD of intensities, and SBRs. Using these figures of merit and the line intensities, trends were studied to develop a system for predicting possible instrument failure using only the blank solution data. Performance was also compared to that provided by the QUID Expert tests using a standard test solution.

Table 2.1 Observed lines or zones in blank solution.

Line	Wavelength (nm)
Ar I	355.431
Ar I	404.442
Ar I	549.587
Ar I	750.387
Ar I	811.531
H I	410.174
H I	434.097
H I	486.133
H I	656.279
Background	200
Background	400

2.3 Experiments and Discussion

2.3.1 General Experiment Information

A Thermo Jarrell Ash Model 25 scanning spectrometer was used in this study with a cross-flow nebulizer attached to a peristaltic pump. All the instrument functions are automated and controlled by an independent computer via an RS-232 port. The solutions used for the first set of experiments were distilled and deionized water, 5% nitric acid blank solution, and the standard test solution used by QUID Expert[2] which consists of 5 ppm of Ba, Mg, and Zn, prepared from Fisher (Pittsburgh, PA) certified 1000 ppm standard solutions, in 5% reagent grade nitric acid (lines listed in Table 2.2). The experiments were performed under the operating conditions listed in Table 2.3. For each solution, three operating parameters, RF power, sample introduction rate (feed rate), and nebulizer gas pressure, were varied (Table 2.3) one at a time while holding all other operating parameters constant thereby generating fifteen different data sets. A single reading of the total signal and one of its background signal were recorded for each of the lines studied (Table 2.1 and Table 2.2, in their respective solutions) at each subset of

operating conditions. The relative intensities were determined with 100 assigned to the standard setting.

Table 2.2 Spectral lines or zones used in QUID Expert solution.

Lines	Wavelength (nm)
Ar I	404.442
Ba II	455.403
Zn II	206.200
Mg II	280.270
Mg I	285.213
Background	200
Background	400

Table 2.3 Instrument parameter settings.

Standard operating conditions used in first set of experiments.	
Operating parameters	*Setting*
RF power	1150 W
Sample introduction rate	0.9 ml/min
Nebulizer gas pressure	0.39 l/min (30 psi)
Integration time	5 sec x 4 repeats
Observation height	15 mm ATOLC (above the top of the load coil)
Operating conditions used and being varied.	
Operating parameters	*Variations in setting*
RF power	750W, 950W, 1150W, 1350W, 1550W, 1750W
Sample introduction rate	0.3, 0.5, 0.8, 1.6, 2.4, 3.1 ml/min
Nebulizer gas pressure	0.28, 0.39, 0.48 l/min (20, 30, 40 psi, respectively)

2.3.2 General Observations

Based on the information obtained with the blank solutions, trends for each line were observed for the variations in operating parameters. The trends are listed as an increase or decrease corresponding to the variation and whether this trend is linear (Tables 2.4 to 2.6). A trend was considered linear if a linear regression produced an r squared greater

than 0.90. A trend was considered almost linear if the linear regression produced an r squared greater than 0.80.

2.3.2.1 Observations: Emission lines as a function of power

Upon examination of the relative line intensities in the blank solutions as a function of power (Table 2.4), it can be seen that the relative line intensities of all the Ar lines increased linearly with increasing power. The relative line intensities of the H lines were seen to increase to a plateau with the sole exception of H (656.279 nm) which simply increased. According to Boumans[4], the intensities of hard atomic and ionic lines initially increase sharply with power and do not reach their maxima in the range of 800W to 2200W. Boumans also observed that soft atomic lines have maxima at the lower end of the power range whereas the ionic lines approach their maxima in the middle of the range. If we take the definition of "soft" lines to be atomic lines of elements with a low to medium ionization potential (≤ 8 eV) and ionic lines of elements with a low second ionization potential and "hard" lines to be all other elements[4], then both the H line and Ar line are hard lines. However, the H line seems to exhibit soft line characteristics when varying the RF power. Considering the relative SBRs of the Ar lines as a function of power, only Ar (549.587 nm) performs in a predictable fashion, decreasing linearly with increasing power. All the H lines exhibit similar decreasing trends (Table 2.4). This results because an increase in power causes the background signal to increase more rapidly than the net signal[4].

Table 2.4 Trends observed while increasing the power setting.

Lines	H_2O (Signal)		SBR H_2O		HNO_3 (Signal)		SBR HNO_3	
Ar 3554	+	L	+/-	N	+	L	+/-	N
Ar 7503	+	L	+/-	N	+	L	+/-	N
Ar 4044	+	L	+/-	N	+	L	+/-	N
Ar 8115	+	L	+/-	N	+	L	+/-	N
Ar 5495	+	L	-	L	+	L	-	L
H 6562	+	L	-	L	+	L	-	AL
H 4101	+	N	-	N	+	N	-	N
H 4340	+	N	-	N	+	N	-	N
H 4861	+/-	N	-	N	+	N	-	N
400 nm	+	AL			+	AL		
200 nm	+	AL			+	AL		
400 nm / 200 nm	+/-	N			+/-	N		

+ increase
- decrease
+/- increase then decrease
L linear
AL almost linear
N Nonlinear

Table 2.5 Trends observed while increasing the sample introduction rate up to 1.6 ml/min.

Lines	H_2O (Signal)		SBR H_2O		HNO_3 (Signal)		SBR HNO_3	
Ar 3554	-/+	N	=	N	-/+	N	=	N
Ar 7503	-	N	=	N	-	N	-/=	N
Ar 4044	-	N	=	N	-	N	=	L
Ar 8115	-	N	=	N	-/=	N	+/=	N
Ar 5495	-	N	=	N	-	N	=	N
H 6562	+	N	=	N	+/=	N	+	N
H 4101	+	N	+	N	+/=	N	+	N
H 4340	+	N	+	N	+	N	+	N
H 4861	+	N	+	N	+/=	N	+	N
400 nm	-	N			-/+	N		
200 nm	=	N			-/+	N		
400 nm / 200 nm	-/+	N			-/+	N		

+ increase
- decrease
+/- increase then decrease
-/+ decrease then increase
= relative stable
L linear
N Nonlinear

Table 2.6 Trends observed while increasing the nebulizer gas pressure.

Lines	H_2O (Signal)		SBR H_2O		HNO_3 (Signal)		SBR HNO_3	
Ar 3554	-	L	+	N	-	L	+/-	N
Ar 7503	-	L	-	L	-	L	+	N
Ar 4044	-	L	+/-	N	-	L	+/-	N
Ar 8115	-	L	-	N	-	L	+/-	N
Ar 5495	-	L	+	L	-	L	+	L
H 6562	+	N	+	N	+/- or =	N	+/-	N
H 4101	+	N	+	N	+	L	+	L
H 4340	+	L	+	L	+	L	+	L
H 4861	+	L	+	N	+	L	+	L
400 nm	-	L			-	L		
200 nm	-	L			-	L		
400 nm / 200 nm	-	N			+/-	N		

+ increase
- decrease
+/- increase then decrease
L linear
N Nonlinear

2.3.2.2 Observations: Emission lines as a function of feed rate

If one considers the relative line intensities as a function of feed rate (e.g., Figure 2.1a), one observes that all the lines exhibit a specific trend until 1.6 ml/min. where there is a noticeable break. When using QUID Expert, one verifies nebulizer efficiency by monitoring the SBR of Mg (285.213 nm). Examining the plot of the SBR of Mg as a function of feed rate (Figure 2.1b), one observes that the trend is also broken at a feed rate of 1.6 ml/min. This would lead us to believe that the maximal aspirating rate of the nebulizer used in our experiment is around the 1.6 ml/min mark. According to Thompson[5], increasing the solution uptake beyond the "free-uptake" level by pumping produces a slight decrease in signal intensity. Therefore, when determining trends as a function of feed rate, only feed rates under 1.6 ml/min were considered. From Table 2.5, it can be seen that all the H lines increase with feed rate whereas all the Ar lines decrease due to the loss of available power. The relative SBRs as a function of feed rate reveal that most of the Ar lines can be considered constant and that the relative SBR of the H lines increases with feed rate (Table 2.5).

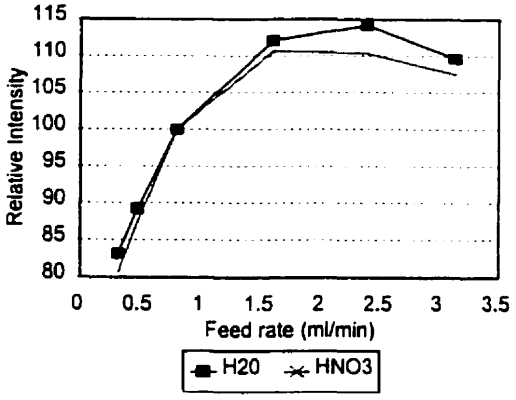

Figure 2.1(a) Relative intensity of the H line (486.133 nm) in both water and 5% nitric acid as the sample introduction rate is varied.

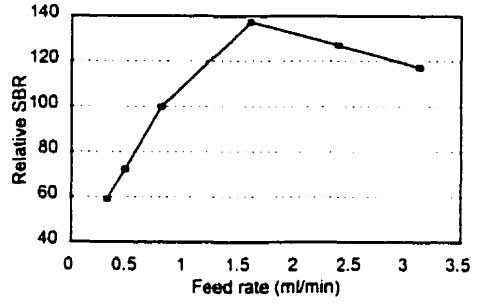

Figure 2.1(b) Relative signal-to-background ratio of Mg (285.213 nm) in the QUID test solution as the sample introduction rate is varied.

2.3.2.3 Observations: Emission lines as a function of nebulizer gas flow rate

The relative line intensities as a function of nebulizer gas pressure (Table 2.6) reveal that the H lines increase linearly whereas the Ar lines decrease linearly. Boumans found that the intensities of soft lines increase with carrier gas flow while hard lines decrease[4]. Again, H behaves like a soft line and Ar behaves like a hard line. Looking at the SBRs as a function of nebulizer gas pressure it can be seen that most H lines increase linearly whereas those of Ar could go either way (Table 2.6). Boumans found that a high carrier gas flow favors the SBRs of soft lines[4] which seems to be the case with H. Inspecting all

of the trends of the lines investigated, it was determined that the H (486.133 nm) line and the Ar (549.587 nm) line would be used for further studies.

2.3.3 Prediction Table Generation and Results

Upon examination of the trends (Tables 2.4 to 2.6), two lines, the H Beta line (486.133 nm) and the Ar (549.587 nm) line, were selected as providing adequate information to formulate general trends. Using the line intensities and SBRs of these two lines, a prediction table was generated (Table 2.7) by inspection. This could easily translate into a decision tree however, for our purposes, the prediction table will be used.

Table 2.7 Prediction table.

Variation	Ar	SBR Ar	H	SBR H
Power -	-	+	-	+
+	+	-	+	-
Sample introduction -	+	=	-	-
+	-	=	+	+
Nebulizer gas -	+	-	-	-
+	-	+	+	+
No variations =	=	=	=	=

+ increase
- decrease
= reasonably stable

Five experiments were performed to ascertain the validity of the prediction table. The experiments were performed using only the 5% nitric acid blank solution. All five experiments were carried out using the same operating conditions (Table 2.3). For these experiments, various initial operating settings for the RF power, the sample introduction rate, and the nebulizer gas pressure, were selected. Ten readings of the total signal and background signal were recorded for each of two lines, H (486.133 nm) and Ar (549.587 nm). The mean and standard deviation of the line intensities and the SBRs were calculated. Following this, a single parameter was varied and, once the data was recorded, the line intensities and SBRs were calculated.

In determining whether there was a change in the system, a value was assigned to one of three states: stable (constant), increase, or decrease. A stable evaluation resulted in a prediction that there was no problem identified in the system. In some cases the

system predicted a problem but not the correct one. This would warn the user that there was a problem, but it would be misleading as to the nature of the problem if no further experiments were done. The two misclassified problems in Experiment 1 of Table 2.8 were caused by increases in power. Due to the parabolic nature of the line intensity of H as a function of power, if one sits at the top of the curve an increase in power will not give an increase in the line intensity as stated in the prediction table, but will produce a decrease. This same problem was observed in all of the other experiments (Experiments 2 and 5) with the last two being the most severe. A high power setting was chosen as an initial operating condition rather than the more common values (Table 2.3) used for generating the prediction table. Not surprisingly, this resulted in errors being produced when decreasing the power. In this case, the prediction table does not always predict that there is a change in power, however it will state that there is a problem and identify it incorrectly as a change in nebulizer gas pressure. This is still an acceptable situation since, by detecting a problem, it will recommend that further diagnostics be run, which could correctly identify the situation as an energy transfer problem. The only other problems observed were in Experiments 2 to 4 where small (and occasionally large) increases in feed rate were often within one standard deviation of the average. This suggests that this method was not sensitive enough to monitor small changes in nebulization and perhaps that small changes in feed rate are not critical to nebulizer performance.

Table 2.8 Diagnosis of problems using prediction table

Exp.	**Initial Settings**			**Number of tests**	**Correct predictions**	**Predicted other problem**	**Predicted no problem**
	Power (W)	Sample introduction (ml/min)	Nebulizer gas (l/min)				
1	1150	0.9	0.39	28	22	5	1
2	1150	1.2	0.39	10	5	3	2
3	1350	1.0	0.39	10	4	4	2
4	1550	0.9	0.39	10	4	3	3
5	1550	0.9	0.39	7	4	2	1
Total				65	39	17	9

2.3.4 Inductive Learning Generated Decision Tree

The results obtained using the prediction table were not as good as we had hoped especially when it came to changes in power. In order to evaluate an automated rather than manual method of selecting evaluation criteria, we extracted rules from the information using inductive learning, an algorithm used to automatically generate rule-based expert systems[6]. We generated a decision tree using the C4.5 induction engine developed by Quinlan[7]. The resulting decision tree is provided in Figure 2.2.

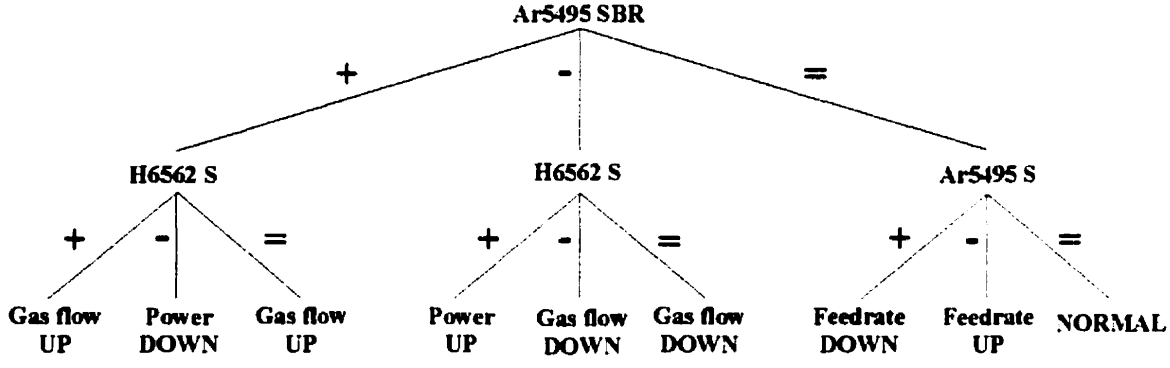

Figure 2.2 Flowchart of decision tree generated by the C4.5 induction engine.

Twelve experiments were performed to see how well this decision tree classified system malfunctions. The two lines used by the decision tree for its classification were H (656.279 nm) and Ar (549.587 nm). These experiments were exactly like those done for the prediction table except that a different hydrogen line was selected by the C4.5 algorithm. For these experiments, various initial operating settings for the RF power, the sample introduction rate, and the nebulizer gas pressure, were selected. Ten readings of the total signal and background signal were recorded for each of two lines, H (656.279 nm) and Ar (549.587 nm). Following this, one of the three parameters was varied, and a single reading of the total and background signal was recorded for each of the two lines. The results are listed in Table 2.9.

Table 2.9 Diagnosis of problems using a C4.5 generated decision tree

Exp.	Initial Settings			Number of tests	Correct predictions	Predicted other problem	Predicted no problem
	Power (W)	Sample introduction (ml/min)	Nebulizer gas (l/min)				
1	1550	0.4	0.39	8	7	0	1
2	1150	0.8	0.28	8	6	1	1
3	750	1.6	0.43	9	5	3	1
4	750	0.4	0.28	8	7	1	0
5	950	0.6	0.39	8	7	1	0
6	1150	0.9	0.48	8	7	1	0
7	1350	1.6	0.39	8	6	1	1
8	1550	1.6	0.28	10	8	1	1
9	750	0.8	0.48	10	5	5	0
10	1150	0.9	0.39	10	10	0	0
11	1350	0.5	0.33	10	8	2	0
12	950	1.2	0.43	10	5	3	2
Total				107	81	19	7

Most of the errors seen in the results (Table 2.9) arose during changes of the feed rate. Some of the changes in the H and Ar signals were so small that the situation was considered normal even though there had been a change in feed rate. Another problem was observed in predicting a change in nebulizer gas pressure. This problem was seen mostly in Experiments 3, 9, and 12 of Table 2.9. These results all have in common that they were obtained using low power and high nebulizer gas pressure. Once again, it should be noted that the initial information about the trends of the three operating parameters was obtained using different operating conditions (Table 2.3). These are "standard conditions" (in the middle of the range of settings) and may not apply to extreme starting conditions such as those with low power and high nebulizer pressure.

If the results from the prediction table (Table 2.8) and those of the decision tree (Table 2.9) are examined side-by-side, it can be seen that the decision tree classified more malfunctions correctly (~75%) than the prediction table (~60%). Both were good at noting that there was a change. The prediction table correctly caught changes 86% of the time while the inductive system caught changes 93% of the time.

2.3.5 Nebulizer malfunctions

The nebulizer is an important part of the instrument and malfunctions can occur from plugging of the nebulizer to air bubbles in the pump tubing. Simulation of these problems was performed with an external peristaltic pump controlled by computer. The pump could be pulsed at various frequencies to simulate poor precision. The sample introduction rate was held constant at 0.8 ml/min. The two solutions used for these experiments were the 5% nitric acid blank solution and the standard QUID Expert test solution. The RSD of ten readings of the background subtracted intensity of Mg (285.213 nm) was recorded as a function of integration time (Figure 2.3). The RSD of the line intensities was plotted against integration time for both Mg (285.213 nm), which is in the standard QUID Expert test solution, and H (486.133 nm) from the nitric acid blank solution (Figure 2.3). From Figure 2.3 it was determined that both the RSD of the intensity of Mg in the QUID Expert solution and that of H in the nitric acid solution did not show any particular trend as a function of integration time. The pump was then pulsed at various frequencies with a duty cycle of 50% while an instrument integration time of 10 seconds was used (Figure 2.4). The RSD of ten readings of the background subtracted intensity of Mg was recorded for each pulsing frequency. This same procedure was repeated for the H line (486.133 nm) in the nitric acid blank solution. Since the variations were observed between 0 and 1 Hz for Mg, the pulsing for the H experiment was kept within this range. By introducing a pulsing frequency (Figure 2.4), the RSD's of the line intensities for both Mg and H increased with lower pulsing frequencies as one would expect. From these plots it can be seen that the line intensity of Mg is more sensitive to these fluctuations than that of H although the RSD of the line intensity of H could still provide an excellent indication of nebulizer precision degradation.

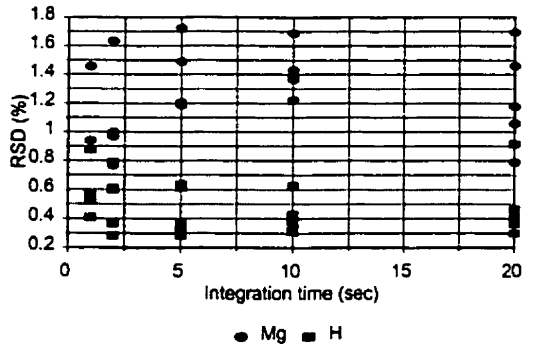

Figure 2.3 Relative standard deviation of Mg (285.213 nm) in the QUID test solution and H (486.133 nm) in 5% nitric acid observed while varying the integration time.

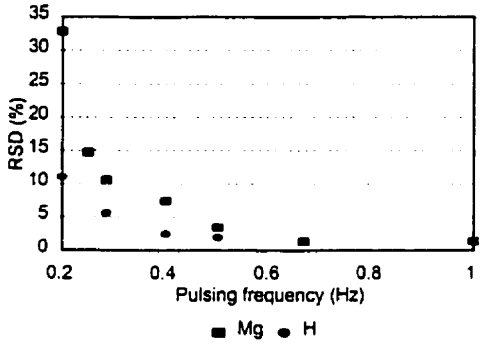

Figure 2.4 Relative standard deviation of Mg (285.213 nm) in the QUID test solution and H (486.133 nm) in 5% nitric acid observed while varying the pulsing frequency at a constant integration time of ten seconds.

Another experiment used a tube on the external pump to introduce air into the system through a T-joint. The pump feed rate was held constant at 0.8 ml/min. and an integration time of 10 sec was used. Line intensities and background signals were recorded for both H and Ar as a function of time. Several readings were taken prior to the introduction of air bubbles so that the line could be used as a reference. The relative line intensity of H, the relative SBR of H, and the RSD of line intensities of H were plotted against time (Figure 2.5). Examining Figure 2.5, in all three plots it can be seen when the air bubbles were introduced into the system both the line intensity and the SBR of H decrease and the RSD of the line intensity of H increases. A following experiment

allowed the pump to run dry (i.e., to run out of nitric acid solution) at 0.8 ml/min (Figure 2.6a). Line intensities and background signals were recorded (integration time of 5 sec) for both H (486.133 nm) and Ar (549.587 nm) starting with a few milliliters of nitric acid solution and continuing until there were no further variations of the signals after the solution was depleted. The relative line intensity and relative SBR of H were plotted against time (Figure 2.6b). When left to run dry (Figure 2.6b) the line intensity and the SBR of H decrease as expected.

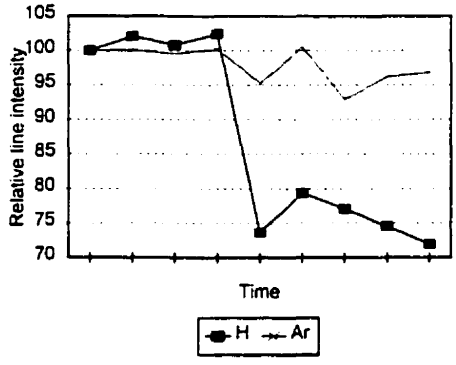

Figure 2.5(a) Monitoring of the relative intensity of both H, in 5% nitric acid, and Ar with the introduction of air bubbles (at the fifth time interval).

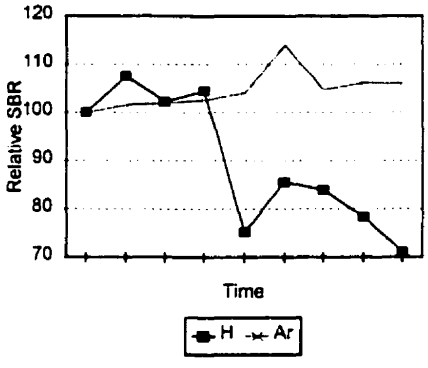

Figure 2.5(b) Monitoring of the relative SBR of both H, in 5% nitric acid, and Ar with the introduction of air bubbles (at the fifth time interval).

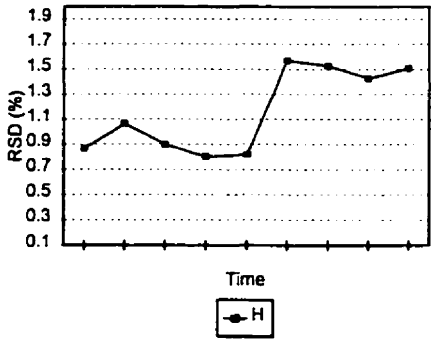

Figure 2.5(c) Monitoring of the RSD of H, in 5% nitric acid, with the introduction of air bubbles (at the fifth time interval).

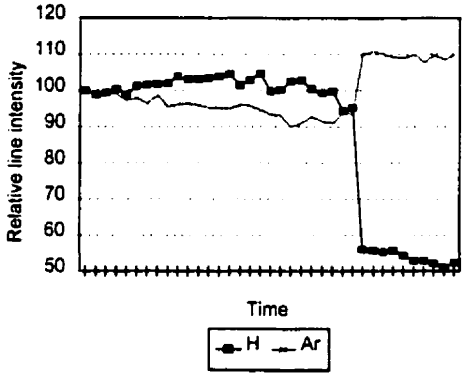

Figure 2.6(a) Monitoring of the relative intensity of both H, in 5% nitric acid, and Ar as the solution finishes.

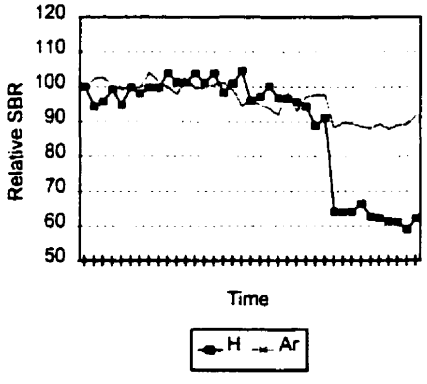

Figure 2.6(b) Monitoring of the relative SBR of both H, in 5% nitric acid, and Ar as the solution finishes.

By monitoring the H line, the diagnostic procedure can identify if there has been a change in the nebulization system.

2.4 Conclusion

It appears that information available in a blank spectrum can be used to predict instrument degradation with a success rate of 93% when using a scheme predicted automatically by the C4.5 induction algorithm. This performance was superior to the 86% obtained with a manually developed algorithm. The C4.5 system had a correct fault prediction rate of 76% as compared to 60% with the manually developed system. Either system provides a good immediate warning. The accuracy of the prediction can be enhanced by the use of QUID Expert with its solution. Hydrogen lines can be used to monitor nebulizer degradation and certain errors in the feed system. In general, real time system monitoring seems viable using only blank solution information.

2.5 References

1 Poussel, E. and Mermet, J.M., *Spectrochim. Acta*, 1993, 48B, 743, and references therein.

2 Eric D. Salin, Jean-Francois Alary, Christine Sartoros, and Jean-Michel Mermet, ICP-AES System Diagnosis using QUID, 1996 Winter Conference on Plasma Spectrochemistry, Fort Lauderdale, Florida, January 7-13, 1996.

3 Botto, R.I., *Spectrochim. Acta*, , 1985, 40B, 397.

4 Boumans, P.W.J.M., ed., Inductively Coupled Plasma Emission Spectroscopy Part I: Methodology, Instrumentation, and Performance, (Wiley-Interscience Publication, New York, 1987).

5 Thompson, M., "Operating Conditions and Analytical Performance", Inductively Coupled Plasmas in Analytical Atomic Spectrometry, A. Montaser and D.W. Golightly, ed., Chap. 5.2 (VCH Publishers Inc.,New York, 1992).

6 Salin, E.D., and Winston, P.H., *Anal. Chem.*, 1992, 64(1) 49A.

7 Quinlan, J. R., C4.5 Algorithms for Machine Learning (Morgan Kaufmann Publishers, San Mateo, 1993).

Chapter 3

The Autonomous Instrument must have the ability to recognize patterns. Several modules require this capability. In the Quality Control module, pattern matching is used to monitor the samples such that any sample, which is found different, will be identified when it is flagged. The pattern recognition algorithm is also used in the modules Learning to Run a New Sample and Analysis of an Unknown Sample. In both these modules, pattern recognition is used to find a sample in the database that is similar to the one of interest. Along with a qualitative and quantitative description of samples, the database includes the instrument operating conditions and the calibration methodology used to analyze each sample. If a similar sample is found in the database, the instrument operating conditions and calibration methodology is used as a starting point for the analyses of the sample of interest.

The first attempt at pattern recognition in our laboratory was done on a data set of reference materials that ranged from biological to geological samples. Using various standard deviations, data was generated from the original mean values of concentrations. The results obtained on this simulated data were good but several remarks were made by other researchers. The first was on the data: it was not real data obtained in a laboratory and therefore did not typify a common laboratory situation. The second remark was that working with a complete database is not common, especially when setting up an instrument. When the Autonomous Instrument is first installed it will begin with an empty database or a very small database (unless data could be shared among instruments). This chapter takes a closer look at the pattern recognition module. It specifically evaluates several candidate techniques for use in ICP-AES. This chapter was published in J. Anal. At. Spectrom., 1997, 12, 827.

3 Pattern Recognition for Sample Classification using Elemental Composition -Application for Inductively Coupled Plasma Atomic Emission Spectrometry

3.1 Abstract

Three pattern recognition techniques were investigated as tools for automatic recognition of samples: *k*-Nearest Neighbors, Bayesian Classification and the C4.5 inductive learning algorithm. Their abilities to classify 20 geological reference materials were compared. Each training and test example used 13 elemental concentrations. The data set was composed of 2582 examples obtained from CANMET in the form of results of analyses performed on these reference materials by different laboratories. It was found that all three pattern recognition techniques performed extremely well with a large data set of real samples. Bayesian Classification and *k*-Nearest Neighbors worked very well with small data sets.

3.2 Introduction

The Autonomous Instrument Project involves developing software and methodologies which allow instruments to run 'intelligently' with an absolute minimum of supervision[1-4]. One characteristic of the ideal autonomous instrument would be the ability to classify samples. The classification can be used for two purposes: (1) selecting operating conditions and calibration methodology (e.g., internal standards, standard additions), and (2) identification of the sample (e.g., 440 stainless steel). The first case consists of (a) performing a preliminary analysis (a semi-quantitative scan), (b) recognizing that the apparent elemental composition is similar to a sample class that has been successfully run with the use of a certain methodology and (c) adopting the same methodology[3]. The second case consists of (a) performing a preliminary analysis, and (b) finding an exact (or very close) match in the sample database using the apparent elemental composition of the sample. In a recent paper,[3] we evaluated the potential of several numeric processing techniques for the identification of samples. A wide variety of reference materials were selected, ranging from clinical through botanical to geological, using their reported elemental concentrations and relative standard deviations to generate validation (test) sets and training sets. The pattern recognition techniques that were used were *k*-Nearest Neighbors (*k*NN)[5], Bayesian classification[6] and Inductive Learning[7,8]. These three techniques were described in some detail[3]. The reference materials used to study the three pattern recognition techniques were dissimilar and would not have posed as much of a problem as in a study in which the materials were similar. In addition, the data was not 'real' in the sense that the standard deviations were not obtained experimentally but were fabricated as described. In this study, geological reference material data was used for test and training sets in the comparison of the three pattern recognition techniques. These geological materials were much more similar than those in the previous study and consequently provide a much more rigorous test of the possibility of using pattern recognition with elemental concentrations for automatic sample identification.

3.3 Experimental

The general method for classifying samples is illustrated in Figure 3.1. The pattern recognition technique is applied to a set of examples, the training set, to develop classification rules. These rules are then tested using another set of examples, the test set. The sample types of the examples in the test set are known and used to evaluate the performance of the classification techniques.

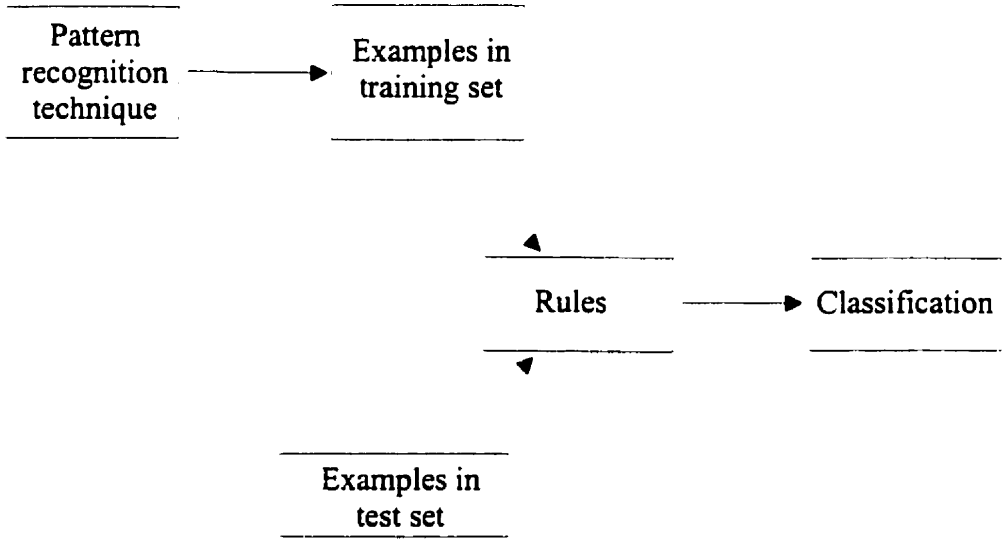

Figure 3.1 Flow chart of steps in pattern recognition.

3.3.1 k-Nearest Neighbors

The *k*-Nearest Neighbors[5] algorithm is a simple statistical technique which does not exactly follow the general method described in Figure 3.1. An example in the training set is denoted as the vector $E_{class,i}(a_j) = (a_1, a_2,..., a_m)$ where *class* is the sample type of the *i*th example in the training set, and a_j is the *j*th attribute in the example. An example in a test set will be the vector $T(a_j) = (a_1, a_2,..., a_m)$. To classify an example in the test set, the Euclidean distance between it and every example in the training set is calculated. Since

large changes in attributes of large values would influence the calculation more than big changes in attributes of small values, a 'relative' Euclidean distance was used.

$$d = \sqrt{\sum_{j=1}^{m} \left(\frac{\left(E_{class,i}(a_j) - T(a_j)\right)}{T(a_j)} \right)^2}$$

These distances are then used to determine the closest neighbors (i.e., smallest Euclidean distance) to the test example. The nearest *k* neighbors are selected and the frequency of each is determined. The class to which the majority of training examples belong is assigned to the test example. If a tie should occur, the class with the closest neighbors is selected.

3.3.2 Bayesian Classification

Bayesian Classification[6] is a probabilistic technique of pattern recognition. It is based on the assumption that the classification problem is posed in probabilistic terms. It also assumes that all the probability values are known. Using the mean and standard deviation of examples of a class in the training set, the Bayesian Classification technique determines the probability that an example in the test set belongs to a particular class. The class with the highest probability is assigned to the example in the test set. In this study the distributions of the examples were assumed to be Gaussian in nature.

3.3.3 C4.5 Inductive Learning

Inductive learning has been mainly used to generate rule-based expert systems although it is also a powerful technique for pattern recognition. By evaluating examples in a training set, inductive learning has the ability to infer general relationships about these examples. In this study, the C4.5 induction engine developed by Quinlan[7] was used. The output of the C4.5 induction algorithm is in the form of a decision tree. The algorithm determines which data attribute best divides the examples in the training set into distinct classes. It separates the examples in such a way that any pattern in the data is made apparent. This results in a hierarchical structure of decisions, i.e., a decision tree. The decision tree can then be used to classify the examples in the test set.

Table 3.1 Reference Materials from CANMET.

Reference Material	**Number of examples in data set**
Copper Concentrate CCU-1b	133
Lead Concentrate CPB-1	274
Zinc Concentrate CZN-1	298
Zinc-Lead-Tin-Silver Ore KC-1a	90
Zinc-Tin-Copper-Lead Ore MP-1a	119
Tungsten-Molybdenum Ore MP-2	79
Iron Ore MW-1	82
Noble Metals Bearing Sulphide Concentrate PTC-1a	98
Noble Metals Bearing Nickel-Copper Matte PTM-1a	97
Sulphide Ore Mill Tailings RTS-1	30
Sulphide Ore Mill Tailings RTS-2	43
Sulphide Ore Mill Tailings RTS-3	58
Sulphide Ore Mill Tailings RTS-4	47
Iron Ore SCH-1	271
Nickel-Copper-Cobalt Ore SU-1a	216
Diorite Gneiss SY-4	248
Diabase Rock PGE Material TDB-1a	101
Gabbro Rock PGE Material WGB-1	96
Mineralized Gabbro PGE Material WMG-1	102
Massive Sulphide PGE Material WMS-1	100

The Data Sets

The data set used in this study consisted of the elemental compositions for 20 reference materials obtained from CANMET, Mineral Science Laboratories (Ottawa, Canada) (Table 3.1). The data set was used for all three techniques, *k*NN, Bayesian Classification and the C4.5 inductive learning algorithm. Computer programs for *k*NN classification and Bayesian classification were written in Borland International's (Otis Valley, CA,

USA) Turbo Pascal 7.0. C4.5 was written in Watcom International's (Waterloo, Ontario, Canada) C/C++ v.10.0 for OS/2. All computer programs were written in our laboratory and were executed on a 66-MHz 486 PC type computer. The data set was composed of results of multiple repeat analyses obtained for each reference material by different laboratories. Each training and test example consisted of the concentration for each of the 13 most commonly analyzed elements in the reference materials. The data set contained unknown attributes since the concentration of each of the 13 elements was not available for each reference material. The C4.5 inductive learning algorithm is capable of handling unknown attributes with their values set to a question mark ('?'). Since the other two techniques, *k*NN and Bayesian classification, require all attributes to be known, the unknown attributes needed to be set to some value. For *k*NN, the unknown attributes (concentrations) were set to zero.

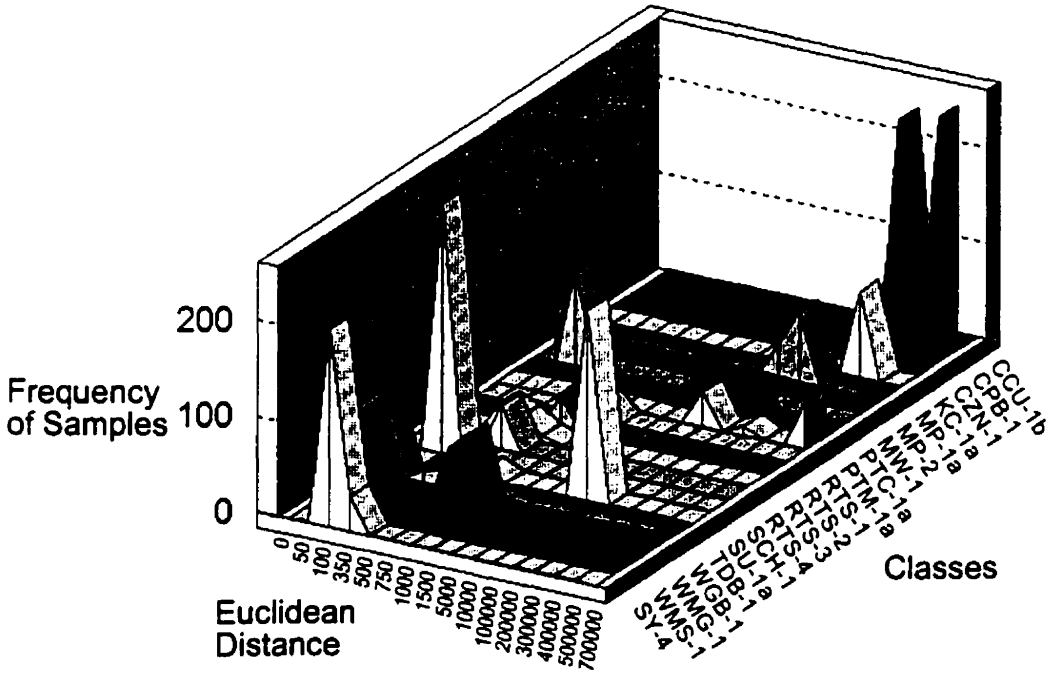

Figure 3.2 Frequency of samples from each class in each Euclidean distance range.

Figure 3.2 depicts the frequency of samples in each class that belong in the different Euclidean distance ranges relative to the zero point. For Bayesian classification, the attributes (concentrations) in a class that were sometimes known were set to the value

of the mean of that attribute in that class; the attributes in a class that were completely unknown were given a mean (999 999.5) far removed from any possible value and a very small standard deviation thereby eliminating that element as a classifier. The average concentrations of each element in each class are shown in Figure 3.3, which illustrates the relative similarity of some materials. (Note: The maximum concentration on the graph is 600 000 μg/g so that the lower concentrations can be seen.) Figure 3.4 shows both the relative standard deviations with a material type as well as deviations across sample types for a given element. The examples used in the test sets were selected at random from the data set. In addition, the sizes of the test sets were varied to provide a variety of testing environments.

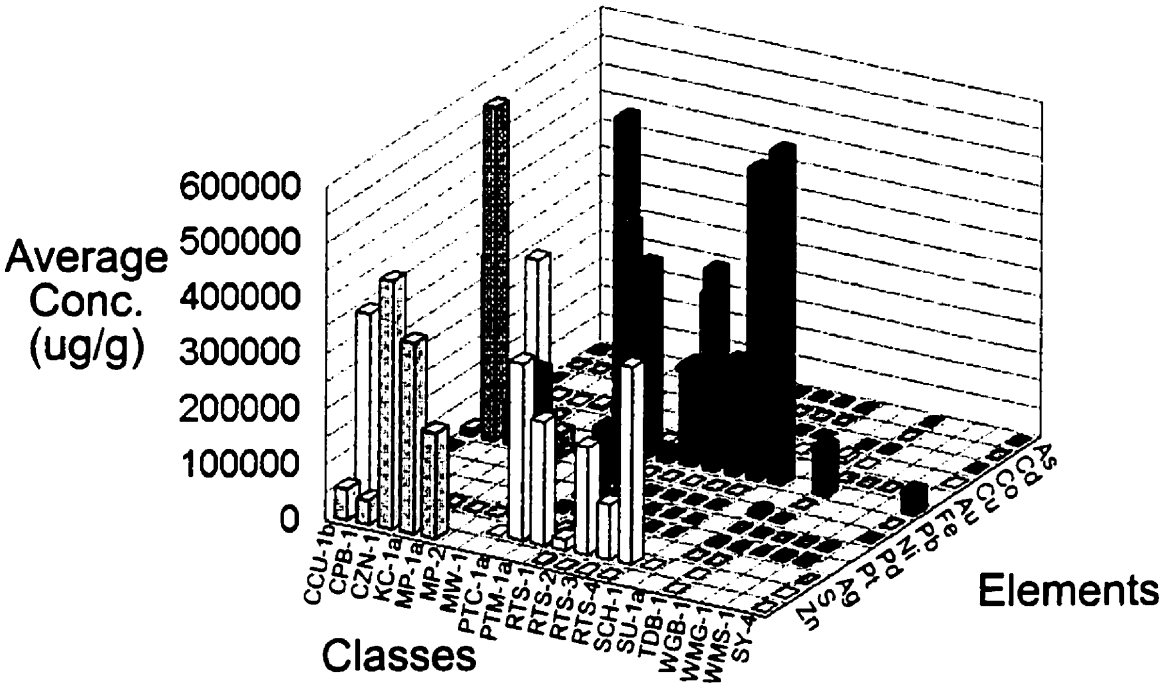

Figure 3.3 Average concentration of each element in each class.

Table 3.2 Reference materials used in subset.

Reference Material	Number of examples in data set
Sulphide Ore Mill Tailings RTS-1	18
Sulphide Ore Mill Tailings RTS-2	25
Sulphide Ore Mill Tailings RTS-3	34
Sulphide Ore Mill Tailings RTS-4	28

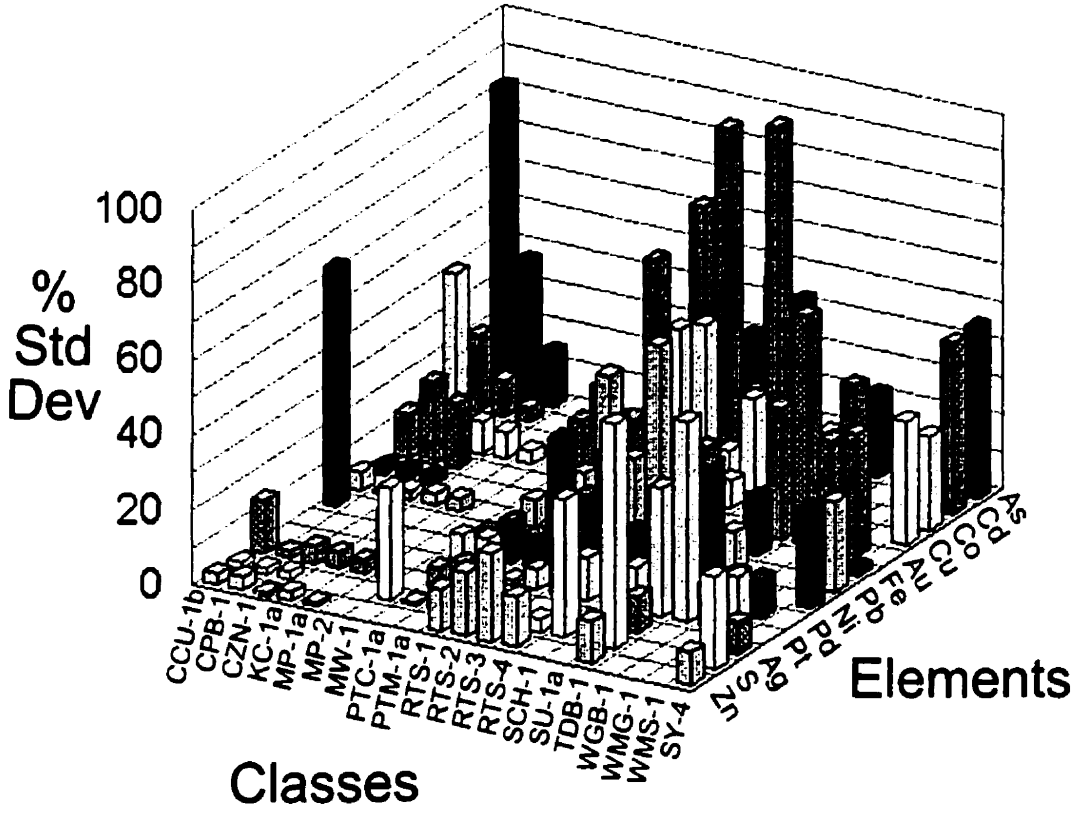

Figure 3.4 Relative standard deviation of the concentration of each element in each class.

Due to the inconvenience of the missing data, further studies were done on a subset of the CANMET data consisting of only the data from the Sulfide Ore Mill Tailings (RTS-1, RTS-2, RTS-3 and RTS-4). The number of elements studied was

reduced from 13 to 9 and all examples with missing data were eliminated. The numbers of remaining examples for each sample type are listed in Table 3.2. This particular set was selected for the similarity of the materials.

3.4 Results and Discussion

Figure 3.2 is a depiction of the number of examples lying in an Euclidean distance range with respect to the origin. The examples in the data set are grouped with their respective sample types. Some of the sample types can be seen to fall in the same range (e.g., CCU-1b and CPB-1) which could make them difficult to distinguish with a technique like *k*NN. Figure 3.3 illustrates the average concentration of the elements in the various sample types. This figure can be read in two different ways. The first is to start at the axis labeled 'Elements' and to go across in parallel with the 'Classes' axis; the concentration of an element can be viewed and compared for the various sample types. The second method is to start at the 'Classes' axis and go in parallel with the 'Elements' axis; the concentration of all elements in a sample type can be viewed. The pattern for a sample type seen by this method can be used for comparison with other sample types. Figure 3.4 has a similar layout except that it shows standard deviations rather than concentrations. This figure can be read in the same manner as Figure 3.3. A casual examination of both Figures 3.3 and 3.4 would suggest that it might be difficult to differentiate between some of the sample types with a technique such as Bayesian Classification.

The classification results of the three techniques are listed in Tables 3.3, 3.4, and 3.5. As can be seen, all three classifications perform extremely well, with Bayesian classification and *k*NN performing the best.

Table 3.3 Classification results for kNN.

Test Set	Size Relative to Data Set	Rate of Success
1	25 %	97.1 %
2	25 %	97.6 %
3	25 %	97.3 %
4	25 %	97.3 %
5	26 %	97.2 %
6	22 %	97.9 %
7	50 %	95.7 %
8	50 %	96.3 %
9	54 %	95.4 %
10	51 %	95.4 %
11	52 %	96.1 %
12	51 %	96.2 %

Table 3.4 Results of Bayesian classification

Test Set	Size Relative to Data Set	Rate of Success
1	25 %	95.8 %
2	25 %	95.9 %
3	25 %	95.6 %
4	25 %	96.6 %
5	26 %	96.1 %
6	22 %	95.6 %
7	50 %	99.3 %
8	50 %	96.5 %
9	52 %	97.8 %
10	52 %	98.7 %
11	52 %	98.4 %
12	54 %	98.5 %

Table 3.5 Classification results of C4.5 inductive learning

Test Set	Size Relative to Data Set	Rate of Success
1	25 %	92.3 %
2	25 %	91.3 %
3	25 %	93.5 %
4	25 %	92.6 %
5	26 %	92.0 %
6	22 %	93.2 %
7	50 %	91.5 %
8	50 %	90.7 %
9	51 %	91.8 %
10	51 %	92.4 %
11	52 %	91.7 %
12	54 %	90.7 %

Even though these results are extremely good and demonstrate how well these three techniques can perform with large data sets, the data and the tests performed are not necessarily representative of all situations. The Autonomous Instrument system that we are developing will not be initially supplied with such a complete set of data. It will have to build it in time with experiments. In addition, this system will always perform a fast analysis (a semi-quantitative scan) at standard conditions of a sample to provide an estimate of the concentrations of all the elements. Since this will be performed every time and the concentrations of all the elements will be known, there will not be any missing data in the training or test set. The system would start with an empty training set the first time it is run. This first analysis would be the first example in the training set and for every other analysis performed an example would be added to the training set as long as the sample type is known. The system will use this training set (or database) when running an unknown sample to find the closest match; that information can then be used to select operating conditions and calibration methodology. Since the number of examples of each class in the training can vary and could be as low as one example, a set of experiments was conducted in which only one neighbor (k=1) was used for k-Nearest Neighbors. For Bayesian Classification, the one-example experiments were conducted using a small percentage of the mean as the standard deviation (e.g., 1%). To simulate

the way our system would work, we started with an empty training set. We used a subset of the CANMET data which only consisted of the four types of Sulfide Ore Mill Tailings with no missing values. A random example of each sample type was put into the training set. The remaining examples were put into the test set. Ten different combinations of training and test sets were created and all three pattern recognition techniques were applied to them, searching for the closest match. This described the first time the system was used for classification of an unknown sample with respect to four sample types; this was also repeated using two, three, five, and ten examples of each sample type in the training set. The average success rates are listed in Table 3.6.

Table 3.6 Classifications based on number of examples in training set.

Number of examples in training set	Number of different cases Tests	Average rate of success of pattern recognition technique (%)		
		k-Nearest Neighbor	Bayesian Classification	C4.5 Inductive Learning
1	10	92	88	44
2	10	92	96	61
3	10	97	83	65
5	5	97	100	83
10	3	100	100	86

Upon examination of the average success rate of the three techniques (Table 3.6), C4.5 inductive learning did not perform well with very few examples in the training set; however, its classification performance did improve significantly as the number of examples in the training set increased. With a small number of examples in the training set it seems that both *k*NN and Bayesian Classification performed well (Figure 3.5).

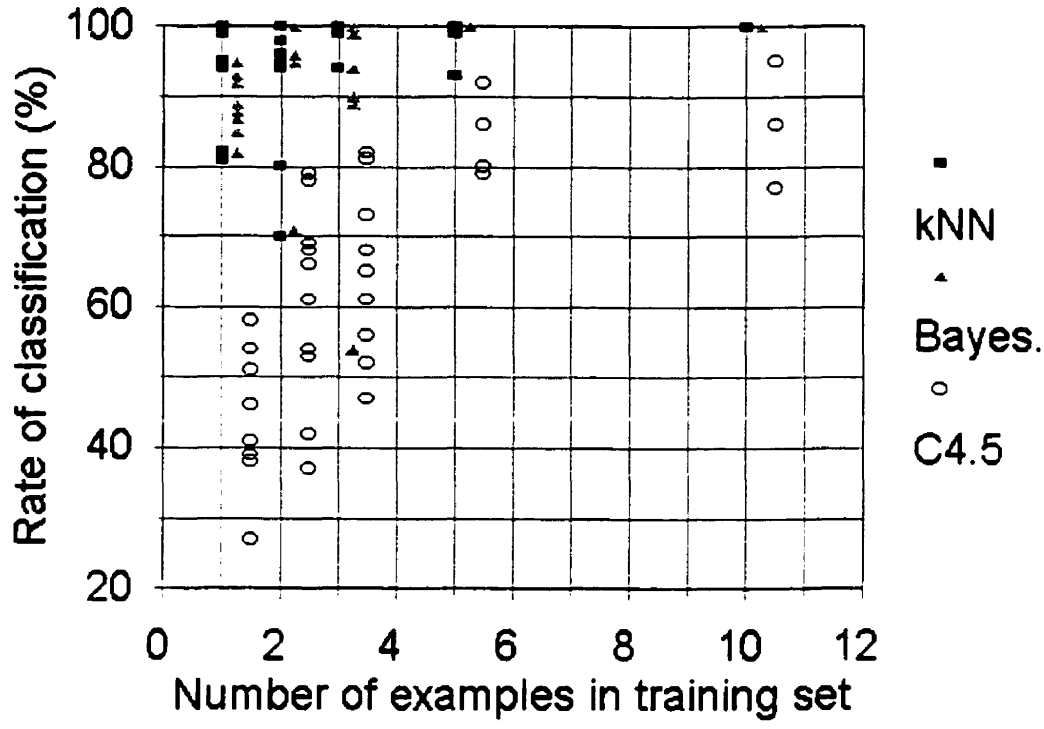

Figure 3.5 Classification of test samples based on number of examples in training set.

In the tests based on two examples of each type in the training set, there were two cases where one technique outperformed the other. In the first, *k*NN had a success rate of 70% whereas Bayesian Classification performed at 96%. The two training examples selected for the RTS-4 sample type were not representative of the whole class. In fact, these two were situated somewhere in between the RTS-2 sample type and the RTS-4 sample type such that the Euclidean distances calculated were so close that the test examples were sometimes classified as the RTS-2 sample type. Bayesian Classification, since it uses means and standard deviations to calculate the probabilities, did not misclassify the test examples. The probabilities of the test examples belonging to either class were nonetheless competitive. In the second case, Bayesian Classification performed at 71% whereas *k*NN had a success rate of 94%. The two training examples selected for the RTS-1 sample type were so similar that the standard deviations of some of their attributes were zero or close to it. When the standard deviation is very low or zero, the probability of a test example's attributes belonging to that particular class becomes zero or close to it.

This results in very few test examples being assigned to the RTS-1 sample type. The *k*NN technique did not exhibit the same difficulties since the technique does not rely on standard deviations. This same phenomenon was observed in one of the cases for the three training examples of the sample types RTS-1, RTS-2 and RTS-3. The training examples of the RTS-4 sample type, on the other hand, had relatively large standard deviations which resulted in most of the examples in the test set being assigned to the RTS-4 sample type. Bayesian Classification was only able to correctly classify 54% of the test set.

Between the two techniques it would seem that *k*NN would suit our purposes best for small numbers of examples. The minimum requirements in our system are that there be at least one example of each sample type in the training set and that the examples in the training set be representative of their class.

3.5 Conclusion

It has been shown that for classification of 20 reference materials with the use of their elemental compositions obtained experimentally by various laboratories, C4.5 inductive learning, *k*NN, and Bayesian classification all performed extremely well. In choosing a pattern recognition technique, there are several important characteristics to consider: speed, classification accuracy, and clarity of results. C4.5 and Bayesian Classification generate their rules and means and standard deviations, respectively, once, and hence take approximately the same amount of time to classify an example. The *k*NN technique can be much slower since the test example must be compared to every training example and the amount of time needed is dependent on the number of examples in the training set. We have seen that in classification accuracy all three techniques performed extremely well when large training sets were used. As for clarity of results, it depends on what information is required. C4.5 provides a decision tree demonstrating which attributes are being used in the classification. Bayesian classification provides a statistical probability of a test example belonging to a particular class and can be used as a measure for possible misclassifications. *k*NN provides the Euclidean distance between the test example and its nearest neighbors, which can be used as a measure of goodness.

Using small training sets, both *k*NN and Bayesian Classification performed well whereas C4.5 required larger training sets. For the Autonomous Instrument system, *k*NN seems to be the appropriate choice for the pattern recognition module. The hypothesis from our last paper[3] (i.e., that pattern recognition for sample identification is highly practicable) has been strongly reinforced by this more recent work. It would seem that modern ICP-AES spectrometer systems, using readily available pattern recognition techniques, have a high probability of being able to extract considerably more useful information than is presently extracted from data which is already present in the system.

3.6 Acknowledgments

The authors gratefully acknowledge William Bowman at CANMET for providing the data set, and financial support from the National Sciences and Engineering Research Council of Canada. C. S. would like to acknowledge financial support from Fonds pour la Formation de Chercheurs et l'Aide à la Recherche.

3.7 References

1 Webb, D. P., Hamier, J., and Salin, E. D., *Trends Anal. Chem.*, 1994, 13, 44.

2 Webb, D. P. and Salin, E. D., *Intelligent Instruments and Computers*, 1992, 5, 185.

3 Branagh, W, Yu, H., and Salin, E. D., *Appl. Spectrosc.* 1995, 49(7), 964.

4 Branagh, W. and Salin, E. D., *Spectroscopy*, 1995, 10, 20.

5 Sharaf, M. A., Illman, D. L., and Kowalski, B. R., Chemometrics (John Wiley and Sons, New York, 1986).

6 Duda, R. O. and Hart, P. E., Pattern Classification and Scene Analysis (John Wiley and Sons, Toronto, 1973).

7 Quinlan, J. R., C4.5 Algorithms for Machine Learning (Morgan Kaufmann Publishers, San Mateo, 1993).

8 Salin, E. D. and Winston, P. H., *Anal. Chem.*, 1992, 64, 49A.

Chapter 4

An optimization procedure is required in two of the modules of the Autonomous Instrument. In the Learning to Run a New Sample module, an analysis method has to be determined for a standard reference material. An important aspect of the analysis method is the selection of operating conditions. The optimization procedure would search for the best operating conditions to be used for the standard reference material. In the Analysis of an Unknown Sample, if a sample cannot be analyzed[1] using standard operating conditions and if there is no prior knowledge of analyzing that type of sample, then the operating conditions need to be determined. The optimization procedure not only determines the best operating conditions to be used with the unknown sample but must perform this operation in a reasonable amount of time.

Most optimization techniques use a single response value in their algorithms to find candidate-operating conditions. In an analysis of a sample, this would be limited to a single analyte signal. In a multi-element analysis, an objective function that combines many values into one is necessary. This chapter looks at the development of an objective function that was applied to ICP-AES. Its performance was compared to an existing function commonly used in ICP-AES. This work was published in *J. Anal. At. Spectrom.*, 12, 1997, 13.

4 Comparison of Two Objective Functions for Optimization of Simultaneous Multi-Element Determinations in Inductively Coupled Plasma Spectrometry

4.1 Abstract

Two objective functions for multi-element optimization in inductively coupled plasma atomic emission spectrometry (ICP-AES) were compared using signal-to-background ratios as a figure of merit. Complete three-dimensional response surfaces were generated for a number of elements (Ca, Cu, Al, Na, Ni, Mn, Ba) and two artificial "elements" to evaluate the performance of both objective functions in locating the optimal compromise instrumental operating conditions in multi-element determinations. In the determination of the best compromise instrument operating conditions for most combinations of the elements used, both objective functions performed equally well; however, one occasionally performs significantly better than the other.

4.2 Introduction

Optimization of instrumental operating conditions may improve analytical accuracy and precision. The instrumental operating conditions of an ICP that may be optimized are rf power, flow rates of gases (the outer or coolant, intermediate or plasma and injector gas flow rates), observation region in the plasma and solution pump rate to the nebulizer.[2] The primary optimization techniques that have been used with ICPs are Simplex[3-12] and the Davidon-Fletcher-Powell[13] algorithm. Traditionally the response functions used have been signal-to-background ratios (SBRs), signal-to-noise ratios (SNRs), precision and accuracy. Thomas and Collins[13] also used detection limits as the response function. Any of these response functions may be directly used for determining optimal instrument operating conditions for single-element analysis[3-6]. Signal-to-background ratios are easily obtained and they require the fewest measurements of the response functions listed above. The SBR is also a good figure of merit since it can be correlated to detection limits. Therefore, SBRs are used throughout this work as calculated using the following equation:

$$S/B = \frac{\text{Total signal - Background}}{\text{Background}}$$

where S/B is the SBR.

The difficulty arises in simultaneous multi-element analysis because optimization techniques generally require a single value representing each set of operating conditions but, using any of the response functions mentioned above, multiple values (one for each element) are obtained for each set of conditions. Galley *et al.*[6], in their automated Simplex optimization of multi-element solutions, used the following choices for optimization criteria: (1) the maximization of the net signal or signal-to-background noise ratio, (2) the minimization of the relative standard deviation of the background and (3) the maximization of the ratio of atomic or ionic lines. An objective function, which by definition would result in a single value for a set of operating conditions, is needed. It

should comprise the SBRs of all the elements studied with the emphasis on the elements closer to the detection limits.

Leary *et al.*[7] developed and tested several objective functions based on SBRs, the best one being represented by the sum of the reciprocals of the SBRs for the elements studied:

$$F = \frac{n}{\sum_{i=1}^{n} (S/B)_i^{-1}}$$

where n is the number of elements studied for the optimization and $(S/B)_i$ are the SBRs of each of the *i*th elements. This equation generates a value for each set of instrumental operating conditions using the SBRs of all the elements. Ebdon and Carpenter[9] used a modified version of Leary's objective function in their study. Kalivas[10] also used Leary's objective function in the optimization of operating conditions for minimal interferences. Instead of SBRs, Kalivas used selectivity, sensitivity, and accuracy, as derived by Lorber,[14] as response functions. Moore *et al.*[11] also used Leary's objective function with SBRs as well as ionization interference as the figure of merits. Belchamber *et al.*[12] developed an objective function based on a measure of the magnitude of the matrix effects such as to minimize or remove these matrix effects.

We tested another approach towards satisfying the two conditions required for obtaining optimal compromise operating conditions: (1) obtaining the maximum compromise SBRs for all elements and (2) emphasizing the maximization of the SBR of the elements close to their detection limits. This objective function is called the Combined Ratio Method (CRM) and is given by:

$$CRM = \frac{\sum_{i=1}^{n} (S/B)_i}{\sum_{j=1}^{k} R_j}$$

where n is the number of elements, k is (n-1) + (n-2) + ...+ 1, $(S/B)_i$ are the SBRs of each of the *i*th elements and R_j is the ratio of the SBRs of two given elements (*j*th

combination) where the maximum SBR of the two is in the numerator such that $R_j \geq 1$. For example, given the following SBRs of three elements Zn, Na, and K, the values for R_1, R_2, and R_3, would be:

$$(S/B)_{Zn} = 1;\ (S/B)_{Na} = 2;\ (S/B)_K = 10$$
$$R_1 = (S/B)_K/(S/B)_{Zn} = 10/1 = 10$$
$$R_2 = (S/B)_K/(S/B)_{Na} = 10/2 = 5$$
$$R_3 = (S/B)_{Na}/(S/B)_{Zn} = 2/1 = 2$$

and the CRM would be calculated as:

$$CRM = \frac{(S/B)_{Zn} + (S/B)_{Na} + (S/B)_K}{R_1 + R_2 + R_3}$$

$$CRM = \frac{1 + 2 + 10}{10 + 5 + 2} = \frac{13}{17} = 0.76$$

The CRM performs a weighted average on the sum of the SBRs and maximizes the individual SBRs while minimizing the difference among these ratios (i.e., minimizing ΣR_j).

In this work, we performed a comparison of Leary's objective function and the CRM by examining the response surfaces generated by each function and evaluating the performance of each function in determining the optimum instrument operating conditions.

4.3 Experimental

The instrument used was a Thermo Jarrell Ash (Franklin, MA, USA) Model 25 sequential scanning spectrometer. The instrument functions are all automated and controlled by an independent computer via an RS-232 port. The solution pump rate to the nebulizer was 0.9 ml min^{-1}. A signal integration time of 1.0 s was used. The background for each line was selected at 0.05 nm on both sides of each spectral line peak. An average of the background was used for all readings. All operating conditions were held constant except for observation height and rf power. The observation height was varied from 3 mm to 24 mm above the top of the load coil (ATOLC) in steps of 3.0 mm and the rf power was varied from 750 to 1550 W in steps of 200 W. All these combinations generated a response surface which characterized the parameter space. While any combination of rf power, observation region in the plasma, flow rates of gases, and solution pump rate to the nebulizer could be optimized, we chose to vary only two of these parameters for simplicity of the graphical representation of the response surfaces. A stock solution was prepared from Fisher (Pittsburgh, PA) certified sodium, calcium, copper, aluminum, nickel, manganese and barium 1000 ppm standard solutions and the concentration and spectral lines of these seven elements studied are listed in Table 4.1 along with their ionization potential. These elements have both hard and soft lines.

Table 4.1 Elements used.

Element	**Concentration /ppm**	**Wavelength /nm**	**Ionization potential[15] /eV**
Al I	10	309.28	5.99
Ca II	10	317.93	11.87
Cu I	10	324.75	7.73
Ba II	2	455.40	10.00
Ni I	10	232.00	7.64
Mn II	2	257.61	15.64
Na I	10	589.59	5.14

The SBRs were determined for all seven elements at each set of instrumental operating conditions. Based on these SBRs, a response surface was generated for each element. Using these seven response surfaces for the seven elements, two other surfaces were generated, one using Leary's objective function and one using the CRM. The optimum operating conditions were determined from these latter surfaces and used in the comparison of the two objective functions. In addition, theoretical models were used to further compare the two objective functions.

4.4 Results and Discussion

Three-dimensional response surfaces were obtained for each element by plotting the SBRs of each element against the observation heights and rf powers (Figures 4.1 to 4.7). The SBRs of each element at each set of operating conditions are listed in Tables 4.2 to 4.8. The optimum instrumental operating conditions for each element are listed in Table 4.9. Low power seems to be the best choice for these elements at their present concentration. This is expected since an increase in power increases the background more than the signal with a subsequent decrease in SBR^2. For example, looking at the combination of manganese and sodium, the optimum operating conditions for manganese are 750 W for rf power and 12 mm ATOLC, whereas those for sodium are 950 W for rf power and 21 mm ATOLC. However, using either of these operating conditions in the simultaneous determination of these two elements would produce poor results for one of them.

Using the data in Tables 4.2 through 4.8, the optimum compromise instrumental operating conditions were determined for all combinations (Table 4.10) of the seven elements studied by applying Leary's objective function and the CRM. The application of these two objective functions to any combination of the elements for all sets of operating conditions produces two response surfaces (one for Leary's objective function and the other for the CRM). For example, in the optimization of operating conditions over all seven elements, the resulting surfaces are depicted in Figures 4.8 and 4.9. The maximum point on a surface indicates the best compromise operating conditions given by

each method. Considering the combination of these seven elements, the resulting surfaces are similar to each other and give the same set of operating conditions as the optimum compromise.

The optimum compromise settings were determined for each combination of the elements using both objective functions and are listed in Table 4.10. In many cases, both objective functions give the same set of instrumental operating conditions as the best compromise. In the cases where they give different operating conditions (Table 4.11), the CRM puts a greater emphasis on decreasing the difference between the SBRs (i.e., decreasing R_j).

Table 4.2 SBRs of aluminum.

	RF power /W				
Observation height/mm	**750**	**950**	**1150**	**1350**	**1550**
3	0.66	0.75	0.57	0.38	0.34
6	1.68	1.03	0.81	0.54	0.40
9	4.10	2.01	1.48	0.78	0.56
12	8.18	4.14	2.77	1.57	1.07
15	13.02	7.09	4.67	2.69	1.97
18	11.96	7.99	7.42	3.86	2.84
21	9.83	10.57	9.89	6.00	3.26
24	10.09	10.50	10.30	8.47	7.05

Table 4.3. SBRs of calcium.

Observation height/mm	RF power /W 750	950	1150	1350	1550
3	0.59	0.75	0.75	0.75	0.61
6	1.55	1.76	1.68	1.36	1.12
9	4.01	3.59	2.99	2.15	1.70
12	7.66	5.89	4.92	3.40	2.66
15	7.81	7.44	6.78	4.80	3.93
18	5.30	6.92	6.55	6.31	5.21
21	2.54	4.61	5.73	5.62	5.65
24	1.19	1.81	3.08	3.85	4.78

Table 4.4 SBRs of copper.

Observation height/mm	RF power /W 750	950	1150	1350	1550
3	4.05	2.46	1.78	1.18	0.92
6	6.92	3.87	2.99	1.79	1.32
9	14.02	7.65	4.93	2.73	1.76
12	25.38	13.73	9.41	5.13	3.32
15	33.97	21.41	16.19	8.72	6.06
18	35.04	26.98	22.53	14.28	9.80
21	33.95	32.95	30.77	23.27	16.28
24	32.83	35.57	38.44	31.99	28.40

Table 4.5 SBRs of barium.

Observation height/mm	RF power /W 750	950	1150	1350	1550
3	0.39	0.29	0.27	0.16	0.13
6	0.85	0.55	0.42	0.26	0.19
9	1.50	0.73	0.52	0.24	0.15
12	3.94	1.61	1.09	0.49	0.32
15	7.65	3.75	2.30	1.05	0.77
18	10.32	5.87	4.20	2.18	1.38
21	9.16	8.64	6.64	3.72	2.57
24	6.35	8.23	7.70	5.68	4.73

Table 4.6 SBRs of nickel.

Observation height/mm	RF power /W 750	950	1150	1350	1550
3	1.28	1.15	0.73	0.67	0.47
6	2.38	2.23	1.55	1.20	0.93
9	6.64	5.51	4.08	2.11	1.54
12	12.61	9.55	6.77	3.84	2.22
15	14.48	12.05	9.03	6.56	4.12
18	8.45	10.55	10.05	6.14	3.83
21	3.23	5.65	5.83	4.99	2.21
24	2.50	2.25	2.35	2.99	3.78

Table 4.7 SBRs of manganese.

Observation height/mm	RF power /W				
	750	950	1150	1350	1550
3	5.47	6.17	5.60	4.60	3.26
6	13.38	12.19	9.95	8.34	6.56
9	26.31	24.57	19.61	12.66	8.70
12	41.05	32.97	28.80	19.58	14.98
15	36.87	39.03	36.83	26.53	20.32
18	27.46	35.66	36.65	32.85	26.49
21	14.08	22.28	22.34	22.73	18.74
24	4.44	6.63	10.57	9.51	11.21

Table 4.8 SBRs of sodium.

Observation height/mm	RF power /W				
	750	950	1150	1350	1550
3	3.20	1.69	1.27	0.75	0.58
6	3.90	2.05	1.37	0.81	0.64
9	5.10	2.45	1.60	0.94	0.63
12	9.50	4.54	2.94	1.60	1.21
15	14.24	7.59	5.31	3.08	2.59
18	15.98	12.37	8.65	5.32	4.09
21	14.87	14.26	11.97	8.82	7.25
24	16.17	17.73	15.81	11.75	10.84

Table 4.9 Best operating conditions for each element.

Element	Power /W	Observation Height /mm
Al	750	15
Ca	750	15
Cu	1150	24
Ba	750	18
Ni	750	15
Mn	750	12
Na	950	24

The similarities between the surface produced with Leary's objective function (Figure 4.8) and that produced with the CRM (Figure 4.9) indicate that neither function would provide a better surface over the other for use with Simplex optimization techniques or the Davidon-Fletcher-Powell algorithm. It is also difficult to tell whether one of the two functions provides better compromise operating conditions over the other for all seven elements. When fewer element responses are combined, such as for the combination of Al, Ba and Mn, (Line 32 in Tables 4.10 and 4.11), Leary's objective function provides better compromise operating conditions than the CRM since the CRM puts more emphasis on minimizing the difference between the SBRs of these three elements. However, for other combinations, such as that of Al, Ba, and Ni (Line 31 in Tables 4.10 and 4.11), it is a question of which is of greater importance, maximizing the smallest SBR obtained (i.e. minimizing the difference between the SBRs of the elements) (CRM) or maximizing the total of the SBRs (Leary's objective function). When considering SBRs which can vary widely, these data suggest that the Leary approach is better, as significant improvements are sometimes found with relatively small losses compared with the CRM approach.

Table 4.10 Best compromise conditions for all the combinations of the elements.

Line	Combination	CRM		LEARY	
		Power (W)	Height (mm)	Power (W)	Height (mm)
1	Al-Ca	750	12	750	15
2	Al-Cu	750	15	750	15
3	Al-Ba	750	18	750	18
4	Al-Ni	750	15	750	15
5	Al-Mn	1150	24	750	15
6	Al-Na	750	15	750	18
7	Ca-Cu	950	15	750	15
8	Ca-Ba	750	15	750	15
9	Ca-Ni	750	12	750	15
10	Ca-Mn	750	15	750	12
11	Ca-Na	950	15	750	15
12	Cu-Ba	750	18	750	18
13	Cu-Ni	750	15	750	15
14	Cu-Mn	750	15	750	15
15	Cu-Na	950	24	950	24
16	Ba-Ni	750	18	750	15
17	Ba-Mn	750	21	750	18
18	Ba-Na	750	18	750	18
19	Ni-Mn	750	15	750	15
20	Ni-Na	750	15	750	15
21	Mn-Na	750	21	750	15
22	Al-Ca-Cu	750	15	750	15
23	Al-Ca-Ba	750	15	750	15
24	Al-Ca-Ni	750	15	750	15
25	Al-Ca-Mn	750	15	750	15
26	Al-Ca-Na	750	15	750	15
27	Al-Cu-Ba	750	18	750	15
28	Al-Cu-Ni	750	15	750	15
29	Al-Cu-Mn	750	15	750	15
30	Al-Cu-Na	750	15	750	18
31	Al-Ba-Ni	750	18	750	15
32	Al-Ba-Mn	750	21	750	18
33	Al-Ba-Na	750	18	750	18

34	Al-Ni-Mn	750	15	750	15
35	Al-Ni-Na	750	15	750	15
36	Al-Mn-Na	750	18	750	15
37	Ca-Cu-Ba	750	15	750	15
38	Ca-Cu-Ni	750	15	750	15
39	Ca-Cu-Mn	750	15	750	15
40	Ca-Cu-Na	750	15	750	15
41	Ca-Ba-Ni	750	15	750	15
42	Ca-Ba-Mn	750	15	750	15
43	Ca-Ba-Na	750	15	750	15
44	Ca-Ni-Mn	750	15	750	15
45	Ca-Ni-Na	750	15	750	15
46	Ca-Mn-Na	750	15	750	15
47	Cu-Ba-Ni	750	15	750	15
48	Cu-Ba-Mn	750	18	750	18
49	Cu-Ba-Na	750	18	750	18
50	Cu-Ni-Mn	750	15	750	15
51	Cu-Ni-Na	750	15	750	15
52	Cu-Mn-Na	750	18	750	15
53	Ba-Ni-Mn	750	18	750	15
54	Ba-Ni-Na	750	15	750	15
55	Ba-Mn-Na	750	18	750	18
56	Ni-Mn-Na	750	15	750	15
57	Al-Ca-Cu-Ba	750	15	750	15
58	Al-Ca-Cu-Ni	750	15	750	15
59	Al-Ca-Cu-Mn	750	15	750	15
60	Al-Ca-Cu-Na	750	15	750	15
61	Al-Ca-Ba-Ni	750	15	750	15
62	Al-Ca-Ba-Mn	750	15	750	15
63	Al-Ca-Ba-Na	750	15	750	15
64	Al-Ca-Ni-Mn	750	15	750	15
65	Al-Ca-Ni-Na	750	15	750	15
66	Al-Ca-Mn-Na	750	15	750	15
67	Al-Cu-Ba-Ni	750	15	750	15
68	Al-Cu-Ba-Mn	750	18	750	18
69	Al-Cu-Ba-Na	750	18	750	18
70	Al-Cu-Ni-Mn	750	15	750	15

71	Al-Cu-Ni-Na	750	15	750	15
72	Al-Cu-Mn-Na	750	15	750	15
73	Al-Ba-Ni-Mn	750	18	750	15
74	Al-Ba-Ni-Na	750	15	750	15
75	Al-Ba-Mn-Na	750	18	750	18
76	Al-Ni-Mn-Na	750	15	750	15
77	Ca-Cu-Ba-Ni	750	15	750	15
78	Ca-Cu-Ba-Mn	750	15	750	15
79	Ca-Cu-Ba-Na	750	15	750	15
80	Ca-Cu-Ni-Mn	750	15	750	15
81	Ca-Cu-Ni-Na	750	15	750	15
82	Ca-Cu-Mn-Na	750	15	750	15
83	Ca-Ba-Ni-Mn	750	15	750	15
84	Ca-Ba-Ni-Na	750	15	750	15
85	Ca-Ba-Mn-Na	750	15	750	15
86	Ca-Ni-Mn-Na	750	15	750	15
87	Cu-Ba-Ni-Mn	750	15	750	15
88	Cu-Ba-Ni-Na	750	15	750	15
89	Cu-Ba-Mn-Na	750	18	750	18
90	Cu-Ni-Mn-Na	750	15	750	15
91	Ba-Ni-Mn-Na	750	18	750	15
92	Al-Ca-Cu-Ba-Ni	750	15	750	15
93	Al-Ca-Cu-Ba-Mn	750	15	750	15
94	Al-Ca-Cu-Ba-Na	750	15	750	15
95	Al-Ca-Cu-Ni-Mn	750	15	750	15
96	Al-Ca-Cu-Ni-Na	750	15	750	15
97	Al-Ca-Cu-Mn-Na	750	15	750	15
98	Al-Ca-Ba-Ni-Mn	750	15	750	15
99	Al-Ca-Ba-Ni-Na	750	15	750	15
100	Al-Ca-Ba-Mn-Na	750	15	750	15
101	Al-Ca-Ni-Mn-Na	750	15	750	15
102	Al-Cu-Ba-Ni-Mn	750	15	750	15
103	Al-Cu-Ba-Ni-Na	750	15	750	15
104	Al-Cu-Ba-Mn-Na	750	18	750	18
105	Al-Cu-Ni-Mn-Na	750	15	750	15
106	Al-Ba-Ni-Mn-Na	750	15	750	15
107	Ca-Cu-Ba-Ni-Mn	750	15	750	15

108	Ca-Cu-Ba-Ni-Na	750	15	750	15
109	Ca-Cu-Ba-Mn-Na	750	15	750	15
110	Ca-Cu-Ni-Mn-Na	750	15	750	15
111	Ca-Ba-Ni-Mn-Na	750	15	750	15
112	Cu-Ba-Ni-Mn-Na	750	15	750	15
113	Al-Ca-Cu-Ba-Ni-Mn	750	15	750	15
114	Al-Ca-Cu-Ba-Ni-Na	750	15	750	15
115	Al-Ca-Cu-Ba-Mn-Na	750	15	750	15
116	Al-Ca-Cu-Ni-Mn-Na	750	15	750	15
117	Al-Ca-Ba-Ni-Mn-Na	750	15	750	15
118	Al-Cu-Ba-Ni-Mn-Na	750	15	750	15
119	Ca-Cu-Ba-Ni-Mn-Na	750	15	750	15
120	all	750	15	750	15

Table 4.11 SBR of elements for the best compromise conditions obtained using the two methods.

Line	**Method**	**SBR of elements**	
1		**Al**	**Ca**
	CRM	8.18	7.66
	Leary	13.02	7.81
5		**Al**	**Mn**
	CRM	10.30	10.57
	Leary	13.02	36.87
6		**Al**	**Na**
	CRM	13.02	14.24
	Leary	11.96	15.98
7		**Ca**	**Cu**
	CRM	7.44	21.41
	Leary	7.81	33.97
9		**Ca**	**Ni**

	CRM	7.66	12.61	
	Leary	7.81	14.48	
10		**Ca**	**Mn**	
	CRM	7.81	36.87	
	Leary	7.66	41.05	
11		**Ca**	**Na**	
	CRM	7.44	7.59	
	Leary	7.81	14.24	
16		**Ba**	**Ni**	
	CRM	10.32	8.45	
	Leary	7.65	14.48	
17		**Ba**	**Mn**	
	CRM	9.16	14.08	
	Leary	10.32	27.46	
21		**Mn**	**Na**	
	CRM	14.08	14.87	
	Leary	36.87	14.24	
27		**Al**	**Cu**	**Ba**
	CRM	11.96	35.04	10.32
	Leary	13.02	33.97	7.65
30		**Al**	**Cu**	**Na**
	CRM	13.02	33.97	14.24
	Leary	11.96	35.04	15.98
31		**Al**	**Ba**	**Ni**
	CRM	11.96	10.32	8.45
	Leary	13.02	7.65	14.48
32		**Al**	**Ba**	**Mn**
	CRM	9.83	9.16	14.08

	Leary	11.96	10.32	27.46	
36		**Al**	**Mn**	**Na**	
	CRM	11.96	27.46	15.98	
	Leary	13.02	36.87	14.24	
52		**Cu**	**Mn**	**Na**	
	CRM	35.04	27.46	15.98	
	Leary	33.97	36.87	14.24	
53		**Ba**	**Ni**	**Mn**	
	CRM	10.32	8.45	27.46	
	Leary	7.65	14.48	36.87	
73		**Al**	**Ba**	**Ni**	**Mn**
	CRM	11.96	10.32	8.45	27.46
	Leary	13.02	7.65	14.48	36.87

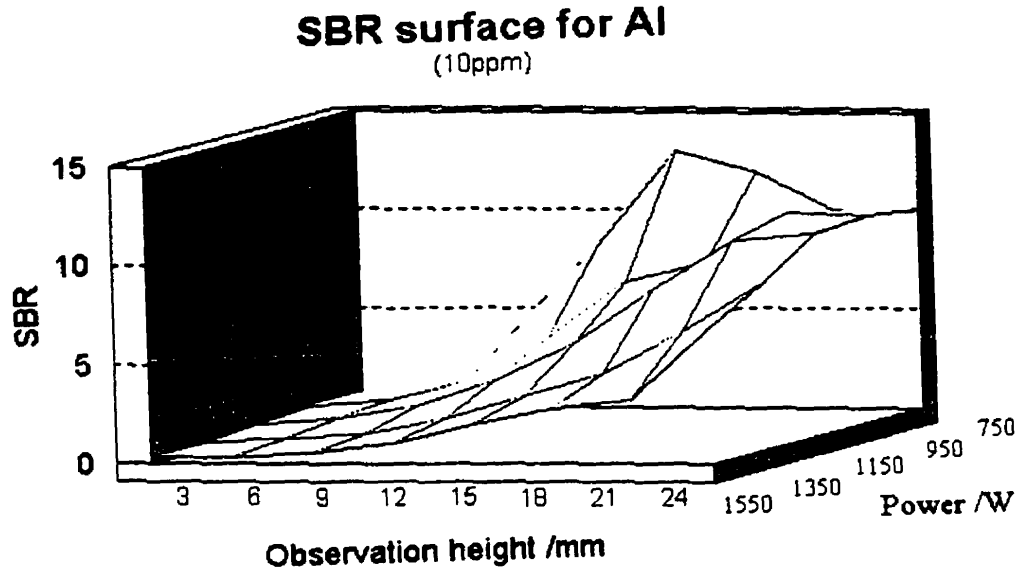

Figure 4.1 Surface of SBRs of Al.

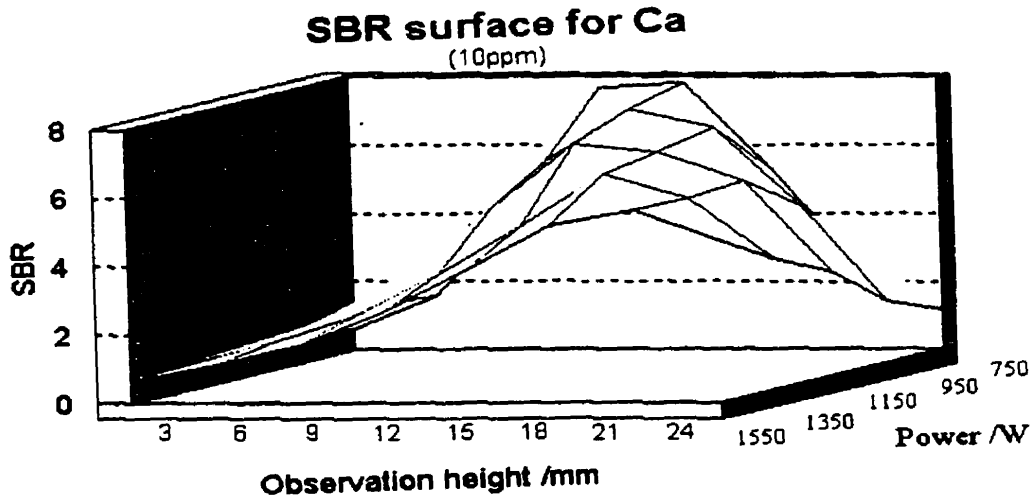

Figure 4.2 Surface of SBRs of Ca.

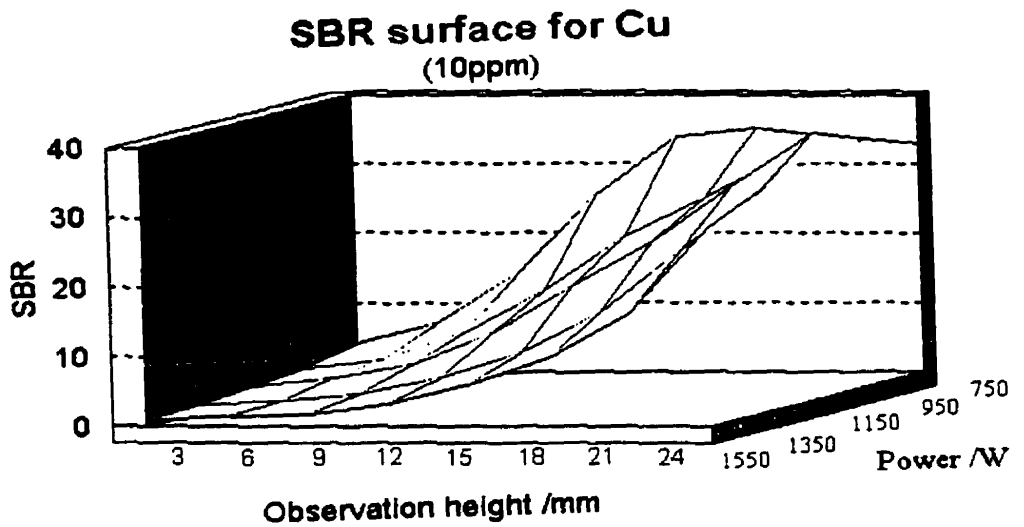

Figure 4.3 Surface of SBRs of Cu.

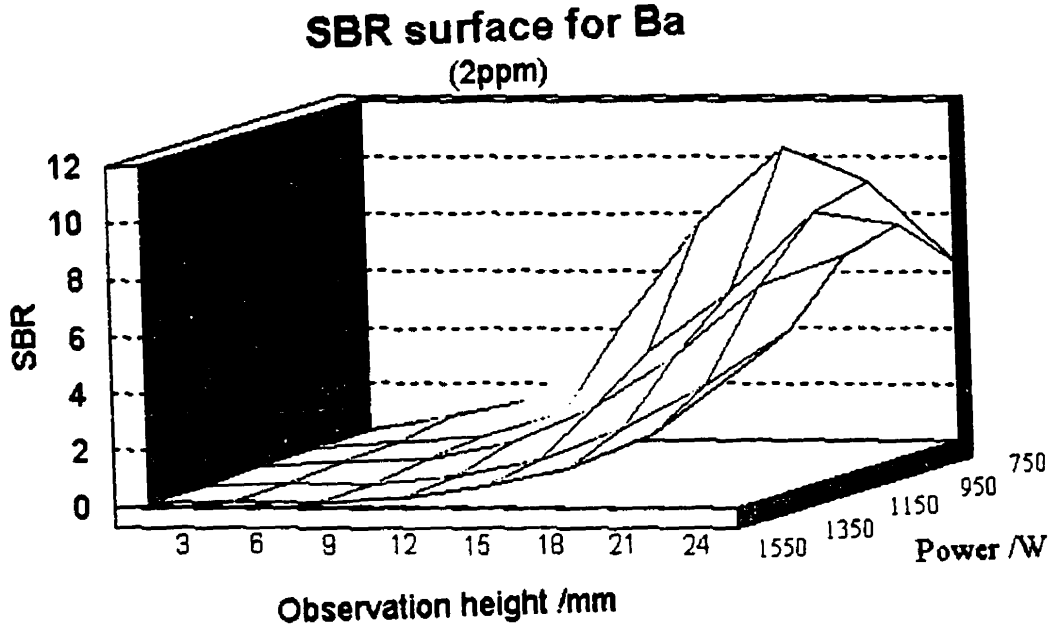

Figure 4.4 Surface of SBRs of Ba.

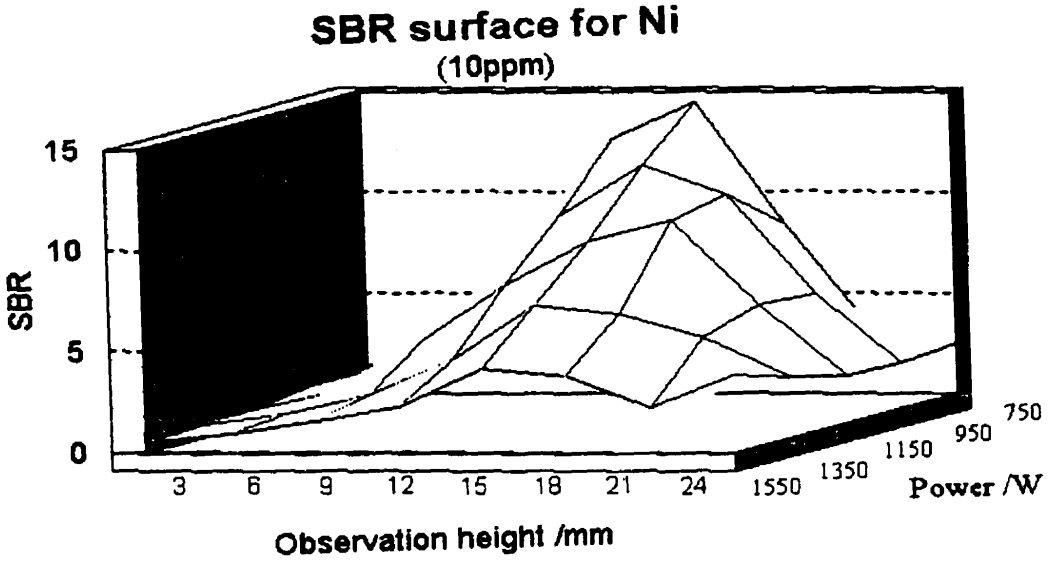

Figure 4.5 Surface of SBRs of Ni.

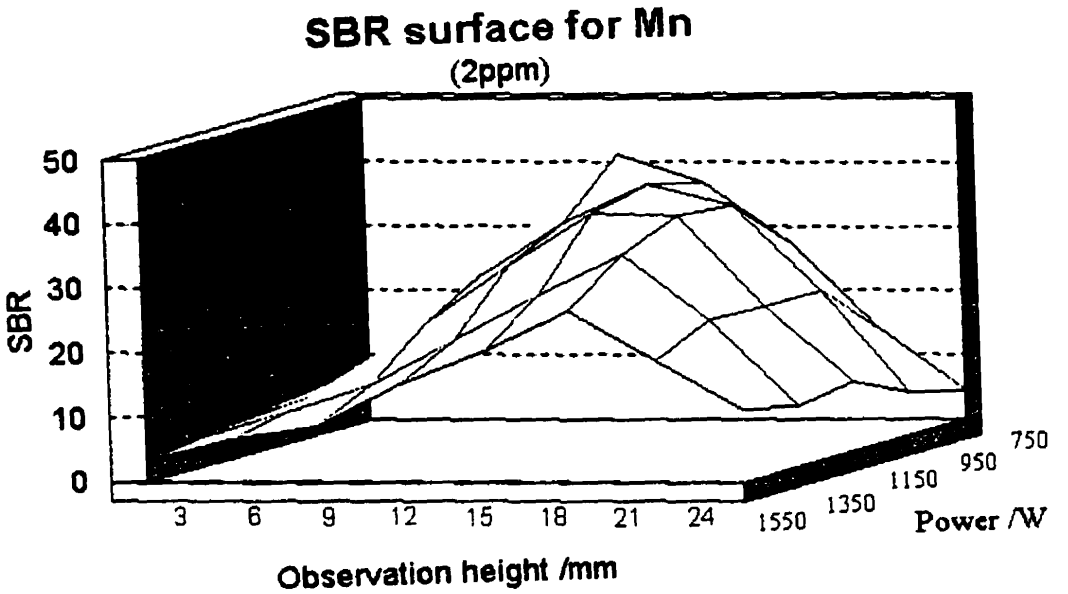

Figure 4.6 Surface of SBRs of Mn.

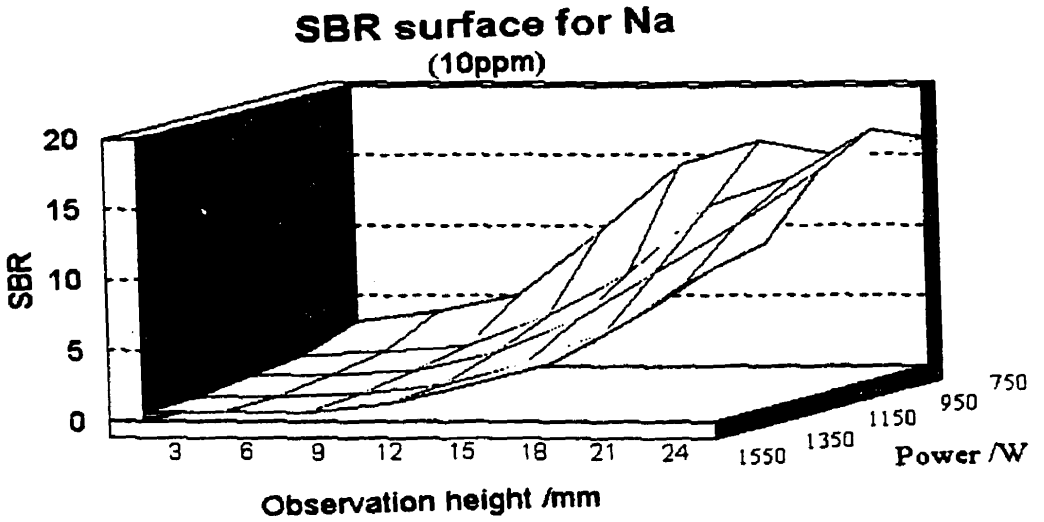

Figure 4.7 Surface of SBRs of Na.

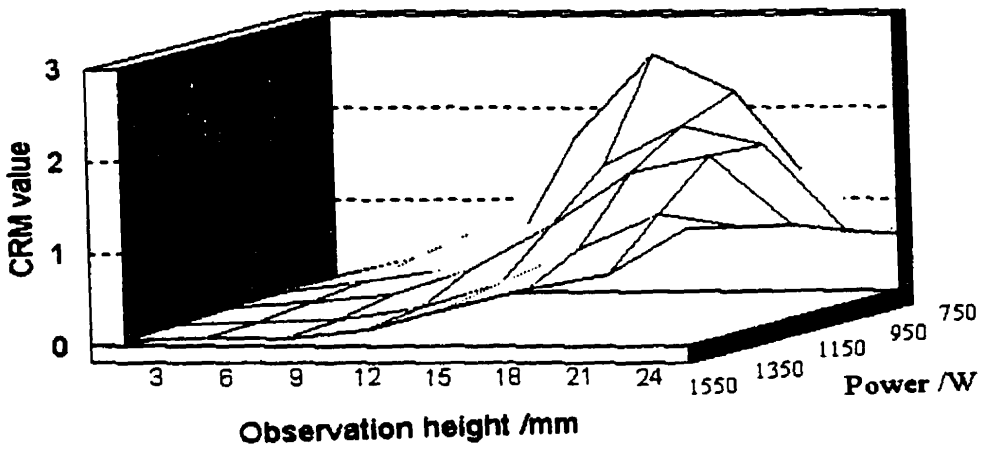

Figure 4.8 Surface obtained using the CRM method.

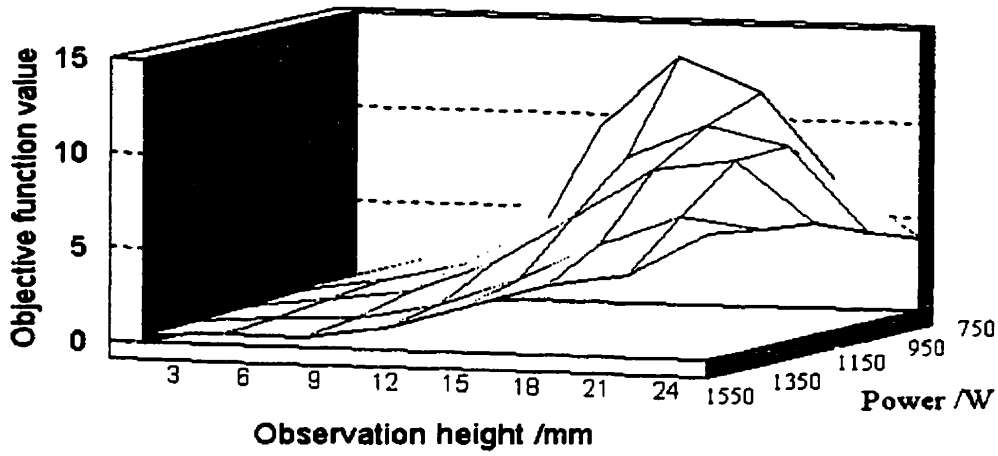

Figure 4.9 Surface obtained using Leary's objective function.

Given that the response surfaces were relatively similar for the various elements, several artificial 'elemental' surfaces were generated to compare the two approaches . Two of these models depicting extreme situations are presented (Figures 4.10 and 4.11). The first model (Figure 4.10) illustrates SBR surfaces of two elements that peak under completely different instrumental operating conditions but with approximately the same SBR at the top of the peak. The surfaces obtained using both the CRM approach and Leary's objective function are very similar, peaking under the same operating conditions. The second model (Figure 4.11) is similar to the first except the SBRs of the two elements at the maximum peak height are completely different. Again, the surfaces obtained using the CRM and Leary's objective function are very similar. All models generated gave the same operating conditions or produced the same situation described earlier where Leary's objective function performed better since the CRM decreased the difference between the SBRs.

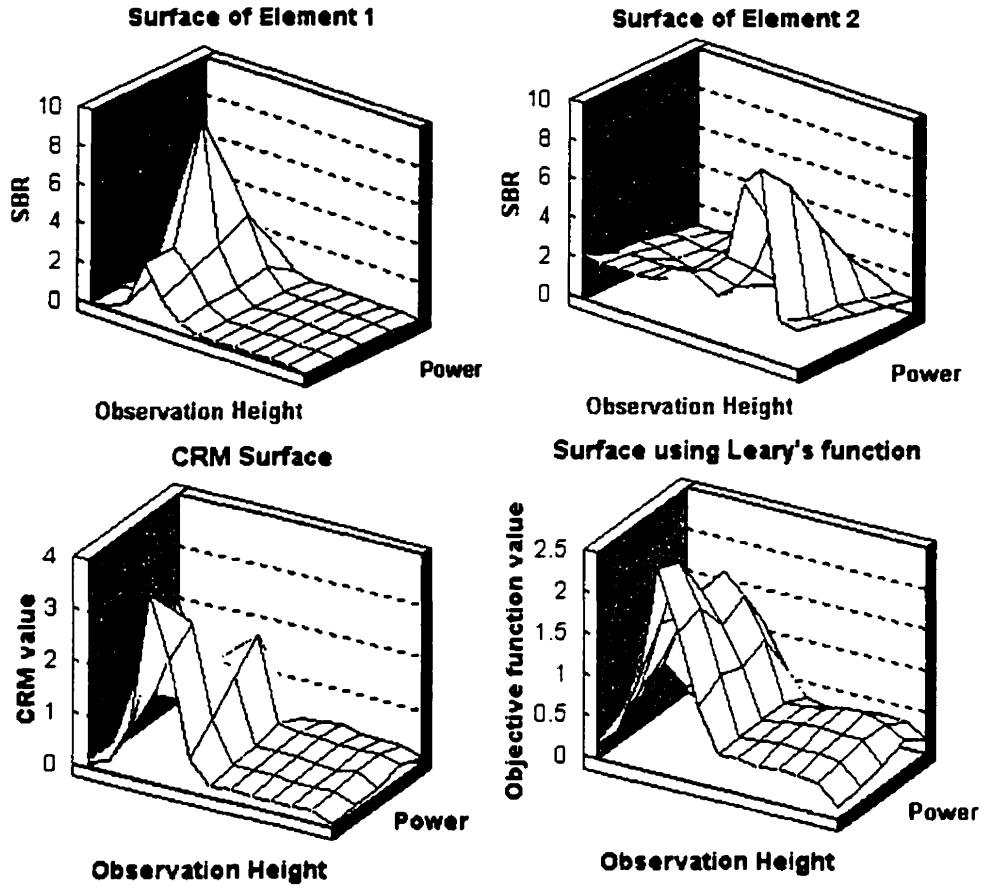

Figure 4.10 Theoretical model of two elements with similar SBRs.

Signal-to-background ratios are convenient to use for optimization since fewer measurements are required compared to SNRs and they often are easily related to detection limits. While one expects SBRs to vary widely, SNRs should be relative similar given concentrations well above the detection limit. In this case the CRM may be advantageous. With many ICP-MS instruments one tends to adjust a variety of operating parameters (e.g. lens settings) to obtain a roughly uniform sensitivity for all elements. Because of its tendency to promote uniformity of performance, the CRM may be more advantageous when used with a technique such as ICP-MS.

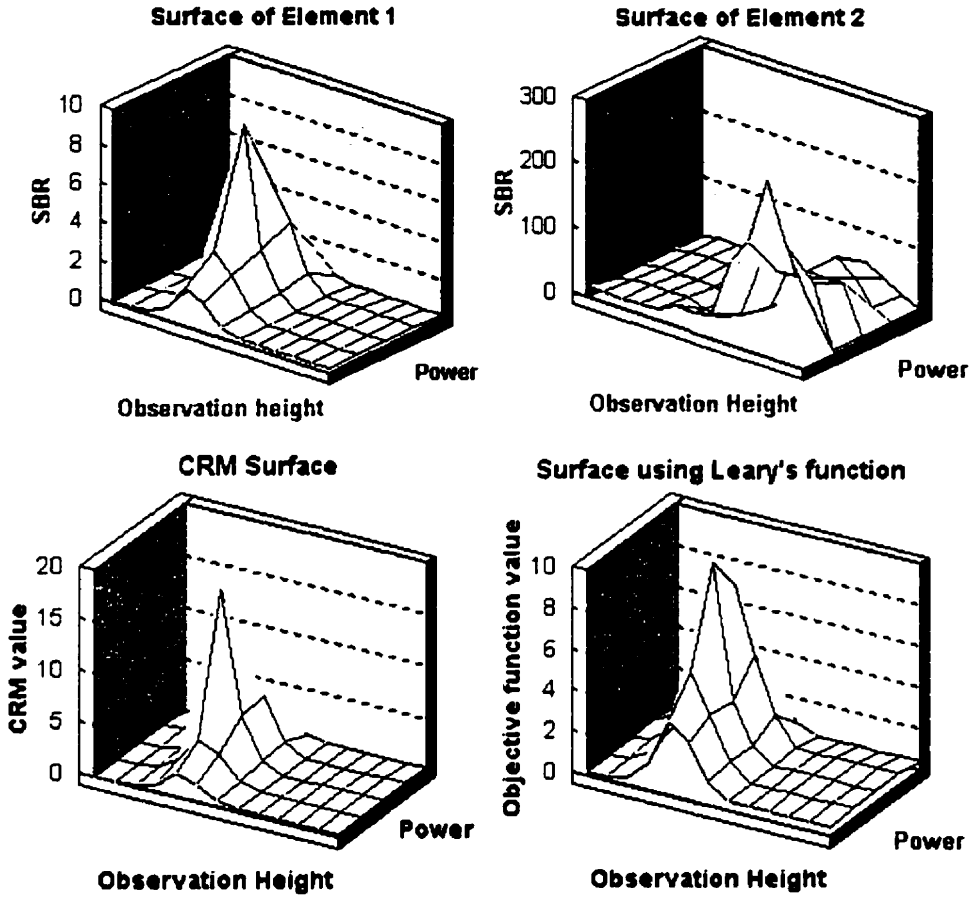

Figure 4.11 Theoretical model of two elements with dissimilar SBRs.

Both objective functions, Leary's and the CRM, could easily use SNRs, accuracy or any of the other figure of merits mentioned previously instead of SBRs in the computation of the objective function values. They could also be applied to optimization of the other instrument parameters (e.g., gas flow rates, solution pump rate to the nebulizer) using any group of analyte elements. With the evolution of instruments, most instruments perform simultaneous multi-element analysis rapidly and are completely computer controlled. The use of these objective functions would be ideal in the optimization of these instruments since the information for the optimization is readily available and the computations involved are trivial relative to the computational power of modern computers.

4.5 Acknowledgments

The authors gratefully acknowledge the financial support from National Sciences and Engineering Council of Canada. C. S. acknowledges financial support from Fonds pour la Formation de Chercheurs et l'Aide à la Recherche.

4.6 References

1 Branagh, W.A., Whelan, C., Salin, E.D., J. Anal. At. Spectrom., 1997, in press.

2 Boumans, P. W. J. M., ed., *Inductively Coupled Plasma Emission Spectroscopy Part I: Methodology, Instrumentation, and Performance*, Wiley-Interscience, New York, 1987, pt. 1, vol. 90, ch. 4. pp. 100-257.

3 Ebdon, L., Cave, M. R., and Mowthorpe, D. J., *Anal. Chim. Acta*, 1980, 115, 179.

4 Norman, P. and Ebdon, L., *Anal. Proc.*, 1986, 23, 420.

5 Werner, P. and Friege, H., *Appl. Spectrosc.*, 1987, 41, 32.

6 Galley, P. J., Horner, J. A., and Hieftje, G. M., *Spectrochim. Acta*, 1995, 50B, 87.

7 Leary, J. J., Brokes, A. E., Dorrzapf, A. F., Jr., and D. W. Golightly, *Appl. Spectrosc.*, 1982, 36, 37.

8 Terblanche, S. P., Visser, K., and. Zeeman, P. B, *Spectrochim. Acta*, 1981, 36B, 293.

9 Ebdon, L. and Carpenter, R. C., *Anal. Chim. Acta*, 1987, 200, 551.

10 Kalivas, J. H., *Appl. Spectrosc.*, 1987, 41, 1338.

11 Moore, G. L., Humphries-Cuff, P. J., and Watson, A. E., *Spectrochim. Acta*, 1984, 39B, 915.

12 Belchamber, R. M., Betteridge, D., Wade, A. P., Cruickshank, A. J., and Davison, P., *Spectrochim. Acta*, 1986, 41B, 503.

13 Thomas, R. J. and Collins, J. B., *Spectroscopy*, 1990, 5, 38.

14 Lorber, A., *Anal. Chem.*, 1986, 54, 989.

15 Lide, D. R., ed., *CRC Handbook of Chemistry and Physics*, 76th ed., CRC Press, New York, 1995-6, pp. 10-207, 10-208.

Chapter 5

Optimization in ICP-AES was suitable for the purpose of the development of an objective function due to the simple response surface. A more challenging application of optimization can be found in ICP-mass spectrometry (MS). In ICP-MS systems, the ion optics settings may discriminate ions based on their mass which can result in poor analyte signals. This phenomenon may be observed when the ion optics settings are adjusted using the response of a light element; the result, poor signals for the heavy analytes. The reverse scenario can also be observed. To ensure that the ion optics settings are optimal for both heavy and light analytes in a sample, these settings must be tuned either manually or using an optimization algorithm.

This chapter evaluates various aspects of the optimization algorithm. It contains a study of the effect of the initial operating conditions, the selection of an objective function, and the performance of multi-element and single element optimizations. This work was published in Appl. Spectrosc., 1998, 52, 643.

5 Program Considerations for Simplex Optimization of Ion Lenses in ICP-MS

5.1 Abstract

The performance of an inductively coupled plasma mass spectrometer (ICP-MS) is dependent on the ion optic bias potentials. A discussion of the multi-element optimization of the ICP-MS ion optics bias potentials using a Simplex algorithm is presented. Three objective functions were tested: a function developed by Leary; the combined ratio method (CRM); and the Euclidean distance from multicriteria target vector optimization. Both the Leary and the target vector optimization's performances were comparable whereas, the CRM optimizations placed an emphasis on obtaining similar signal intensities. Experiments determined that an initial Simplex starting size of 20% of the parameter space was optimal. A method for the selection of an appropriate target vector by predicting analyte signal intensity was also investigated. Signal intensities for all elements could be predicted with an acceptable margin of error (10-30 %), provided the same conditions were used. Comparisons of optimizations using a single mid-mass element versus multi-element optimizations revealed that the multi-element approach is only slightly better. If the analyst wished to optimize lens settings to favor heavy or light elements, then an average mass was better than a mid-mass optimization.

5.2 Introduction

In the inductively coupled plasma mass spectrometer (ICP-MS), ions produced in the plasma are extracted through a sampling interface region using sampler and skimmer cones. The extracted ions are focused into a narrow beam using one or more ion lenses before entering the quadrupole mass filter. The Elan 250-5000 series of ICP-MS instruments use a number of ion lenses including Einzel lenses (E1), Photon Stop (S2), Plate lenses (P) and Bessel Box (B). Optimization of the voltage settings of the ion lenses is critical for optimal performance of this type of ICP-MS.

An earlier study by Schmit and Chtaib[1] demonstrated that analyte signals of an Elan 250 ICP-MS were dependent on the applied bias potentials of the input ion optics. The transmission efficiency of the ion optics is dependent on the mass of the analyte and can vary significantly for widely different masses (e.g. B and Tl). This is due to the higher kinetic energy of the higher mass elements which results in lower sensitivity to changes in the ion lens voltage. For example, if one optimizes the ion lenses using a low mass element, the sensitivity of the high mass elements are negatively affected and vice versa. In general, if one optimizes lens voltages at some compromise for both light and heavy elements, then the response signals for both light and heavy elements will be compromised.

Optimization studies of the plasma operating parameters and ion lens voltages have appeared in the literature for most, if not all commercially available systems. In most routine laboratories, optimization of ion lenses using the Elan 250-5000 series of ICP-MS instruments is carried out manually using a univariate optimization procedure, with one or two elements. The process is tedious and can be quite subjective depending on the operator's choice of elements. Frequent ion lens optimization is generally not required for single operator, routine analysis, however, in laboratories with many operators and with many applications using different settings, tuning of the ion lenses may be required. Univariate optimization techniques become time consuming and inefficient when dealing with many variables that require a large number of

measurements to cover a wide range of instrument settings. The range of instrument settings can be considered a multi-dimensional surface for the optimization. Univariate optimizations do not cover the whole surface (parameter space), making it possible for the operator to miss the maximum. If the variables being optimized are dependent on each other then a change in one variable affects other variables. A univariate optimization would not perform well in such a situation since this approach assumes that the variables are independent. Relatively few studies in optimization of the ICP-MS have made use of the Simplex technique which is simple, rapid and efficient in such a system[2-5]. Evans and Caruso[3] used Simplex optimization of ion lenses for reducing matrix induced signal suppression by tuning the ion lenses in the presence of the matrix. Schmit and Chauvette[4] used the Ar_2^+ (m/z=76) signal intensity to test their Simplex optimization of the ion lens voltages. They also compared the signals obtained using their Simplex approach to the manual optimization of ion lenses by a skilled operator and found improvements in ion transmissions of 33% for Li and up to 380% for U. Evans and Ebdon[5] and van der Velde-Koerts and de Boer[2] demonstrated the use of the Simplex technique in the optimization of the plasma operating parameters. Ford *et al.*[6] used the Simplex technique for the multi-element optimization of the plasma parameters and the ion optics, though their study was focused on signal-to-background ratios (SBRs) of the analytes. This Simplex approach was used to optimize operating conditions across the elemental mass range for argon and mixed gas plasmas.

The objective of this study was to investigate the best approach to ICP-MS optimization using a Simplex algorithm. Another goal of this study was the development of a practical procedure for the optimization of ion lenses. The procedure should be at least as fast as an expert operator would determine the best settings manually. Aspects of the multi-element optimization algorithm such as the selection of the initial search size and the selection and application of objective functions based on analyte response were examined.

5.3 Experimental

A Perkin-Elmer Sciex Elan 500 ICP-MS, with Elan 5000 software, was used throughout with the operating conditions found in Table 5.1. Sample was introduced into the ICP-MS at a flow rate of 1 ml min^{-1} using a peristaltic pump. The operating conditions shown in Table 5.1 were chosen, because they are typical for routine ICP-MS analysis. The uncertainty of analyte signal intensity presented in all of the tables and figures was determined using 25 replicate measurements with a typical relative standard deviation of approximately 5%. Each of the four lenses of the ion optics in the ICP-MS has its own voltage range (Table 5.1) which is individually controlled and scaled from 0 to 99 on the instrument control panel. Adjustment of the ion lens voltages was carried out manually. The Simplex program was run on a separate personal computer. Standards and blank solutions were prepared in 0.2% HNO_3. Standards containing 100 ng ml^{-1} of analyte were prepared by serial dilution from stock solutions (1000 ug ml^{-1}).

Table 5.1 Instrumental operating and data acquisition parameters of ICP-MS.

ICP Mass Spectrometer	
RF power	1000 W
Coolant Ar flow	15.0 l min^{-1}
Auxiliary Ar flow	1.4 l min^{-1}
Nebulizer Ar flow	1.0 l min^{-1}
Sample introduction	1.0 ml min^{-1}
Data Acquisition	
Dwell Time	20 ms
Scan mode	peak hopping
number of masses (m/z) monitored	2-7
number of replicates	25
signal measurement	counts s^{-1}
resolution	0.7 a.m.u. at 10% peak height.
Lens voltages	
Einzel lenses E1	-0.1 to -20.3 V
Photon Stop S2	-0.01 to -20.2 V
Plate lenses P	-0.2 to -60.1 V
Bessel box B	+0.1 to +10.1 V

5.3.1 Simplex Optimization

The optimization algorithm used in this study was the modified Simplex described by Morgan and Deming[7]. Optimization techniques generally require a single value representing the response at a set of operating conditions but multiple response values (one for each element) are actually obtained. For single element optimization in ICP-MS the objective function is the analyte signal intensity. For multi-element analyses, an objective function was used to convert the multiple response values into a single value. There are several types of objective functions for multi-element responses that may be used[8]. Two will be considered for this study. In the first, response values for m analyte signals ($y_1,...,y_m$) are united to form a new artificial one, $y^* = f(y_1,...,y_m)$. The optimization technique would use y^* as a multiple compromise value and the optimal conditions will result in the best compromise for all m analyte signals. Such an objective function for optimizing the ICP-MS could take the same form as an objective function developed for inductively coupled plasma atomic emission spectrometry (ICP-AES) using SBRs by Leary *et al.*[9]. The objective function was:

$$F = \frac{n}{\sum_{i}^{n} (SBR)_i^{-1}}$$

where n is the number of analytes and SBR_i is the SBR of the *i*th analyte. The purpose of this function is to find the best compromise by maximizing the lower SBRs at the expense of the larger SBRs. For the optimization of the ICP-MS the objective function studied was:

$$y^* = \frac{n}{\sum_{i}^{n} (S)_i^{-1}}$$

where n is the number of analytes and $(S)_i$ is the response of the *i*th analyte.

Another objective function of this type was investigated. It was originally developed in our laboratory for optimizing ICP-AES and it can also be applied to ICP-MS. This objective function was called the Combined Ratio Method[10] (CRM) and takes the form:

$$CRM = \frac{\sum_{i}^{n}(S)_i}{\sum_{j}^{k} R_j}$$

where n is the number of analytes, $(S)_i$ is the response of the *i*th analyte, k is (n-1) + (n-2) +...+ 1, and R_j is the ratio of two given analytes (*j*th combination) where the maximum response of the two is in the numerator such that $R_j \geq 1$. The CRM performs a weighted average on the sum of the analyte responses. For these objective functions the Simplex algorithm tries to maximize the y* or CRM value.

The second type of objective functions is based on multicriteria target vector optimization[8]. This optimization requires that the operator select "optimal" values for the signals for the analytes. The algorithm then tries to find settings that would produce analyte signals that are closest to the "optimal." The actual response value vector for the m analytes will be defined as $(y_1(a),...,y_m(a))$, where (a) stands for actual and y(a) is the experimentally obtained response value for an analyte. The goal of this approach is to achieve a desired response target vector $(y_1(t),...,y_m(t))$, where (t) stands for target and y(t) is the target response value set by the operator. The objective function then becomes the Euclidean distance, $d_E(t-a)$, between the target and the actual response vectors

$$d_E(t-a) = \left(\sum_{i}^{m} [y_i(t) - y_i(a)]^2 \right)^{1/2}$$

In the optimization of the ICP-MS, $y_i(a)$ will be the signal intensity counts obtained for the *i*th analyte and $y_i(t)$ will be the desired signal intensity counts for that analyte. The Euclidean distance was not calculated using the above equation since changes in smaller values would not be weighted as much as changes in larger values; the normalized Euclidean distance was used instead.

$$d_E(t-a) = \left(\sum_{i}^{m} \left[\frac{y_i(t) - y_i(a)}{y_i(t)} \right]^2 \right)^{1/2}$$

The Simplex algorithm's goal is to minimize the distance between the actual and target vector. Prior to performing a multicriteria target vector optimization, an appropriate target must be selected. The values in the target vector must always be greater than the

maximum obtainable responses. If the responses are greater than the target values then the values in the target have been underestimated. Due to the nature of the calculation of the Euclidean distance ($\sqrt{(distance^2)}$) this would result in a distance that may not be considered as a good response even though it is better than the target vector. The value of each element in the target vector plays an important role in how well the optimization will perform. Consider two elements, Al and Pb, whose maximum obtainable signals are, for example, 50000 and 100000 counts, respectively and which will be denoted by the vector [50000,100000]. If an arbitrary target vector was chosen to be, [60000,200000] then changes in Al are weighted move heavily than those of Pb. This is because the values in the target vector for Al and Pb are 120% and 200%, respectively, of the maximum obtainable signals. A good target vector would be [60000,120000] since both values would be 120% of the maximum obtainable signals. In general, to obtain a good target vector, all the values of the analytes in the target vector should be set at the same percentage level with respect to the maximum obtainable signals. This may be difficult in practice since the maximum possible signals may be unknown.

The initial settings for the lenses for the optimization were set to cover 20% of the parameter space unless indicated otherwise. The optimization was terminated when the search space was reduced by the Simplex to 5% of the total parameter space.

5.4 Results and Discussion

5.4.1 Comparison of objective functions

In simultaneous multi-element optimizations, the objective function determines the best compromise for all the elements. Three objective functions were tested: Leary's function, the CRM and the multicriteria target vector optimization function. Two sets of optimizations were performed to cover the mass range of the periodic table. One set of optimizations included Al and Pb and the other set included B and Tl. The best compromise lens voltages found by the Simplex for both sets of optimizations are listed in Table 5.2. The lens voltages obtained are similar for all three objective functions within each set of optimizations. Both Leary's function's and the multicriteria target vector optimization function's performances are comparable. In terms of total counts, the

multicriteria target vector optimization function does slightly better (~10%) than Leary's function. The CRM's compromise places more emphasis on obtaining similar and maximal intensities. The number of steps taken by the Simplex did not differ significantly among objective functions.

Table 5.2 Best settings obtained from the optimizations of Al and Pb, and B and Tl.

Function		**Lens voltages (V)**				**Intensity (Counts s^{-1})**	
	Steps	B	E1	P	S2	Al	Pb
Leary	15	5.3	-10.7	-30.5	-10.6	58400	27000
CRM	20	5.4	-10.5	-25.0	-9.6	37910	39790
Target	20	4.1	-15.0	-28.1	-11.7	60050	33350
						B	Tl
Leary	34	4.9	-18.0	-31.7	-12.1	9735	15440
CRM	24	5.7	-15.0	-31.1	-9.6	11050	12270
Target	33	5.6	-15.2	-29.9	-9.8	10630	17480

5.4.2 Initial Simplex starting sizes

The selection of an initial starting size of the search space for the Simplex algorithm is not an obvious one. Three starting sizes of the search space were examined on an optimization of two elements, Cu and Tb (Table 5.3) using a multicriteria target vector optimization. The three starting sizes studied were 20%, 50% and 70% around the center of the parameter space. All three initial starting sizes resulted in relatively similar compromise values for the two elements although the Simplex did not necessarily find the same lens settings since the response surface has many local minima[4]. The number of steps and therefore the time required for the Simplex optimization was the deciding factor in the selection of the initial starting size. A Simplex starting with 20% of the parameter space required approximately half the number of steps to completion compared to starting sizes of 50% and 70% of the parameter space. In terms of signal intensity, a starting size of 20% was sufficient. Therefore for the remainder of the experiments in this study, a starting size of 20% was used.

Table 5.3 Selection of initial starting size.

Starting Size		Lens voltages (V)				Intensity (Counts s^{-1})	
	Steps	B	E1	P	S2	Cu	Tb
20%	16	3.2	-10.5	-25.0	-8.4	13680	103600
50%	31	2.9	-7.2	-15.4	-5.7	17230	75210
70%	37	2.8	-5.6	-14.7	-5.5	14070	83680

5.4.3 Presence of drift

A potential limitation in this type of optimization study is the presence of instrumental drift which we observed and which has been reported in other studies[3,6]. Drift is a common problem with older electronics and instruments such as the Elan 500. The first 3-5 steps of the optimizations, independent of the objective function used, were the same and therefore they could be used as indicators of drift since they were looked at 3 different times. To verify the presence (or lack) of drift, the ratio of the 2 elements studied, one heavy and one light, was calculated since heavier elements tend to drift more than lighter ones on our spectrometer. For each step taken by the Simplex, the ratios did not exhibit significant variation, so it was concluded that the line intensities were not drifting significantly within the time period of these optimizations. It is also worth noting that the experimental drift may have been observed in some previous studies because their Simplex optimizations required 2-5 hours, whereas 10-15 minutes was usually required in this study.

5.4.4 Determination of a Target Vector

The approach used for determining a good target for all of the elements in the periodic table required the optimization of the ion lenses for a single reference element, which could be used to predict optimum signal intensities of all of the elements in the periodic table. By knowing the optimum signal intensity of one element it should possible to calculate the optimum signal intensities for any single element using the same Simplex and instrumental settings (rf power and carrier flow). It is possible to estimate the optimum signal intensity of any element relative to another provided the atomic mass,

kinetic energy, natural abundance and degree of ionization are known. The kinetic energy of the ions[11] provides information about the transmission efficiency of ions through the sampler and skimmer cones as well as through the ion lenses[12]. In general heavier ions, with higher momentum should have high transmission efficiencies as they are less prone to problems such as spaces-charge effects. For a given atomic mass m, the kinetic energy[11], KE, can be calculated in units of eV using:

$$KE = a*m + b \text{ eV}$$

In our system, the values for a and b were 0.026 and 2.0, respectively, and m is the atomic mass. Parameters such as natural abundance and degree of ionization[13], provide information about the populations of ions in the plasma and therefore signal intensities should be proportional. The assumptions made were that identical analyte concentrations are used; the analytes are in the same matrix and identical conditions are used. Using the signal intensity from a reference element (e.g. ^{103}Rh), the relative signal intensity counts of each element in the test sample could be predicted using:

$$\text{Pred. Signal}_A = \text{Signal}_{Ref} * \frac{Ab_A * Ion_A * KE_A}{Ab_{Ref} * Ion_{Ref} * KE_{Ref}}$$

where A is the element of interest, Ref is the reference element, Pred. $Signal_A$ is the signal predicted for element A, $Signal_{Ref}$ is the signal obtained for the reference element, Ab is the percent abundance, Ion is the degree of ionization[13], and KE is the kinetic energy. ^{103}Rh was selected as the reference element because its mass lies in the middle of the mass range. A Simplex was performed using ^{103}Rh to obtain its maximum signal for use as a reference point. The Predicted Signal was then calculated for seven elements (Table 5.4). Simplex optimizations were performed for each of the seven elements to acquire the maximum obtainable (or close to it) signal. A comparison of the Predicted Signal and the maximum experimentally obtained signal intensities are summarized in Table 5.4. For most of the elements, the Prediction Signal was within 20% of the maximum signal intensity obtained by experiment. Copper was the only element whose signal intensity was not predicted accurately. This approach was then used to predict appropriate values for the target vector by setting the values in the target vector to 120% of the Predicted Signal for each analyte. Overall, this approach for selecting a target

vector was successful, however, it must be kept in mind that the purpose of this study is not to accurately predict the signals of elements but to find a good target vector.

Table 5.4 Predicted and experimentally obtained signal intensities for selected elements.

Element	Kinetic Energy (eV)	Degree of Ionization	Predicted Signal (Counts s^{-1})	Experimental Signal (Counts s^{-1})	Error (%)
^{103}Rh (100%)	4.68	0.96	-	58770	-
^{111}Cd (13%)	4.89	0.85	7113	6444	10
^{140}Ce (88%)	5.64	0.98	65361	66980	-2
^{159}Tb (100%)	6.13	0.99	81161	121800	-33
^{208}Pb (52%)	7.41	0.98	50228	61560	-18
^{45}Sc (100%)	3.17	1.00	42244	37800	12
^{63}Cu (69%)	3.64	0.92	30233	18190	66

5.4.5 Approaches to Mass Selection for Optimization

It is more time consuming to optimize the ion lenses for each of the analytes present in a sample. Optimizing for a single element takes less time and finding an objective function is not necessary. One of the goals of these experiments was to compare optimizations using a mid-mass element and a multi-element response function. A mid-mass element is routinely used for operating parameter adjustments prior to the analysis of samples. To simplify this study, the multi-element optimizations were performed using only two elements. The middle of the atomic mass range of the elements is calculated by:

$$\text{mid - mass} = \frac{\text{Mass}_{high} + \text{Mass}_{low}}{2}$$

where Mass_{high} is the atomic mass of the heaviest element and Mass_{low} is the atomic mass of the lightest element in the analysis. The element, that has an atomic mass closest to the calculated mid-mass, is used as the mid-mass element. Optimizations using mid-mass elements (Tables 5.5 and 5.6) provided higher signal intensities (~8 and 9 %) for the heavier elements than the multi-element optimizations. Multi-element optimizations performed significantly better (~29 and 61 %) for the lighter elements as compared to mid-mass optimizations. The number of steps taken by the Simplex to perform each optimization did not vary considerably and was not a factor. Overall, multi-element

optimizations achieve better results than mid-mass element optimizations, however, the lens voltages obtained using mid-mass element optimizations may be adequate for most routine analyses.

Table 5.5 Best settings obtained in the multi-element (Al and Pb) ptimization and the mid-mass (Sn) optimization.

Elements Optimized	Steps	**Lens voltages (V)** B	E1	P	S2	**Analytes** Al	Pb
Al-Pb (27-208)	20	4.1	-15.0	-28.1	-11.7	52810	30660
Sn (118)	19	5.4	-9.5	-29.9	-10.8	40960	33290

Table 5.6 Best settings obtained in the multi-element (B and Tl) optimization and the mid-mass (Ag) optimization.

Elements Optimized	Steps	**Lens voltages (V)** B	E1	P	S2	**Analytes** B	Tl
B-Tl (11-203)	21	4.8	-12.5	-26.2	-10.6	20570	24030
Ag (107)	15	6.1	-8.2	-24.4	-8.2	12800	25980

In a sample containing more than two analytes, the equation used to calculate the mid-mass element will always give the middle atomic mass between the two elements at the extremes of the sample's mass range regardless of the other analytes in the sample. If a sample consisted of five light elements and one heavy element, it may not be reasonable to use the mid-mass element. An alternative is to calculate the average atomic mass of the analytes, and find an element with corresponding atomic mass. The mid-mass and average-mass elements were used for the optimizations of two sample types. One sample consisted of five heavy and one light element and the second consisted of five light and one heavy element. The optimizations on the first sample (containing the analytes Li, Ba, Ce, Tl, Pb, and Bi) were done using Ag as the mid-mass element and Eu as the average-mass element (Figure 5.1). All the elements with atomic weights above that of Eu saw an increase in signal when the average-mass element, Eu, was used as compared

to the signals obtained when the mid-mass element, Ag, was used; however, all the elements with atomic weights lower than that of Eu saw a decrease in signal when the average-mass element, Eu, was used and the signal for Li suffered the most. The optimizations on the second sample (containing the analytes Li, B, Al, Mn, As, and Bi) were done using Ag as the mid-mass element and Zn as the average-mass element (Figure 5.2). Using the result of the optimization of the average-mass element, Zn, showed an improvement in all the analyte signals except for Bi, which decreased, as compared to using the result of the optimization of the mid-mass element, Ag. The two average-mass elements, Eu and Zn, used in these two samples were both approximately 44 mass units away from the mid-mass element, Ag. Two other samples were made such that the average-mass element and the mid-mass element did not have such a large difference in mass. The first sample contained the analytes B, Co, Ag, and Tl where the mid-mass element was Ag and the average-mass element was Mo.

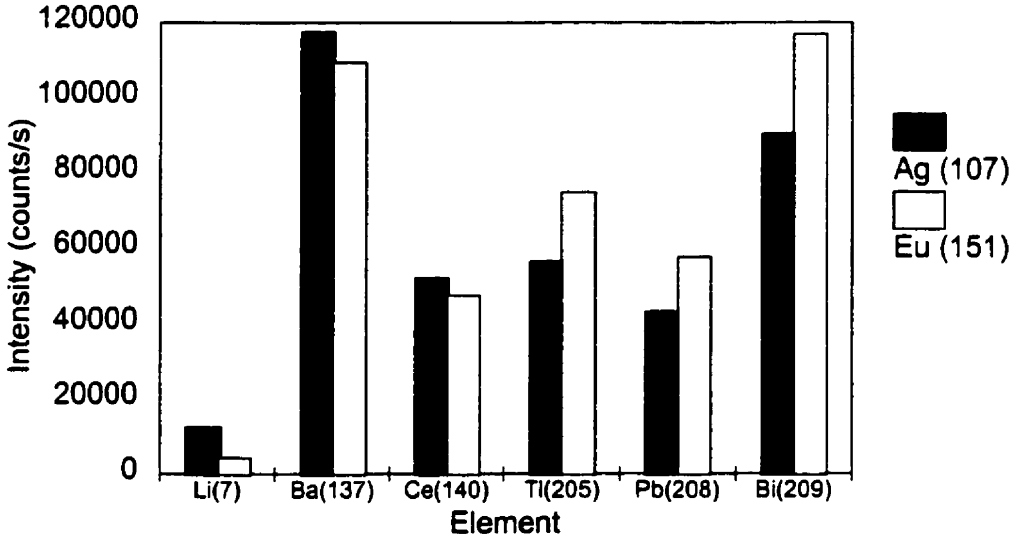

Figure 5.1 Optimization for a solution containing the elements ^{7}Li, ^{138}Ba, ^{140}Ce, ^{203}Tl, ^{208}Pb, and ^{209}Bi. Optimizations were done with a mid-mass element (^{107}Ag) and an average mass element (^{151}Eu).

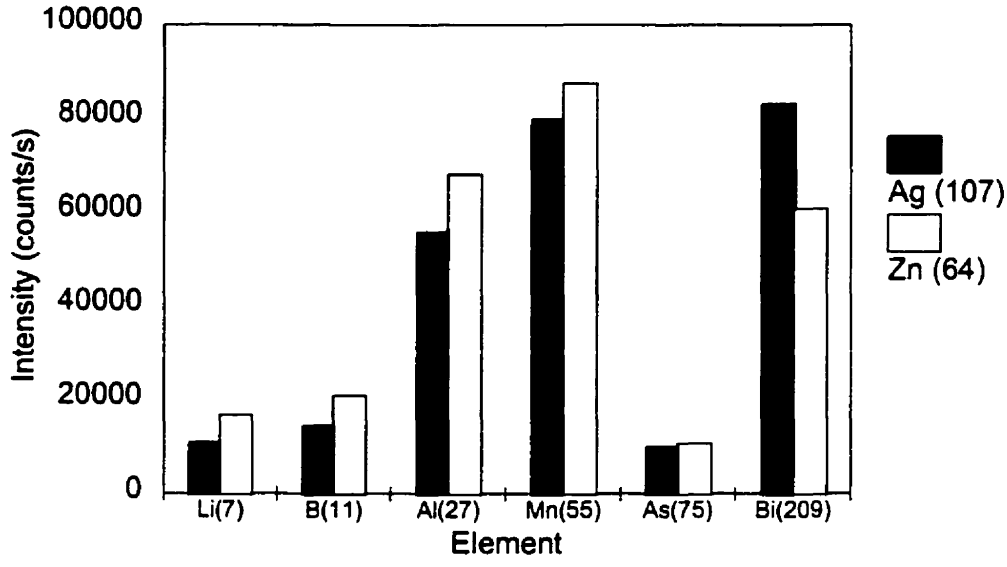

Figure 5.2 Optimization for a solution containing the elements ^{7}Li, ^{11}B, ^{27}Al, ^{55}Mn, ^{75}As, and ^{209}Bi. Optimizations were done with a mid-mass element (^{107}Ag) and an average mass element (^{64}Zn).

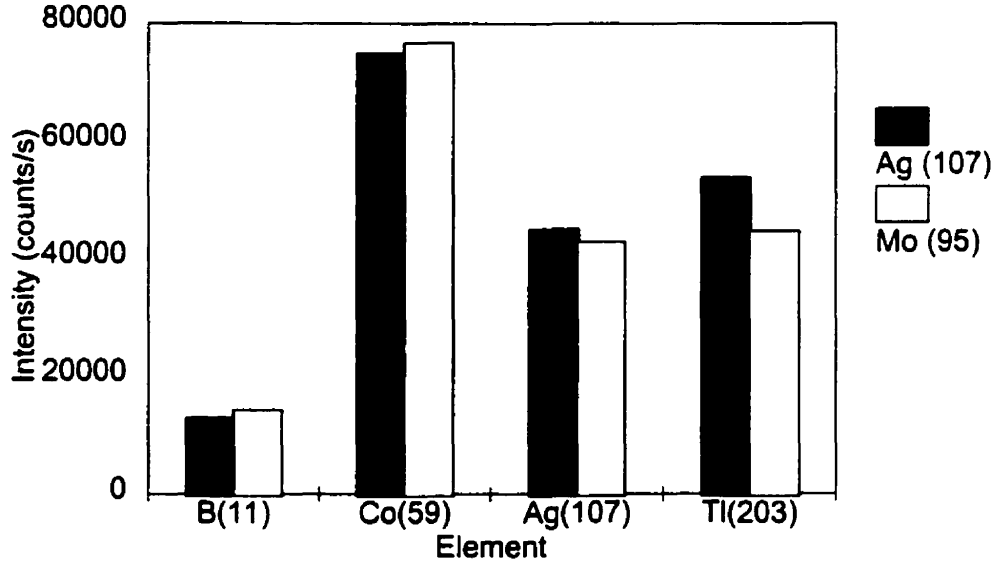

Figure 5.3 Optimization for a solution containing the elements ^{11}B, ^{59}Co, ^{107}Ag, and ^{203}Tl. Optimizations were done with a mid-mass element (^{107}Ag) and an average mass element (^{95}Mo).

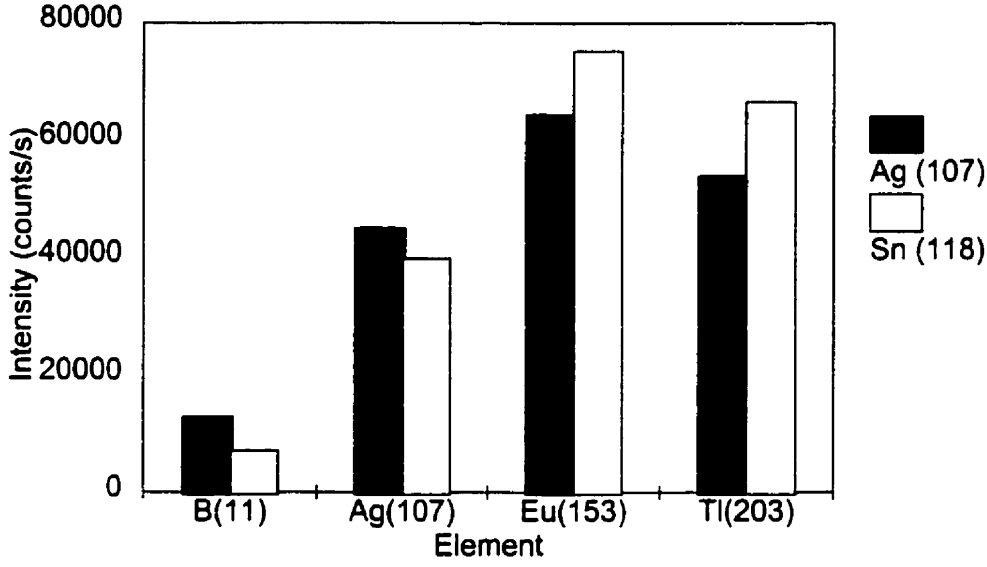

Figure 5.4 Optimization for a solution containing the elements ^{11}B, ^{107}Ag, ^{151}Eu, and ^{203}Tl. Optimizations were done with a mid-mass element (^{107}Ag) and an average mass element (^{118}Sn).

The second sample contained the analytes B, Ag, Eu, and Tl where the mid-mass element was Ag and the average-mass element was Sn. In these samples, both Mo and Sn are approximately 12 mass units from Ag in either direction. The results are depicted in Figures 5.3 and 5.4. For the first sample, Mo is slightly better for the lighter elements at the expense of the heavy element when compared to Ag. The second sample showed an improved signals for the heavier elements at the expense of the light element.

In general the selection between using the mid-mass element and the average-mass element depends on whether it is desirable to bias towards the mass region with the most analytes. Biasing the ion lenses using an average mass rather than a mid-mass can have significant effects on analyte signal intensity.

5.5 Acknowledgments

The authors would like to acknowledge Dr. D. Conrad Gregoire for his collegial support and instrumental expertise. DG thanks the Natural Sciences and Engineering Research

Council of Canada (NSERC) for scholarship support. CS gratefully acknowledges support by FCAR of the Province of Quebec. The authors wish to acknowledge the general support of NSERC.

5.6 References

1 Schmit, J.P. and Chtaib, M., *Can. J. Spectrosc.*, 1987, 32, 56.

2 van der Velde-Koerts, T., and de Boer, J.L.M., *J. Anal. At. Spectrom.*, 1994, 9, 1093.

3 Evans, E.H. and Caruso, J.A., *Spectrochim. Acta*, 1992, 47B, 1001.

4 Schmit, J.P. and Chauvette, A., *J. Anal. At. Spectrom.*, 1989, 4, 755.

5 Evans, E.H. and Ebdon, L., *J. Anal. At. Spectrom.*, 1991, 6, 421.

6 Ford, M.J., Ebdon, L., Hutton, R.C., and Hill, S.J., *Anal. Chim. Acta*, 1994, 285, 23.

7 Morgan, S.L. and Deming, S.N., *Anal. Chem.*, 1974, 46, 1170.

8 Wienke, D., Lucasius, C., and Kateman, G., *Anal. Chim. Acta*, 1992, 265, 211.

9 Leary, J.J., Brokes, A.E., Dorrzapf, A.F., Jr., and Golightly, D.W., *Appl. Spectrosc.*, 1982, 36, 37.

10 Sartoros, C. and Salin, E.D., *J. Anal. At. Spectrom.*, 1997, 12, 13.

11 Fulford, J.E. and Douglas, D.J., *Appl. Spectrosc.*, 1986, 40, 971.

12 Niu, H. and Houk, R.S., *Spectrochim. Acta*, 1996, 51B, 779.

13 Houk, R.S., *Anal. Chem.*, 1996, 58, 97A.

Chapter 6

The calibration methodology selection component is found in both the Analysis of an Unknown Sample module and the Learn to Run a New Sample module. In both modules, this component is responsible for determining the best calibration methodology to be used for an analysis. One of the calibration methodologies that might be selected is the methodology external calibration with internal standards. If the Autonomous Instrument selects this methodology, the question becomes "How does it select elements to be used as internal standards?".

In ICP-MS, the use of internal standards is very common and the Autonomous Instrument will be required to find suitable elements to be used as internal standards for samples to be analyzed. There are several rules that trained operators use for the selection of internal standards which involve the matching of the mass and the ionization potential of the internal standard to the analyte of interest. This chapter examines the use of these rules in the development of an algorithm for the automatic selection of internal standards. This work was accepted for publication in Spectrochimica Acta.

6 Automatic Selection of Internal Standards in ICP-MS

6.1 Abstract

The automatic selection of internal standards in inductively coupled plasma-mass spectrometry was performed using a cluster analysis algorithm. The samples contained twenty-five analytes, spanning the atomic mass and ionization potential ranges, and a single interfering element. The interferents examined were Na, Mg, K, Zn, Ba, and Pb. The cluster analysis algorithm used kinetic energy, ionization potential, oxide bond strength, hydride bond strength, and electronegativity, to group the analytes. These variables were weighted differently in the various matrices. The performance of the clustering method and selection of internal standards was good for most analytes in the various matrices.

6.2 Introduction

Most analytical techniques are susceptible to interferences and inductively coupled plasma mass spectrometry (ICP-MS) is no different. ICP-MS does not suffer from spectral interferences to the same extent that inductively coupled plasma atomic emission spectrometry (ICP-AES) does whereas the opposite can be said of chemical-induced matrix effects. Several calibration techniques can be used to determine the concentration of analytes in a sample[1]. External calibration is one of the easiest and most used techniques; however, it is also the one most prone to errors arising from ionization interferences. The external calibration methodology involves the preparation of standards, containing varying amounts of the analyte in a clean solvent, and the generation of a calibration curve. The response of the analyte is generally assumed to be linearly dependent on its concentration. Inaccuracies in the results can occur if the standards do not accurately represent the sample matrix. The technique of standard additions provides higher accuracy in difficult samples but this technique can be very time consuming to perform since at least two measurements must be taken on each sample: one on the sample itself and one (or more) after the sample has been spiked. Another technique used in ICP-MS is isotope dilution. This is a very accurate technique but it has two disadvantages: the first is that it is not applicable to monoisotopic elements. The second is that it can be very expensive to buy many enriched isotopes. One of the most common calibration methodologies used on ICP-MS is external calibration with internal standardization. The selection of internal standards is not always easy. In selecting internal standards, several rules must be followed: (1) The internal standard must be present in low abundance (or not at all) in the sample; (2) the internal standard must not have any spectral interferences; and, (3) the internal standard must not cause any spectral interferences. Thompson and Houk[2] examined the response of over fifty elements to a sodium matrix under different operating conditions. They found that the amount of suppression and relative order of suppression of various analyte elements can differ for various matrix elements and various operating conditions. They stated that the criteria that they recommend for the selection of internal standards are to closely match the mass and the ionization potential of the internal standard to the analyte of

interest. Doherty[3] found that mass matching was the only criterion necessary for the selection of internal standards for the analysis of rare earth elements. Vanhaecke *et al.*[4] also found a mass dependence in the selection of internal standards for analyses in various matrices (e.g., acidic, organic, high solids). Chen and Houk[5] found that the use of polyatomic ions as internal standards improved both accuracy and precision of the analysis. Vandecasteele *et al.*[6] found a mass dependence for elements in a NaCl matrix. They found that four internal standards were necessary for the analysis of elements in biological samples: ^{9}Be for low mass, ^{59}Co for transition elements, ^{115}In for medium mass, and ^{205}Tl for high mass.

The purpose of this study is to develop a method to automatically determine, when given a particular sample containing an interferent and N analytes, the number of internal standards necessary to achieve the accuracy desired and which elements should be used as internal standards. The most limiting assumption to this work is that a single interferent is present at a high concentration. The second assumption is that standard operating conditions are used. The isotopes in this study were selected such that there were no major spectral interferences. Otherwise, spectral interferences were not considered in this study. An algorithm was developed based on the idea that elements will behave similarly in samples with interfering elements. With this in mind, analytes in a particular sample are grouped together using the cluster analysis technique and the selection of internal standards was based on atomic mass, kinetic energy, ionization potential, oxide bond strength, hydride bond strength and electronegativity.

6.3 Experimental

Since looking at all the elements in the periodic table is not realistic at this juncture, a smaller universe of 26 elements (Table 6.1) covering most of the mass range was considered. Solutions of the analytes at a concentration of 100 ppb were prepared in various single interferent matrices. The analytes were added in the form of a multi-element standard (SCP Science, St-Laurent, Quebec). Six interfering elements were examined: Na, Mg, K, Zn, Ba, and Pb. All matrix elements were prepared from reagent grade nitrates (Alfa Aesar, Ward Hill, MA) with the exception of Mg and Zn which were prepared from reagent grade oxides (Alfa Aesar, Ward Hill, MA). A matrix-matched blank was prepared and used for each sample to minimize any concerns of contamination from the reagents. The matrix-matched blank also eliminated any spectral interferences from the interfering elements. A Sciex ELAN 5000 was employed using standard operating conditions of 1.0 kW of power and a nebulizer gas flow rate of 1.0 l/min. Prior to running any samples, a multicriteria target vector optimization of the ion lenses using the Simplex algorithm was performed[7]. The ion lenses were optimized for maximum signals of Li and Pb to provide a compromise between heavy and light elements.

Table 6.1 Elements used in this study with their monitored isotope and their ionization potentials.

Element	Mass	Ionization potential (eV)	Element	Mass	Ionization potential (eV)
Li	7	5.932	Zn	66	9.394
Be	9	9.322	Se	77	9.752
B	11	8.298	Sr	88	5.695
Na	23	5.139	Y	89	6.380
Mg	25	7.646	Mo	95	7.099
Al	27	5.986	Ag	107	7.576
K	39	4.341	Cd	111	8.993
Ca	44	6.113	Sb	121	8.461
V	51	6.740	Ba	137	5.212
Cr	52	6.766	La	139	5.577
Fe	57	7.870	Pt	195	9.000
Ni	61	7.635	Pb	208	7.416
Cu	63	7.726	Bi	209	7.289

6.3.1 Prior information

The initial step in this study was to determine the suppression or enhancement of elements in a sample containing an interfering element. The analytes were at a concentration of 100 ppb and the interferent was 1000 ppm. The amount of suppression or enhancement is expressed as %Error and was calculated using Equations 1 and 2.

$$ECa,samp = \left(\frac{Sa,samp - Sa,mblk}{Sa,std - Sa,blk} \right) * Ca,std \qquad \{1\}$$

$$\%Error = \left(\frac{ECa,samp}{Ca,samp} - 1 \right) * 100 \qquad \{2\}$$

where a is a given analyte; blk is the blank which consists of distilled water; std is the standard containing 100 ppb of all analytes; samp is the sample containing 100 ppb of all analytes along with 1000 ppm of the interferent; mblk is the matrix matched blank which solely contains the interferent at 1000 ppm; Sa,std is the signal of the analyte in the standard; Sa,samp is the signal of the analyte in the sample; Sa,blk is the signal of the analyte in the blank; Sa,mblk is the signal of the analyte in the matrix matched blank; Ca,std is the concentration of the analyte in the standard; Ca,samp is the concentration of the analyte in the sample; Eca,samp is the estimated concentration of the analyte in the sample.

6.3.2 Selection of internal standards (General Method)

A cluster analysis algorithm[8,9] was used to select internal standards for a particular sample containing N analytes.

1. Sample Data Matrix

The first step involved the preparation of a data matrix. This matrix contains the analytes with the characteristics that will be used to group them (e.g., ionization potential, kinetic energy, etc...).

2. Distance matrix

The second step was the determination of the distance matrix. The distance matrix contains the values that describe how similar elements are to each other and will be used to group the elements. To determine how the distance matrix would be calculated, two interfering elements were considered: Na, a light easily ionizable element, and Pb, a heavy non-easily ionizable element. These two elements are relatively close to the extremities of the atomic mass and ionization potential scales; therefore, they were used to calibrate the method for all elements. The amount of suppression (or enhancement) was calculated as described above for twenty-five analytes in both matrices. In the determination of any possible relationship between the amount of suppression (or enhancement) and characteristics of the elements, five parameters[10] were considered. These were ionization potential, kinetic energy, oxide bond strength, hydride bond strength, and electronegativity. For any atomic mass, m, the kinetic energy[11] can be calculated using

$$KE = 0.026 * m + 2.0\ eV \qquad \{3\}$$

Applying a multiple linear regression[12] (MLR) on the %Error of the analytes in the Na matrix and the five parameters, it was found, based on the correlation coefficient, that the suppression was most correlated to the ionization potential of elements. Electronegativity, hydride bond strength, and oxide bond strength made almost equal contributions whereas the kinetic energy of elements made the least. Kinetic energy was used instead of atomic mass since it was better correlated to the amount of suppression observed. For the data obtained with the Pb matrix, the opposite was observed; the suppression was most correlated to the kinetic energy of analytes whereas there was very little correlation to the ionization potential of elements. It was decided that all five parameters would be included in the calculation of the distance matrix; however, these parameters would be weighted differently. The distance between two analytes was calculated using

$$d_{ij} = \sqrt{[a * ((KE_i - KE_j)/(KE_H - KE_L))^2 + b * ((IP_i - IP_j)/(IP_H - IP_L))^2 + c * ((OBS_i - OBS_j)/(OBS_H - OBS_L))^2 + d * ((HBS_i - HBS_j)/(HBS_H - HBS_L))^2 + e * (ELN_i - ELN_j)/(ELN_H - ELN_L))^2]} \quad \{4\}$$

where the subscripts i and j denote the *i*th and *j*th analytes, respectively; the subscripts H and L denote the highest and lowest value of a characteristic for all elements in our small "universe"; KE is the kinetic energy of an element; IP is the ionization potential of an element; OBS is the oxide bond strength of an element; HBS is the hydride bond strength of an element; and, ELN is the electronegativity of an element. There are five weighing constants, a, b, c, d, and e.

Table 6.2 The weight values of a and b for the six interferents.

Interferent	a	b
Na	1	10
Mg	1	10
K	2	13
Zn	3	1
Ba	7	10
Pb	10	1

The correlation coefficients obtained for the five parameters in the Na and Pb matrices were used to calibrate the five weights. For each matrix, the most correlated parameter was assigned a weight value of ten and the least correlated was assigned a weight value of one. Since the relationship between the oxide bond strength, hydride bond strength, and electronegativity and the amount of suppression was not well known, it was decided that they would be treated equally. The weights for these parameters were arbitrarily assigned to a weight value of 3 (Table 6.2) due to their low correlation with the amount of suppression observed in both matrices. Using the weights assigned for the Na and Pb matrices, two scales, one for kinetic energy and one for ionization potential, were established. These scales could be used to find weights for other matrices. For example, consider a sample containing the matrix element Ba which has an atomic mass of 137. To find the weights for this Ba sample, first the relationship between the parameters and the weights are established. Sodium, with an atomic mass of 23 and a weight value of 1

for a, and lead, with an atomic mass of 208 and a weight of 10 for a, produce the relationship a = 0.049m - 0.12, where m is atomic mass and a is the weight for the kinetic energy parameter. Using this relationship, the weight value of a for the Ba sample was calculated as 6.6 and was rounded to the nearest integer (Table 6.2). The same was done for the weight values of b using ionization potentials. The weight values for c, d, and e were always set to three.

3. Clustering method

The next step was to run the clustering method. A clustering method converts a distance matrix into a tree. It does this by a series of steps, each reducing the distance matrix and building the tree. In the final step, the tree is completed and the distance matrix disappears. A cluster is defined as a set of objects (elements) that are similar to each other. A cluster can consist of one object (element) or all of the objects (elements). At the start of the clustering method, each element is considered to be in a separate cluster. For example, consider a hypothetical sample with four analytes, Li, B, K and Sr, in a Na matrix. The clustering method will begin with four clusters. Each step will merge the two most similar clusters that exist at the start of the step; this will decrement the number of clusters by one. The unweighted pair-group method using arithmetic averages (UPGMA)[8] was used. The process will be illustrated by our example of four analytes. The distance matrix (Table 6.3) for these four analytes was determined using Equation 4.

Step 1. Find the smallest entry in the distance matrix (Table 6.3). Clearly, this is Li and Sr. Merge clusters Li and Sr, giving (Li Sr), B, K. Recalculate (Equations 5 and 6) the distance matrix (Table 6.4) and build tree (Figure 6.1a).

$$d_{(Li\ Sr),B} = (d_{Li,B} + d_{Sr,B}) * 0.5$$
$$= (7.35 + 6.8) * 0.5 = 7.08 \qquad \{5\}$$

$$d_{(Li\ Sr),K} = (d_{Li,K} + d_{Sr,K}) * 0.5$$
$$= (2.01 + 2.63) * 0.5 = 2.32 \qquad \{6\}$$

Step 2. Find the smallest entry in the new distance matrix (Table 6.4). Merge clusters (Li Sr) and K, giving (Li Sr K) and B. Recalculate (Equation 7) the distance matrix (Table 6.5) and build tree (Figure 6.1b).

$$d_{(Li\ Sr\ K),B} = (d_{(Li\ Sr),B} + d_{K,B}) * 0.5$$

$$= (7.08 + 9.34) * 0.5 = 8.21 \qquad \{7\}$$

Step 3. Find the smallest entry in the new distance matrix (Table 6.5). Merge clusters (Li Sr K) and B giving (Li Sr K B). Complete the tree (Figure 6.1c).

Table 6.3 Distance matrix of four elements: Li, B, K, and Sr.

	Li	B	K	Sr
Li	---	---	---	---
B	7.35	---	---	---
K	2.01	9.34	---	---
Sr	0.85	6.80	2.63	---

Table 6.4 Distance matrix after first step of the cluster analysis algorithm.

	(Li Sr)	B	K
(Li Sr)	---	---	---
B	7.08	---	---
K	2.32	9.34	---

Table 6.5 Distance matrix after second step of the cluster analysis algorithm.

	(Li Sr K)	B
(Li Sr K)	---	---
B	8.21	---

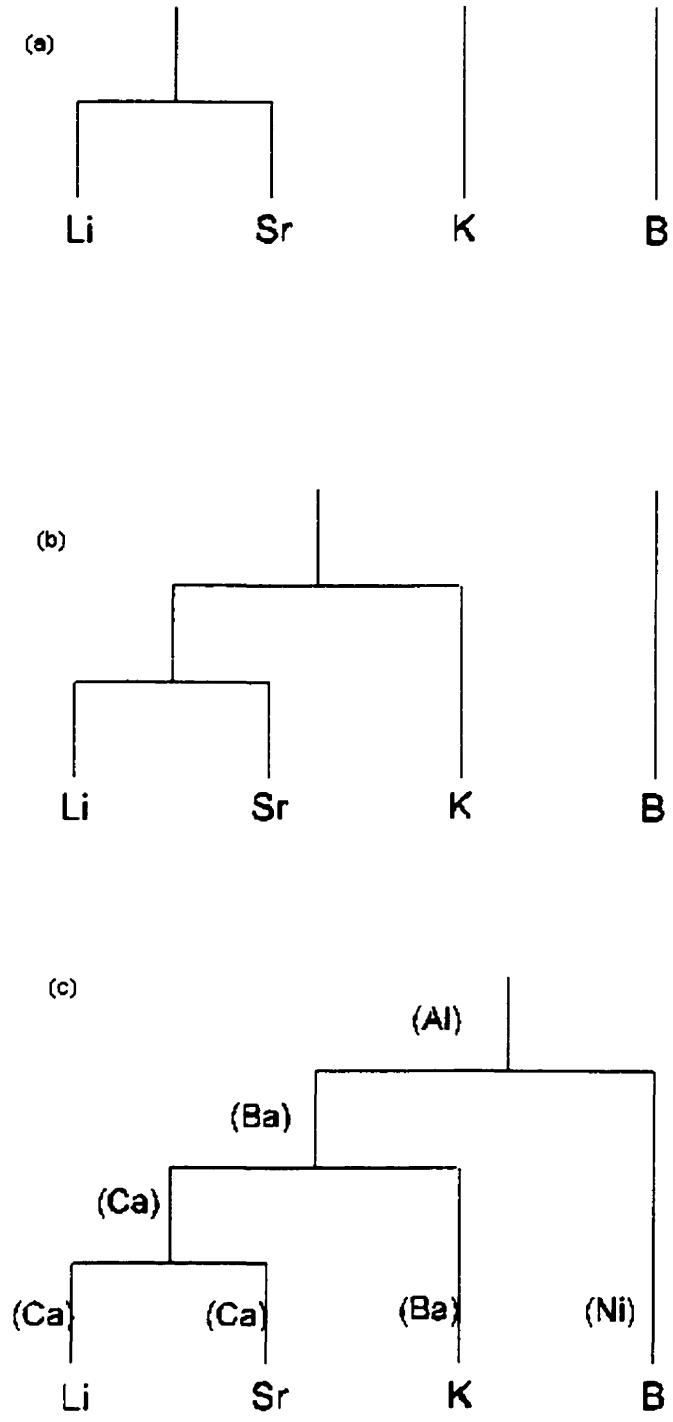

Figure 6.1 Example of (a) Step 1, (b) Step 2, and (c) Step 3 of cluster analysis algorithm, internal standards selected are in brackets.

4. Selection of internal standards

At each level of the tree, internal standards are selected for each cluster. The selection is performed by comparing the analytes in a cluster with the remainder of the elements (Table 6.1) not present in the sample. The comparison is done by using

$$\text{Compare\_value}_i = \sqrt{[a * ((KE_i - AvgKE)/AvgKE)^2 + b * ((IP_i - AvgIP)/AvgIP)^2 + c * ((OBS_i - AvgOBS)/AvgOBS)^2 + d * ((HBS_i - AvgHBS)/AvgHBS)^2 + e * ((ELN_i - AvgELN)/AvgELN)^2]} \{8\}$$

where i is the internal standard candidate from the available elements not present in the sample; AvgKE, AvgIP, AvgOBS, AvgHBS, and AvgELN are the average kinetic energy, ionization potential, oxide bond strength, hydride bond strength, and electronegativity, respectively, of the elements in the cluster. This equation is based on Equation 4 and the weights a, b, c, d, and e are the same as for Equation 4 (Table 6.2). The closest match is used as an internal standard (Table 6.6). It should be noted that the same element can be used as an internal standard for several different clusters; therefore, the number of internal standards at a certain level of a tree does not always correspond to the level number (where level 1 is at the top and level N (number of analytes) is at the bottom).

Table 6.6 Selection of internal standards at each level of the dendrogram.

Level					
4					
	Cluster	Li	Sr	K	B
	Internal Standard	Ca	Ca	Ba	Ni
3					
	Cluster	(Li Sr)	K	B	
	Internal Standard	Ca	Ba	Ni	
2					
	Cluster	(Li Sr K)	B		
	Internal Standard	Ba	Ni		
1					
	Cluster	(Li Sr K B)			
	Internal Standard	Al			

6.3.3 Selection of internal standards (Sample Specific)

Another methodology for selection of internal standards is possible. If samples, such as the Na sample, have been previously run and the %Errors for the analytes have been calculated, this information can be used to find internal standards for samples containing the same matrix element. For example, the 1000 ppm Na sample with the twenty-five analytes can be used to determine appropriate internal standards for other Na samples.

1. Sample Data Matrix

In this case, the Sample Data Matrix contains the analytes and the %Error is calculated using Equation 2.

2. Distance Matrix

The distance between two analytes, i and j, is calculated by

$$dij = \sqrt{[\%Error_i - \%Error_j]^2} \qquad \{9\}$$

3. Clustering Method

The clustering analysis is the same as described previously.

4. Selection of internal standards

The selection is performed by comparing the analytes in a cluster with the elements in Table 6.1 not present in the sample. The comparison is done by

$$Compare\_Value_{is} = \sqrt{[\%Error_{is} - \%ErrorAvg]^2} \qquad \{10\}$$

where $\%Error_{is}$ is the amount of suppression (enhancement) of the internal standard candidate and the %ErrorAvg is the average %Error of the analytes in a cluster.

6.4 Results and discussion

6.4.1 Collection of prior knowledge

6.4.1.1 Interfering element: Na.

The accuracies (or errors) of the determination of analyte concentrations using an external standard were calculated for a sample containing all the analytes listed in Table 6.1 and 1000 ppm Na, a light easily ionizable element. Figure 6.2a illustrates the %Error associated with each analyte. The analytes along the x-axis are listed in order of increasing mass. There is no obvious trend of %Error with respect to mass. Figure 6.2b shows the %Error with respect to ionization potential; although there is considerable scatter, one can see that the suppression increases with ionization potential. Thompson and Houk[2] also found some dependence of the amount of suppression on ionization potential.

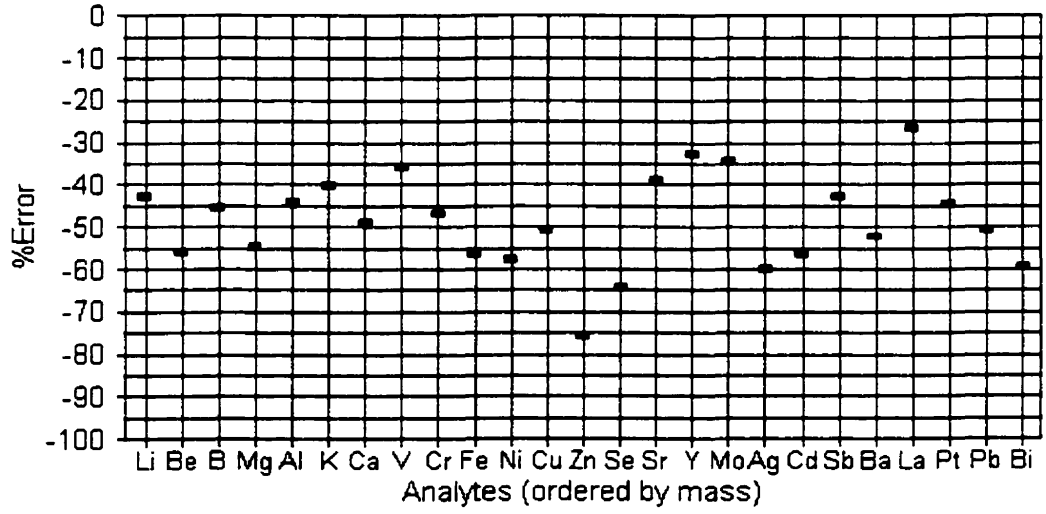

Figure 6.2(a) The amount of suppression obtained for 25 analytes in an 1000 ppm Na sample as a function of atomic mass.

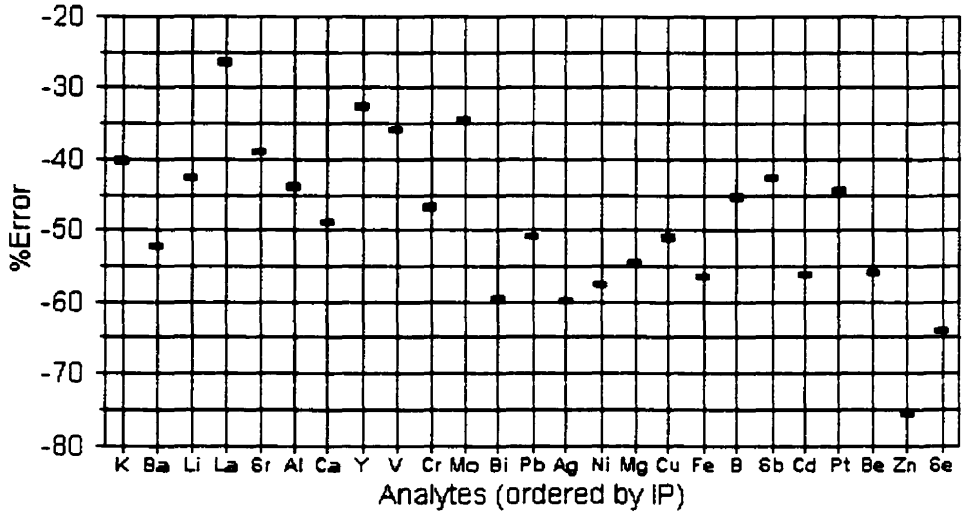

Figure 6.2(b) The amount of suppression obtained for 25 analytes in an 1000 ppm Na sample as a function of ionization potential.

6.4.1.2 Interfering element: Pb

The same analysis was performed using Pb, a heavy element, as the interfering element. Examining Figure 6.3a, it was observed that the lighter elements were more affected in the presence of the Pb interferent than the heavier elements. This was not seen with the Na interferent. The rule regarding the selection of an internal standard close in mass would be appropriate in this case; however, selecting an internal standard close in ionization potential (Figure 6.3b) would lead to erroneous results.

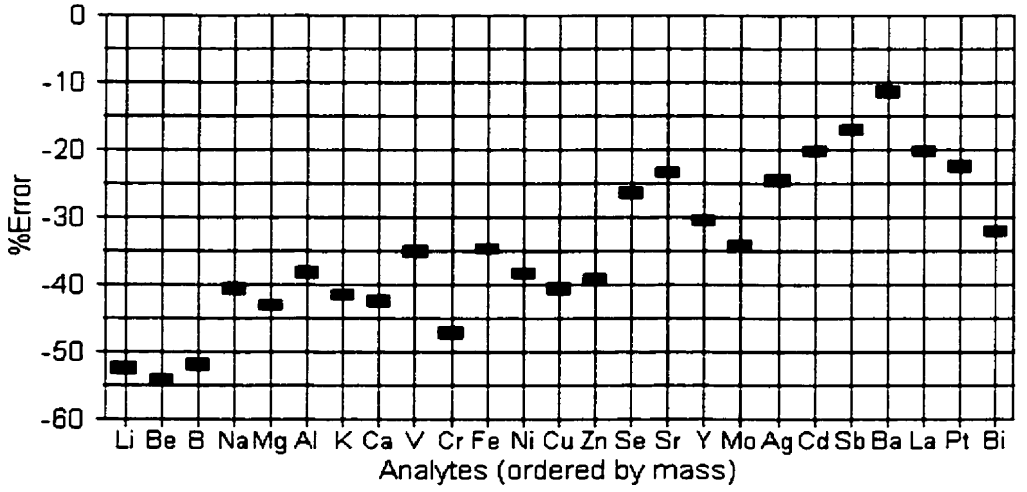

Figure 6.3(a) Amount of suppression obtained for 25 analytes in an 1000 ppm Pb sample as a function of atomic mass.

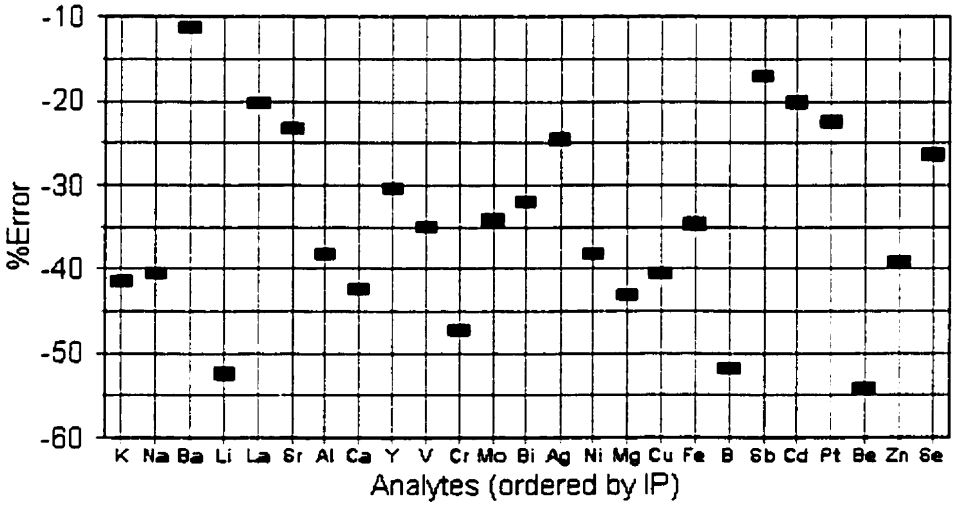

Figure 6.3(b) Amount of suppression obtained for 25 analytes in an 1000 ppm Pb sample as a function of ionization potential.

6.4.2 Selection of internal standards (General Method)

Three different groups of analytes were used as though they were samples to verify the methodology (Table 6.7). This choice of analytes illustrates the difficulty in selecting internal standards for a sample where the analytes cover a large mass range and a wide range of ionization potentials.

Table 6.7 Three groups of analytes used to validate the cluster analysis algorithm.

Group	Analytes
A	^{9}Be, ^{39}K, ^{51}V, ^{63}Cu, ^{89}Y, ^{111}Cd, ^{195}Pt, ^{209}Bi
B	^{11}B, ^{44}Ca, ^{77}Se, ^{111}Cd, ^{137}La, ^{209}Bi
C	^{27}Al, ^{51}V, ^{57}Fe, ^{66}Zn, ^{88}Sr, ^{95}Mo, ^{121}Sb

The selection of internal standards was performed using cluster analysis as described previously. The cluster analysis produced a dendrogram (tree) for each group of analytes in a matrix with an interfering element. Six interfering elements at various concentrations were examined: Na, Mg, K, Zn, Ba, and Pb. These interfering elements cover a wide range of atomic mass and ionization potential. The matrix elements, Mg and Zn, were only investigated at a concentration of 1000 ppm since the errors obtained were small at lower concentrations. At lower concentrations of these elements there would be no need to use an internal standard calibration methodology. The concentrations examined for the four other interfering elements were 500 ppm and 1000 ppm. Using the internal standards selected at every level of the tree, the analyte concentrations were determined. The error in this determination was calculated and its absolute value was determined. The absolute value was taken because the sign of the error in this case was not important. The results obtained using the internal standards are presented in Figures 6.4 to 6.6. The average error (in percentage) for all the analytes in a group is plotted against the number of internal standards used for the analysis. As stated earlier, the cluster analysis algorithm does not always produce a different element as an internal standard for each cluster. This can be seen on the plots since the maximum number of internal standards is not always equal to the number of analytes. In some plots, there are also multiple points for a certain number of internal standards since an

increase in clusters does not always equal an increase in the number of internal standards. When the number of internal standards is zero, only external calibration was performed.

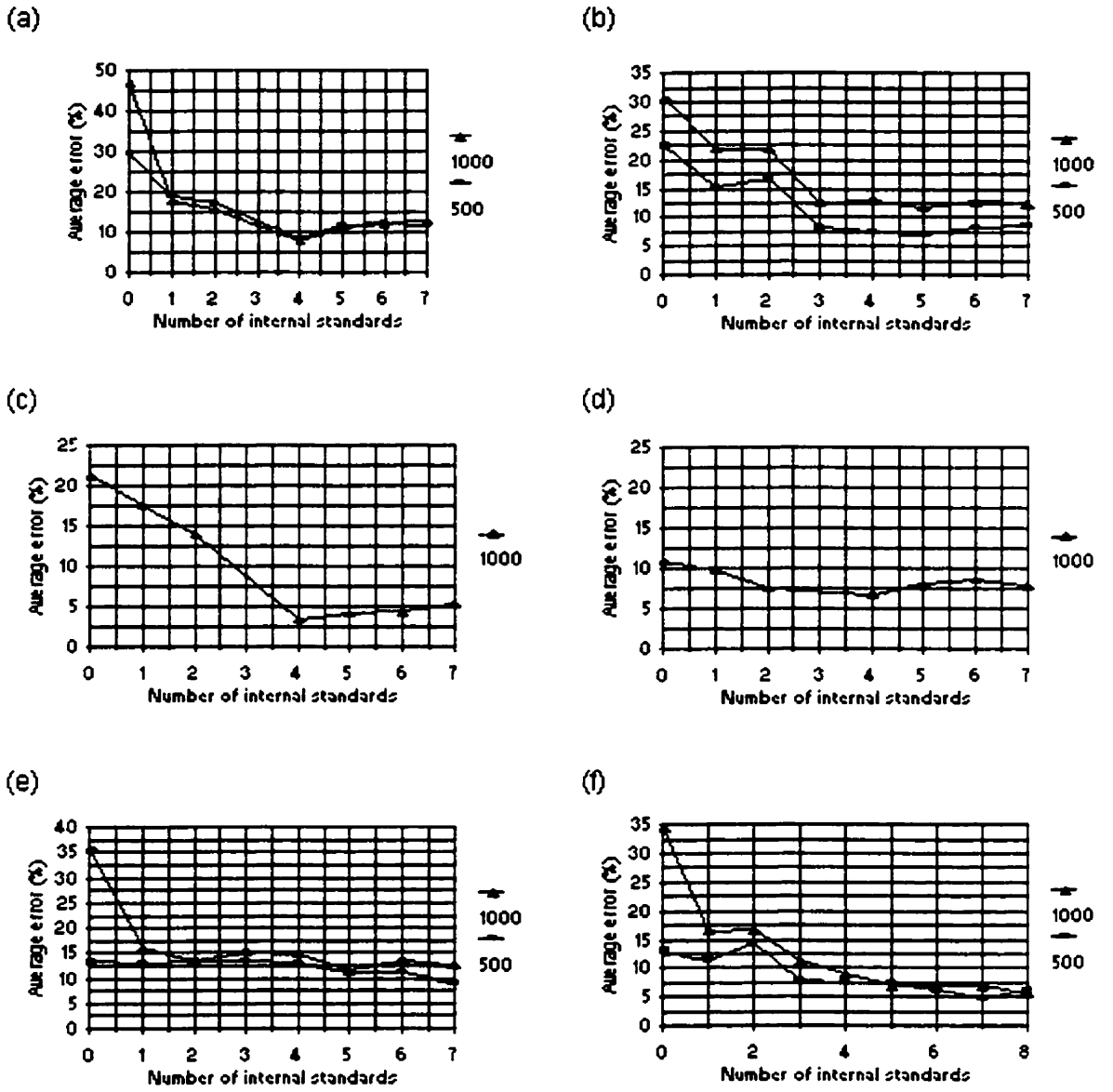

Figure 6.4 Performance of the General Method cluster analysis algorithm for analytes of Group A in (a) Na, (b) K, (c) Mg, (d) Zn, (e) Ba, and (f) Pb samples.

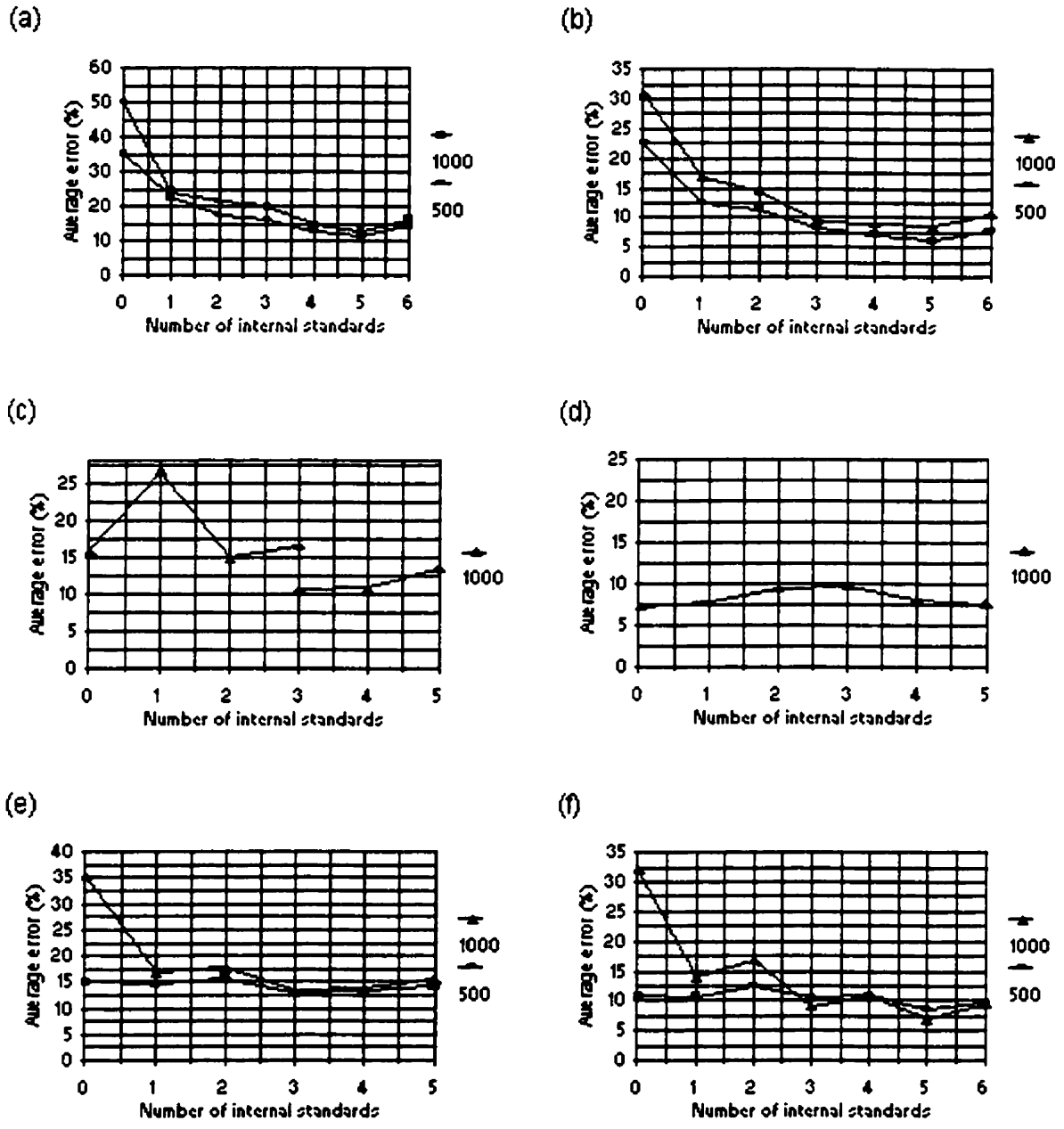

Figure 6.5 Performance of the General Method cluster analysis algorithm for analytes of Group B in (a) Na, (b) K, (c) Mg, (d) Zn, (e) Ba, and (f) Pb samples.

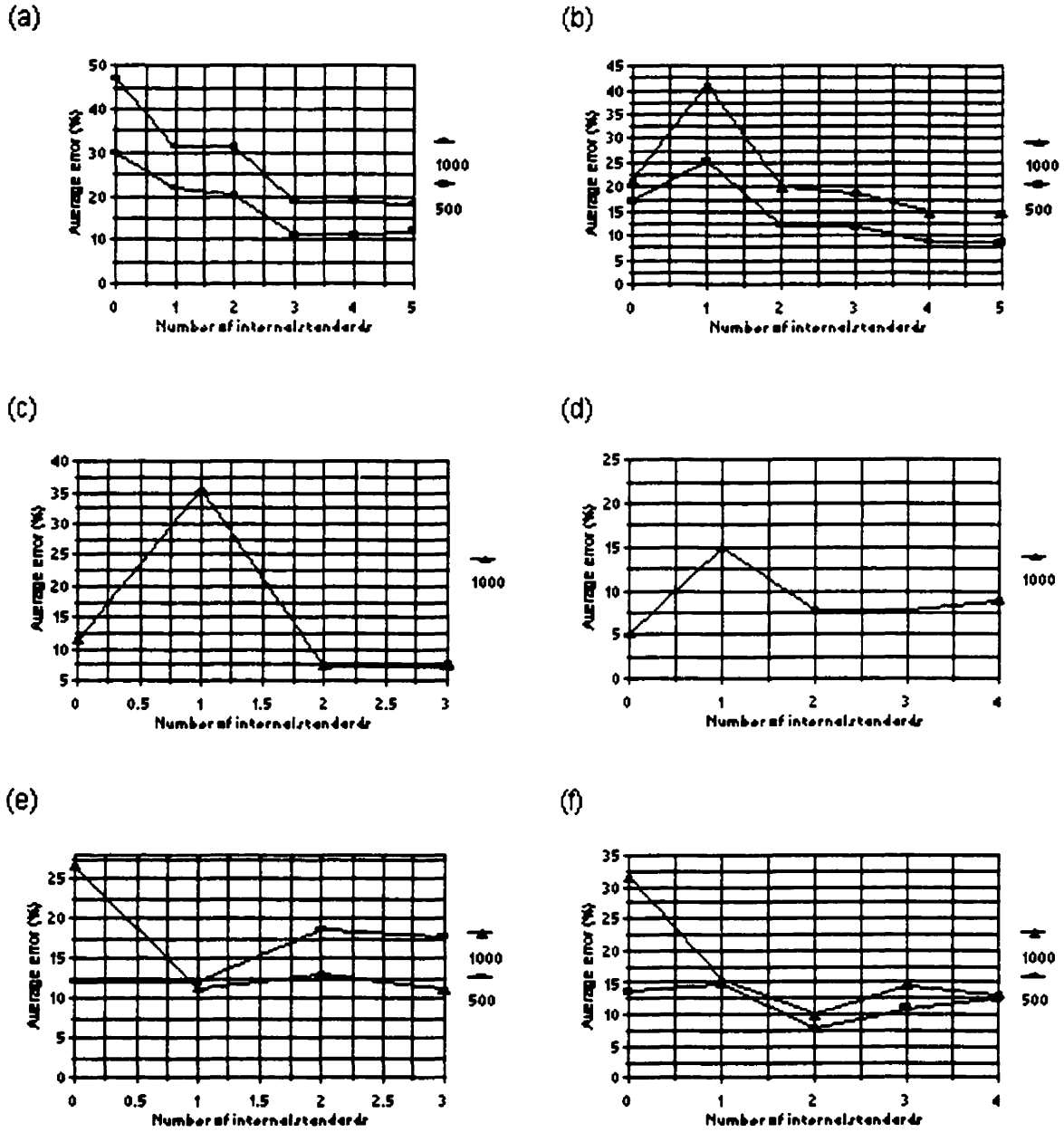

Figure 6.6 Performance of the General Method cluster analysis algorithm for analytes of Group C in (a) Na, (b) K, (c) Mg, (d) Zn, (e) Ba, and (f) Pb samples.

6.4.3 Performance of cluster analysis

Examining the results (Figure 6.4) obtained for the samples containing the analytes of Group A (Table 6.7), it can be seen that the average error initially decreases, then reaches a point where no significant improvement was seen with the addition of internal standards. The only exception is Zn at 1000 ppm where the error obtained with an external calibration was small and no real improvement was observed with the use of more internal standards. Similar trends were observed with the analytes in Group B (Figure 6.5) with the sole exception of Mg. In the case of the Mg interferent, the cluster of all analytes in the group with the addition of one internal standard does not improve performance; in fact, it does the opposite. At the addition of two internal standards, the average error decreases significantly. The only explanation for this phenomenon is that the internal standard chosen for the cluster of all the analytes in Group B was not a good compromise for all analytes. This phenomenon is also observed with the analytes in Group C (Figure 6.6). The internal standards for the analytes of Group C in the Ba matrix (500 ppm) did not perform well as an increase in the average error was observed. In particular, the analyte/internal standard pair of Sr/Ca does not appear to be the appropriate choice. Although these two elements are relatively close in ionization potential, Ca was suppressed twice as much as Sr in the Ba matrix.

One of the assumptions made at the beginning of this study was that there was only one interferent element present in a sample. In real samples, more than one element can be present at high concentration. Further studies would need to be done on how the analytes are affected in samples with many interferents, and whether the effect could be correlated to ionization potential, kinetic energy, oxide bond strength, hydride bond strength, and electronegativity.

6.4.4 Selection of internal standards (Sample specific)

The interferents Na, K, Ba, and Pb, were all run at 1000 ppm with the twenty-five analytes and the %Error for the analytes were calculated. Using this data, the cluster

analysis algorithm was applied to the three group of analytes listed in Table 6.7. The performance of the cluster analysis was studied using a sample with 500 ppm of the interferent. The reverse was also done using the 500 ppm for the selection of internal standards for the 1000 ppm samples. The results are depicted in Figures 6.7 to 6.9. Compared to the results of the General Method (Figures 6.4 to 6.6), it can be seen that a lower average error was obtained when the internal standards are selected with the knowledge of how the elements were affected in a similar matrix. The most dramatic difference appears as one increases the number of internal standards, indicating that fewer internal standards are required to obtain good results with this method. Also, it does not seem to make much difference as to which concentration of interferent in the sample is used with the cluster analysis; both, the 500 ppm and 1000 ppm, samples produce similar trends in the plots. Several other observations were made when the two samples of different interferent concentration were used with the cluster analysis algorithm. First, the clusters produced for a group of analytes in the 1000 ppm sample were not the same for that same group of analytes in the 500 ppm sample of the same interferent. Second, the internal standards selected for the clusters were also different for the two concentrations of interferent. Third, the total number of internal standards selected for a group of analytes also differed for the two samples of the same interferent. These observations would imply that elements are not always similarly affected when the concentration of the interferent is varied.

The sample specific method produces less error; however, care should be taken in selecting the interferent concentration for the sample used with the cluster analysis. If the concentration is too low, the amount of suppression observed for the analytes may be small and not representative of a more difficult sample.

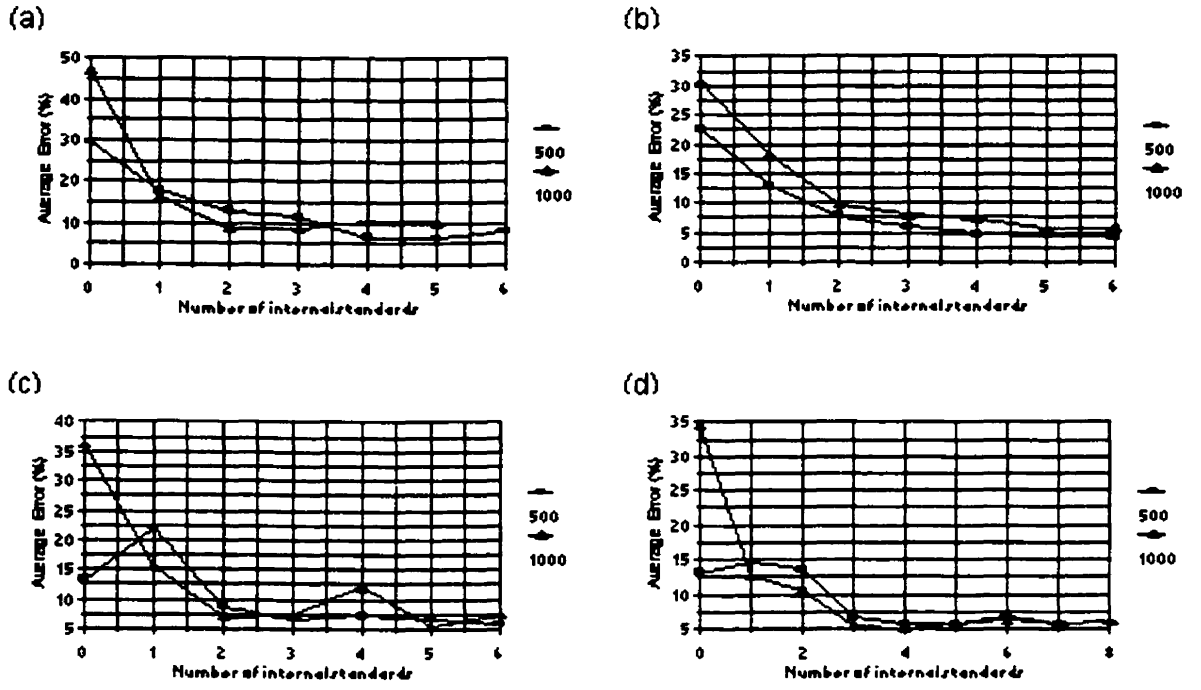

Figure 6.7 Performance of the Sample Specific cluster analysis algorithm for analytes of Group A in (a) Na, (b) K, (c) Ba, and (d) Pb samples.

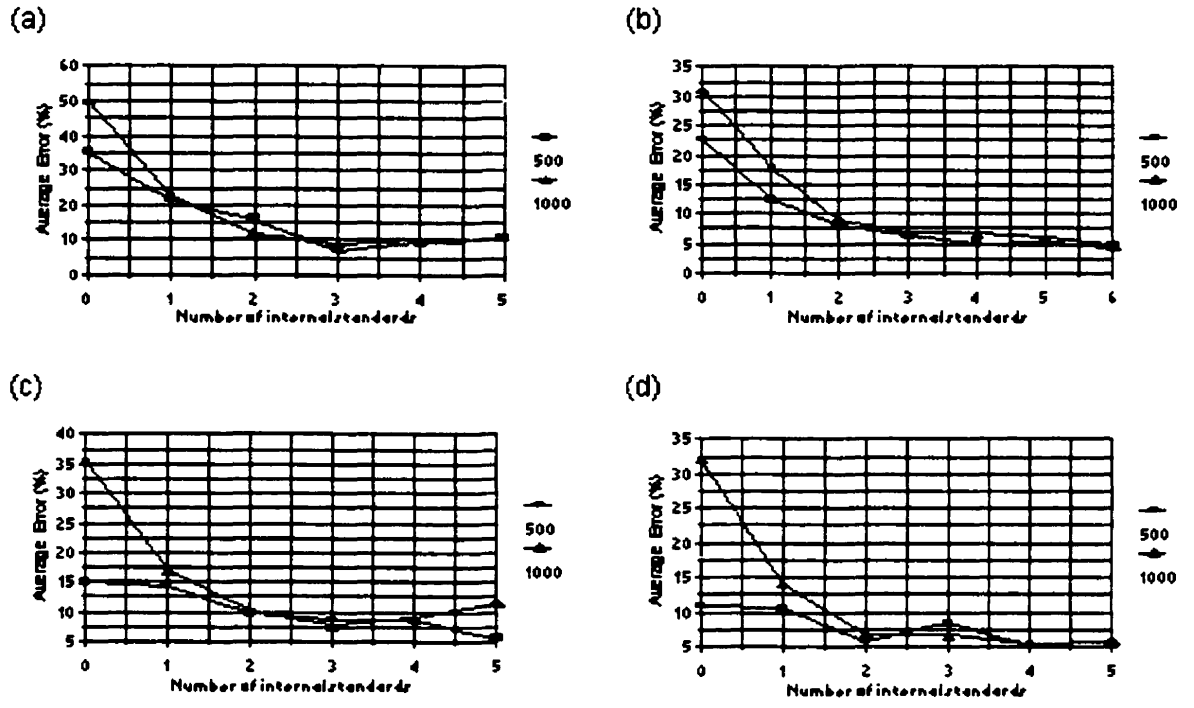

Figure 6.8 Performance of the Sample Specific cluster analysis algorithm for analytes of Group B in (a) Na, (b) K, (c) Ba, and (d) Pb samples.

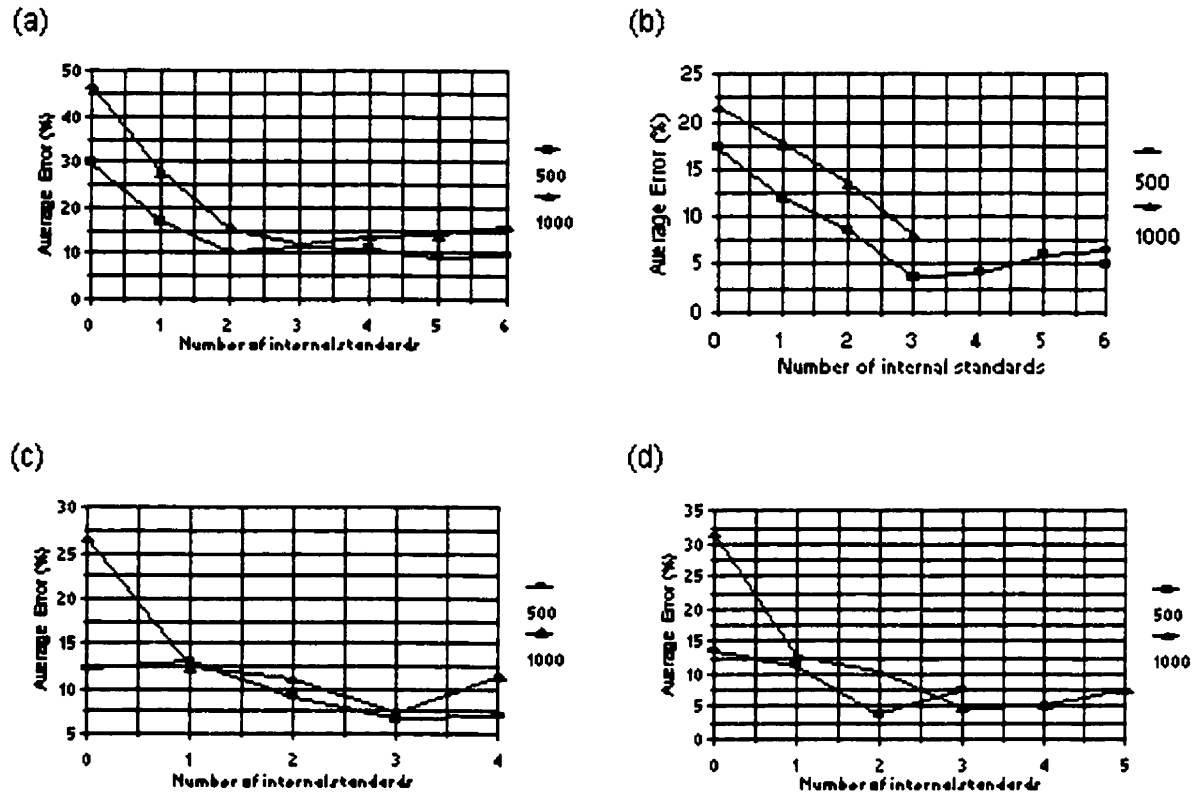

Figure 6.9 Performance of the Sample Specific cluster analysis algorithm for analytes of Group C in (a) Na, (b) K, (c) Ba, and (d) Pb samples.

6.5 Conclusion

The selection of internal standards can be done automatically using a cluster analysis algorithm and using the characteristics: kinetic energy, ionization potential, oxide bond strength, hydride bond strength, and electronegativity. A single set of operating conditions was used throughout this study and the analyte/internal standard pair may not be appropriate under different operating conditions. A change in the weights in Equations 4 and 8 would be required to compensate for a change in operating conditions. This would be done by running samples with single element interferent, Na and Pb, at high concentrations and using multiple linear regressions to determine the contribution of the various characteristics on the amount of suppression (or enhancement) of analytes. The weights to be used for other matrices would be adjusted, accordingly, based on the kinetic energy and ionization potential of the interfering element.

If data has been collected with the specific interferent and analytes in question, then the clustering method can be used to automatically select internal standards that provide even more accurate results than the more general method.

6.6 References

1 Montaser, A. and Golightly, D.W., ed., Inductively Coupled Plasmas in Analytical Atomic Spectrometry, (VCH Publishers Inc.,New York, 1992), and references therein.

2 Thompson, J.J. and Houk, R.S., *Appl. Spectrosc.*, 1987, 41, 801.

3 Doherty, W., *Spectrochim. Acta*, 1989, 44B, 263.

4 Vanhaecke, F., Vanhoe, H., Dams, R., and Vandecasteele, C., *Talanta*, 1992, 39, 737.

5 Chen, X. and Houk, R.S., *J. Anal. At. Spectrom.*, 1995, 10, 837.

6 Vandecasteele, C., Vanhoe, H., and Dams, R., *J. Anal. At. Spectrom.*, 1993, 8, 781.

7 Sartoros, C., Goltz, D.M., and Salin, E.D., *Appl. Spectrosc.*, in press.

8 Romesburg, H.C., Cluster Analysis for Researchers, Lifetime Learning Publications, CA, 1984.

9 Späth, H., Cluster Analysis Algorithms for Data Reduction and Classification of Objects, Ellis Horwood Limited, Chichester, 1980.

10 Lide, D. R., ed., *CRC Handbook of Chemistry and Physics*, 76th ed., CRC Press, New York, 1995-6.

11 Fulford, J.E. and Douglas, D.J., *Appl. Spectrosc*, 1986, 40, 971.

12 Geladi, P. and Kowalski, B.R., *Anal. Chim. Acta*, 1986, 185, 1.

Chapter 7

7 Conclusions and Future Work

The Autonomous Instrument now has modules for pattern recognition, instrument diagnosis, multi-element optimization, and selection of internal standards. There are a few aspects of the Autonomous Instrument that still need to be developed or implemented for ICP-AES and ICP-MS. We have seen that diagnostic modules were successfully developed for ICP-AES. The same framework could be applied to ICP-MS. The QUID Expert module for ICP-AES examined the energy transfer, the sample transfer, nebulizer precision and accuracy, and the optical system (resolution and collimation) using a standard test solution. Most of these same components could be diagnosed for ICP-MS except for the optical component, as it differs; however, other components that could be diagnosed are the ion optics and sampling interface (sampler and skimmer cones). In ICP-AES, the warning diagnostic module used signals and signal-to-background ratios (SBRs) of H and Ar lines to monitor the system's performance. In ICP-MS there are several species that could be monitored; these are the hydrogen, oxygen, and argon ions along with several molecular combinations of these elements (OH^+, ArO^+, ArH^+, Ar_2^+, etc...). If these ions are monitored while varying the rf power, the sample introduction rate, and the gas flow rates, rules for predicting changes to the system could be obtained by using an inductive learning algorithm.

The study on pattern recognition revealed that k-Nearest Neighbors and Bayesian Classification could be used on small databases with relatively high recognition rates. The purpose of the pattern recognition module is to find samples that are similar so that the same operating conditions and calibration methodologies could be used. The next step would be to see if the results obtained when using these operating conditions and calibration methodology are significantly better than those obtained with standard operating conditions.

The Autonomous Instrument can now automatically select internal standards for analyses in ICP-MS. This is one of the components of the Calibration Methodology

Selection module. Several other components also need to be implemented. For example, how should an external calibration with matrix matching be performed. The matrix matching could be done on total salt content, match all the majors, or match the major with the highest concentration. The question would be which one works better and/or takes the least amount of time. The rules for the selection of a calibration methodology also need to be developed and tested.

The framework for the Learn to Run a New Sample module needs to be developed. It can be divided into two components: optimization and calibration methodology selection. Since the optimization component has been developed and implemented, once the rules for the calibration methodology selection have been developed, the two components could be bridged to form this new module. The Learn to Run a New Sample module would begin by optimizing the operating conditions for best accuracy in the results. Once the operating conditions are established, it would pass control to the Calibration Methodology Selection module. This latter module would try to find the best calibration methodology that would suit constraints such as time of analysis, cost of analysis (e.g., isotope dilution can be very expensive if enriched isotopes have to be purchased for many analytes), and volume of sample.

With the addition of the intelligent components yet to be developed, the Autonomous Instrument will be able to perform complete analyses of samples without any assistance from human operators. The Autonomous Instrument will not only be a powerful tool in ICP spectrometry but it will be able to serve as a framework for many other analytical instruments.